THE EFFECTS OF HYDROGEN SULFIDE ON HEK-293 CELLS AND HUMAN PRIMARY BRONCHIAL FIBROBLASTS

Vikas Kaura (B.Sc, B.M.)

MSc by Thesis

The University of Hull and The University of York

Hull York Medical School

October 2015

Abstract

Hydrogen sulfide (H_2S) is a key biologically relevant signalling molecule and has been recognised as the third endogenous gasotransmitter. H_2S modulates various biological functions through complex mechanisms which may involve Transient Receptor Potential (TRP) channels such as TRPA1. TRPA1 is postulated to play a prominent role in pulmonary inflammation and airway hypersensitivity. H_2S has been found to also modulate cell growth and survival, with high concentrations leading to reactive airway disease, acute respiratory failure and pulmonary fibrosis. N-Acetylcysteine (NAC) is a thiol precursor of L-Cysteine which elicits antioxidant effects and has been implicated in preventing the progression of pulmonary fibrosis. The aim of the study was to examine the effects of H_2S on TRPA1 and human primary bronchial fibroblasts (HPBF).

Initial experiments sought to examine the effects of NaHS on HEK293 cells transfected with TRPA1 (HEK-TRPA1) using fluorometric calcium assays. These assays were hampered by a direct reaction between the H_2S donor NaHS and the fluorescent dye. However this has led to the identification of a putative new H_2S sensor.

Next, untransfected HPBF and HEK-TRPA1 were treated with NaHS or with NAC, and the effects assessed using a five-day growth assay. Chronic NaHS exposure induced a significant reduction in the growth of HEK-TRPA1 cells. Furthermore an acute 30 minute treatment with NaHS significantly reduced the growth of both HEK-TRPA1 cells and HPBFs, whereas NAC only inhibited growth of the latter.

The NAC mediated inhibition in HPBF growth provides *in vitro* evidence for the potential anti-fibrotic actions of NAC in the lung. The inhibitory effects on growth at day five following a brief 30 minute NaHS exposure is a novel finding that requires further investigation to elucidate the mechanism of action. This could potentially provide a better understanding of the effects of H_2S in modulating the progression from inflammation to fibrosis.

Table of Contents

This thesis is dedicated to my parents,

Mr CK Kaura and Mrs P Kaura

….and to my wife….

Dr Christine Kaura.

Acknowledgements

This MSc by thesis was funded by the Health Education Yorkshire and the Humber Academic Clinical Fellowship programme in Anaesthetics, to whom I am grateful.

I would like to thank my supervisors Dr Laura Sadofsky and Professor Alyn H Morice for giving me the opportunity to work on this project, their guidance during the research and whilst writing it up. I am also very grateful to Dr Kevin Morgan for his incredible patience, knowledge and the training that he provided during the course of this work.

I also am thankful to Chris Crow, Jiah Wong, Simon Fraser, Dr Vicky Green and Dr Simon Hart for their expertise during various parts of the project. I would also like to thank the other researchers working within the Daisy 2nd floor laboratories, including Ramsah, James, Jonathan and Liz.

Most importantly I would like to acknowledge the support and encouragement from my mum, Sumit, Anu and everyone else in my family. A very special thank-you goes to my wife Christine for her patience, love and incredible support, especially during the late nights and weekends that I spent working on this research.

Declaration

I confirm that this work is original and that if any passage(s) or diagrams(s) have been copied from academic papers, books, the internet or any other sources these are clearly identified by the use of quotation marks and the references(s) is fully cited. I certify that other than where indicated, this is my own work and does not breach the regulations of HYMS, the University of Hull or the University of York regarding plagiarism or academic conduct in examinations. I have read the HYMS Code of Practice on Academic Misconduct, and state that this piece of work is my own and does not contain any unacknowledged work from any other sources.

List of Abbreviations

ACS6	S-Sildenafil
ACS14	S-aspirin
ACS15	S-diclofenac
AITC	Allyl isothiocyanate
AM	Acetoxymethyl
ATB-346	Naproxen
ATP	Adenosine triphosphate
BrdU	Bromodeoxyuridine
Ca^{2+}	Calcium
$CaCl_2$	Calcium chloride
CAT	Cysteine aminotransferase
CBS	Cystathionine beta-synthase
CGA	Cell Growth Assay
CHO	Chinese hamster ovary
CO	Carbon monoxide
COPD	Chronic obstructive pulmonary disease
COS	Carbonyl sulfide
CSE	Cystathionine gamma-lyase
CSLV	Capsaicin sensitive lung vagal
ddH_2O	Double-distilled water
DMEM	Dulbeco's modified Eagle's medium
DMSO	Dimethyl sulphoxide
DNA	Deoxyribonucleic acid
DRG	Dorsal root ganglion
ECM	Extracellular matrix
EC_{50}	Effective Concentration causing a 50% response
EDRF	Endothelium derived relaxing factor
EE	Ethylmalonic encephalopathy
EMT	Epithelial to mesenchymal transition
ERK	Extracellular-signal-regulated kinases
EV	Empty plasmid vector
FCS	Foetal calf serum
Fluo-3 AM	Fluo-3 acetoxymethyl ester
GA	General anaesthetic
GI	Gastrointestinal
GYY4137	Morpholin-4-ium- 4 methoxyphenyl(morpholino)phosphinodithioate
HEK	Human Embryonic Kidney
HEK293	Human Embryonic Kidney-293
H^+	Hydrogen
H_2O_2	Hydrogen Peroxide
HPBF	Human primary bronchial fibroblasts
H_2S	Hydrogen sulfide
HS^-	Hydrogen sulfide anions
ICU	Intensive care unit
IL-1α	Interleukin-1alpha
IPF	Idiopathic pulmonary fibrosis

K	Potassium
K_{ATP}	ATP-dependent potassium channel
LPS	Lipopolysaccharide
3-MST	3-mercaptopyruvate sulfurtransferase
α-MEM	α-modified essential medium
mRNA	Messenger RNA
Na	Sodium
NAC	N-Acetylcysteine
NaCl	Sodium Chloride
NaHS	Sodium hydrosulfide
Na_2S	Sodium sulfide
NMDA	N-methyl-D-aspartate
NO	Nitric oxide
NSAIDs	Non-steroidal anti-inflammatory drugs
O_2	Oxygen
OD	Optical density
PBS	Phospate buffered saline
PI	Propidium iodide
ppm	Parts per million
RCF	Relative centrifugal force
RFU	Relative fluorescent unit
ROS	Reactive oxygen species
RNA	Ribonucleic acid
S^{2-}	Sulfide anions
SEM	Standard error of the mean
SFM	Serum-free media
SMC	Smooth muscle cells
SRB	Sulforhodamine B
TCA	Trichloroacetic acid
TGF-β1	Transforming growth factor-β1
TNFα	Tumour necrosis factor alpha
TRP	Transient receptor protein
TRPA1	Transient receptor protein ankyrin type 1
TRPC	Transient receptor protein canonical type
TRPM	Transient receptor protein melastatin type
TRPML	Transient receptor protein mucolipin type
TRPP	Transient receptor protein polycystin type
TRPV1	Transient receptor protein vanilloid type 1
VAP	Ventilator associated pneumonia
VEGF	Vascular endothelial growth factor
VSMC	Vascular smooth muscle cells

1.1 Gasotransmitters

The human body utilises many different molecules for intercellular and intracellular communication. These range from neurotransmitters and hormones to gaseous transmitters (gasotransmitters). The first gasotransmitter to be identified was nitric oxide (NO) (Furchgott and Vanhoutte, 1989; Olson, 2013). The discovery of this molecule as the much evasive endothelium derived relaxing factor (EDRF) initiated a new frontier of knowledge by introducing gaseous molecules as viable biological ligands. The gaseous nature of these messengers allows them to work in a much more diverse as well as rapid manner, for example they are not reliant on release from vesicles that are targeted towards the plasma membrane, instead they can diffuse out of the cell as a radical as soon as they are synthesised (Myers *et al*., 1990). However, they can also be released in a more conventional manner through binding to carrier molecules (Myers *et al*., 1990). The gaseous nature also affords a greater diversity in the sites of action on the effector cell; these range from proteins on the plasma membrane to an array of intracellular targets which can be reached by the gasotransmitters rapidly diffusing through the cell membrane due to their low molecular weight and high lipid solubility. Such flexibility allows gasotransmitters such as NO to mediate a host of physiological processes from the regulation of organ function such as the vascular tone or respiration, to its involvement in the inflammatory cascade including a putative direct effect in the destruction of microorganisms by the immune system. Furthermore, NO has also been found to modulate intracellular cascades that result in host cell survival or death (Moncada and Higgs, 2006; Fago *et al*., 2012).

The characterisation of NO as EDRF in the late 1980s initiated the search for other endogenously produced gasotransmitters which have so far yielded two novel systems; carbon monoxide and hydrogen sulfide (Mancardi *et al*., 2009; Olson, 2011; Olson, 2013). The former was the first of the two to be discovered, and as with NO has been shown to modulate a host of cellular functions such as metabolism, the redox state and cell death, with these activities primarily mediated by the mitochondria (Almeida *et al*., 2015).

1.2 Hydrogen Sulfide

Hydrogen sulfide (H_2S) is the third recognised endogenous gasotransmitters (Abe and Kimura, 1996; Wang, 2012). It is a colourless flammable gas that was first discovered in 1777 by Carl Wilhelm Scheele. It has the characteristic odour of 'rotten eggs' and is soluble in water, however it has a five-fold greater solubility in lipophilic solvents which facilitates its rapid ability to penetrate the plasma membrane (Mancardi *et al*., 2009; Wagner *et al*., 2009). It is found naturally in the environment as a result of anaerobic metabolism of organic substrates and is particularly concentrated in swamps and sewers (Stein and Bailey, 2013). Conversely H_2S is also produced naturally through inorganic reactions that occur in volcanic gases and well waters (Bates *et al*., 2002). It has also been found to be present in mammalian cells.

1.2.1 Discovery of H_2S as a Gasotransmitter

The discovery that endogenous H_2S could be produced in mammals (Stipanuk and Beck, 1982), together with the presence of the relatively high concentrations of H_2S in the brain (Goodwin *et al*., 1989), led to the original experiments which revealed that H_2S exists as an endogenous neuromodulator (Abe and Kimura, 1996). In their studies, Abe and Kimura provided evidence for a selective enhancement of N-methyl-D-aspartate (NMDA) receptor-mediated responses by H_2S; this was consequently shown to facilitate the induction of hippocampal long-term potentiation (LTP) (Abe and Kimura, 1996). Hippocampal LTP is known to be an important mechanism in the formation of memories. These findings sparked a growing field of research into this small gaseous molecule, with the ensuing publications confirming the importance of H_2S as a key biologically relevant signalling molecule (Hosoki *et al*., 1997; K R Olson, 2011; Kenneth R Olson, 2011; Wang, 2012).

1.2.2 H_2S Chemistry

A brief discussion of the chemistry behind this gaseous compound will allow a greater understanding of its role in biological systems. H_2S has a molecular weight of 34 grams per mole, and a boiling point of -60.2 °C, which renders it a gas at room temperature and pressure. At very low concentrations it has the characteristic smell of 'rotten eggs', this changes to a 'sickeningly sweet' smell at 30 parts per million (ppm), however the ability to smell it is then dulled at 50 ppm and completely lost at 100 ppm (Kenneth R Olson, 2011). The sulphur atom in H_2S contains two lone pair of electrons which render H_2S a polar molecule; this thus allows it to be dissolved in aqueous solutions with a solubility of around 80 - 110 mM at 37 °C. During dissolution it is thought to form equilibrium between three species dissolved hydrogen sulfide, hydrogen sulfide anions (HS^-) and sulfide anions (S^{2-}) (for simplicity water has not directly been shown in the equation):

$$H_2S_{aq} \overset{1}{\leftrightarrow} HS^- + H^+ \overset{2}{\leftrightarrow} S^{2-} + H^+$$

The pK_a for the first and second steps in the equation above are $pK_{a1} = 6.9$ and $pK_{a2} = 11$. Hence at the pH of 7.4, HS^- predominates in a ratio of approximately 3:1 relative to H_2S, with minimal amounts of S^{2-} also present (Olson, 2012; Kashfi and Olson, 2013; Zhao *et al*., 2014). It is not fully understood which of the three species (if not all) is the active form in biological systems, hence all three are inferred to when making reference to H_2S in biological experiments (Kashfi and Olson, 2013).

1.2.3 H_2S Metabolism

It has been known for over three-decades that the human body contained enzymes that were capable of producing H_2S (Figure 1). However, the synthesis of H_2S was thought to simply represent a by-product of two constitutively expressed enzymes involved in the metabolism of cysteine; cystathionine gamma-lyase (CSE) and cystathionine beta-synthase (CBS) (Fago *et al*., 2012). The true significance of the synthesis of H_2S only became apparent after its endogenous role in biological systems was reported by Abe and Kimura (Abe and Kimura, 1996). Both CBS and CSE are present in various tissues

in the body including the vascular endothelium, pulmonary smooth muscle cells (SMC) and fibroblasts, but they are also found in the plasma where they have a role in generating H_2S from cysteine and/or homocysteine (Chen and Wang, 2012; Kimura, 2014). However, in contrast to CSE, CBS possesses a haem domain which allows CBS to have additional functionality as a redox sensor as well as providing a mechanism for cross-talk between the three gasotransmitter systems as NO and CO are able to bind to the haem domain and inhibit CBS activity (Puranik *et al.*, 2006). There is evidence now emerging for the presence of novel endogenous pathways involved in the synthesis of H_2S (Kimura, 2014; Wallace and Wang, 2015). One such mechanism is through the actions of the enzymes cysteine aminotransferase (CAT) and 3-mercaptopyruvate sulfurtransferase (3-MST), which in a multi-step reaction lead to the production of H_2S from cysteine.

The therapeutic properties of sulphurous compounds have been known about for centuries, this is evidenced by the reported health benefits attributed to the consumption of garlic, or bathing in sulphur springs (Prandelli *et al.*, 2013). On the other hand, it has also been known that exposure to high concentrations of H_2S can be fatal (Kamijo *et al.*, 2013). H_2S is the second leading cause of gas-related fatalities in the workplace, but it has also been used in acts of suicide (Olson, 2011; Kamijo *et al*., 2013). The principal mechanism underlying this toxic effect is thought to involve the inhibition of cytochrome-c oxidase in the mitochondrial electron transport chain; although this still remains controversial (Dorman *et al*., 2002; Olson, 2011). Due to the toxic nature of high concentrations of H_2S, the body has developed tight regulatory systems to maintain levels of H_2S within a physiological range. In mammals sub-lethal concentrations of H_2S are rapidly oxidised to sulphate by mitochondrial enzymes and excreted in the urine (Predmore *et al.*, 2012). Three enzymes are involved in this mitochondrial process; a membrane-bound sulfide:quinone oxidoreductase, a sulphur dioxygenase in the mitochondrial matrix and a sulfurtransferase (Figure 1) (Predmore *et al.*, 2012). This oxidation occurs in the majority (if not all) of tissues which include the liver, lungs, kidney, and brain, but is particularly prominent in the colonic mucosa where large quantities of H_2S are generated by colonic bacteria (Kabil and Banerjee, 2010).

The clinical importance of regulating sulfide levels may be highlighted in the rare disease known as Ethylmalonic encephalopathy (EE). In EE there is an autosomal recessive deletion of the *ETHE1* gene that encodes a mitochondrial sulphur dioxygenase (Di Meo *et al.*, 2015). The ensuing syndrome is characterized by developmental delay, acrocyanosis, petechiae, together with chronic diarrhoea, and can be fatal in the first few years of life. Patients with this disease have elevated levels of urinary and tissue thiosulfate and H_2S (Di Meo *et al.*, 2015). Furthermore, symptomatic improvement occurs with metronidazole and N-acetylcysteine (NAC) treatment. Interestingly, it has been proposed that both of these drugs prevent the accumulation of toxic levels of H_2S (Viscomi *et al.*, 2010).

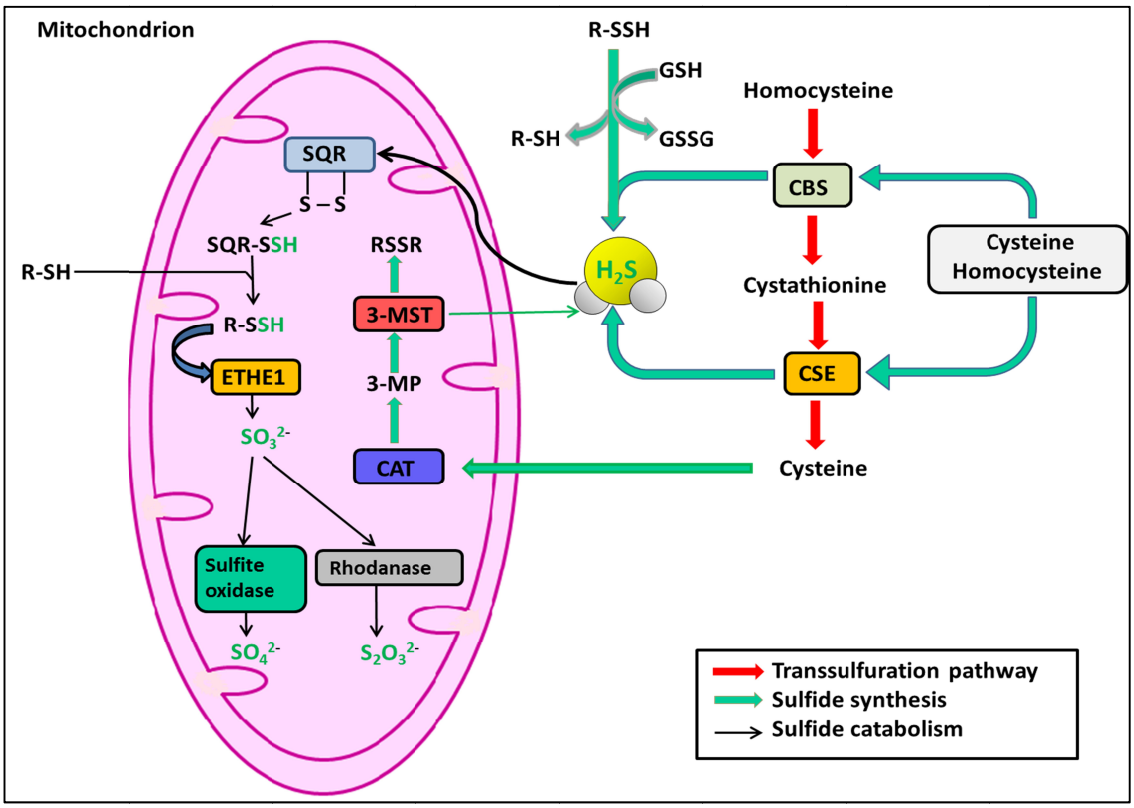

Figure 1: The metabolic pathways in the biosynthesis and degradation of H_2S. The H_2S synthesis pathway incorporates both sulfide synthesis (green arrows) and transulfuration pathways (red arrows). The enzymes cystathionine β synthase (CBS) and cystathionine γ-ligase (CSE) are capable of synthesising H_2S independently as well in tandem from homocysteine or cystathionine during the synthesis of cuysteine. Cysteine itself can be indirectly utilised in the production of H_2S via the novel pathway involving cysteine aminotransferase (CAT) which metabolises cysteine to 3-mercaptopyruvate (3-MP), this then undergoes further metabolism by 3-mercaptopyruvate sulfur transferase (3-MST, in the presence of thioredoxin which is not shown) to produce H_2S. The oxidation of reduced glutathione (GSH) to the oxidised glutathione disulfide (GSSG) can also synthesise H_2S via persulfide (R-SSH). The H_2S degradation pathway occurs in the mitochondria through the sulfur:quinone oxidoreductase enzyme (SQR) which generates a persulfide, this combines with a thiol group (R-SH) and is further oxidised by the persulfide dioxygenase (ETHE1) to sulfite (SO_3^{2-}). The sulfite is eventually converted to thiosulfate ($S_2O_3^{2-}$) and sulfate (SO_4^{2-}) by rhodanase and sulfite oxidase, respectively. Adapted from Yuan *et al.*, 2015.

1.2.4 The Role Hydrogen Sulfide in Physiology and Disease

The recent explosion in the published literature on H_2S has provided a plethora of evidence which indicates that this gasotransmitter affects virtually every organ system (Olson, 2013). Thus, it is not surprising that an increasing number of physiological and pathological processes are thought to be related to alterations in the synthesis of H_2S (full reviews and detailed references in Olson, 2011; Wang, 2012). The effects of H_2S in normal physiology as well as pathophysiology are too complex to delineate it simply in a binary manner as a 'good' or 'bad' molecule, thus its effects will be examined by looking at two of the major organ systems that relate to this thesis, with a specific focus on the respiratory system.

1.2.4.1 Pulmonary System

The gross effects of H_2S on the human pulmonary system are evident from the toxic effects observed when increasingly high concentrations of H_2S are inhaled. An exposure to 300 ppm of H_2S causes respiratory complications such as pulmonary oedema, however becomes acutely lethal at 1000 ppm (Zhao *et al*., 2014). Indeed, what is becoming increasingly recognised are the vast number of more subtle effects this gasotransmitter has on the respiratory system. Moreover, one of the most profound physiological roles that H_2S has been postulated to play is as a key molecule involved in sensing oxygen (Olson, 2011; Kashfi and Olson, 2013).

1.2.4.1.1 Oxygen Sensing

The dependence of eukaryotes on oxygen to sustain life renders it highly likely that complex organisms such as mammals must have a mechanism to detect the presence of oxygen in order to institute states of adaptation during hypoxia. The molecular mechanism underlying the detection of hypoxia is not fully understood, but there are several lines of evidence pointing towards H_2S representing the foundation of the eukaryote oxygen sensing/transduction mechanism (Olson *et al.*, 2010; Kimura, 2013;

Olson, 2013). The Olson group have shown treatment with hypoxia or H_2S produce temporally and quantitatively identical responses in the vasculature of several different vertebrate species (Olson, 2011). They have also shown that the inhibition of H_2S synthesis in these vessels prevents the hypoxic response. In contrast, the addition of cysteine augmented the effects of H_2S (Olson *et al.*, 2006). Others groups have also provided data showing the important role of H_2S in mediating oxygen sensing in the mammalian carotid body (Peng *et al*., 2010). Alterations in the levels of H_2S do not only affect the pulmonary vasculature but also the airways. Pre-contracted murine and porcine bronchi have been shown to relax in the presence of H_2S through a mechanism that is independent of cyclooxygenases, soluble guanylyl cyclase and adenosine triphosphate (ATP) dependent potassium (K_{ATP}) channels *(Kubo et al.*, 2007; *Chen et al., 2009*). However there is conflicting evidence that questions the theory that H_2S is an O_2 sensor, for example a reduction in the partial pressure of oxygen in the pulmonary circulation does not necessarily lead to an increase in H_2S levels (Wallace and Wang, 2015). Although the importance of H_2S as an oxygen sensor remains inconclusive, the increasing literature on the effects of H_2S in the lungs does highlight the importance of this gasotransmitter in pulmonary physiology.

1.2.4.1.2 Pulmonary Diseases

Variations in levels of H_2S have also been implicated in acute and chronic pulmonary pathologies such as acute lung injury, asthma, chronic obstructive pulmonary disease (COPD), and pulmonary fibrosis (Chen and Wang, 2012). In acute lung injury exogenous H_2S was found to improve the arterial oxygenation and attenuate the inflammatory response (Li *et al.*, 2008; Chen *et al.*, 2009). The latter was observed through a reduction in the polymorphonuclear leukocytes, interleukins 6 and 8 as well as reduced activation of inducible nitric oxide synthetase (Li *et al.*, 2008; Chen *et al.*, 2009).

1.2.4.1.3 COPD

COPD is a chronic inflammatory condition which consists of progressive airway obstruction, mucus hypersecretion, and lung destruction (Decramer *et al.*, 2012). It is the fourth leading cause of death worldwide, with smoking as the predominant risk factor (Dekhuijzen and van Beurden, 2006; Decramer *et al*., 2012). The pathogenesis of this pulmonary inflammatory condition is not completely understood, however there is an increasing body of evidence to suggest H_2S may play a role in this disease (Chen and Wang, 2012). For example, it has been found that smokers with COPD have a significantly lower level of serum H_2S compared to control patients who do not have COPD or smoke (Chen *et al.*, 2005). Furthermore patients with an acute exacerbation of COPD have also been shown to have significantly lower levels of serum H_2S relative to patients with stable COPD (Chen *et al.*, 2005). Newer data have led to the proposal that the sputum-to-serum ratio of H_2S can serve as a useful marker of disease severity as well as subtype in COPD, and could help guide treatment (Saito *et al*., 2014). Furthermore, rodent models of chronic cigarette-smoke exposure have shown that increased endogenous H_2S levels were associated with an anti-inflammatory and bronchodilatory effect (Chen *et al.*, 2011). Consistent with this, the administration exogenous H_2S donors induced a reduction in several markers of airway inflammation such as airway reactivity, the thickness of bronchial walls, the amount of pulmonary inflammatory cells and pro-inflammatory cytokines (Chen *et al.*, 2011; Han *et al.*, 2011). Consequently there was a reduction in certain cardiovascular sequelae of this condition such as pulmonary hypertension (Chen *et al.*, 2011; Han *et al.*, 2011). In humans, the progression of COPD results in the development of chronic hypoxia and pulmonary hypertension; both of which have also been associated with a reduction in the plasma and lung tissue production of H_2S (Qingyou *et al.*, 2004). Furthermore, pulmonary hypertension has been shown to be potentiated by inhibitors of H_2S synthesis and reduced with exogenous H_2S (Chunyu *et al.*, 2003; Qingyou *et al*., 2004; Olson, 2011).

1.2.4.1.4 Asthma

Asthma is another chronic inflammatory condition of the airways. It affects over 330 million people worldwide, making it one of the most common diseases in the world (Martinez and Vercelli, 2013; Beasley *et al.*, 2015). It has a complex multicellular pathology characterised by the infiltration of inflammatory cells such as eosinophils, basophils, mast cells and CD4+ T-helper cells into the airway submucosa. This then leads to mucus hypersecretion, airway wall remodelling, airway hyper-responsiveness, and in severe disease, airway fibrosis (Martinez and Vercelli, 2013; Chung, 2015). Patients with stable asthma have been shown to have lower levels of serum H_2S compared to non-asthmatics, with the levels declining further during an acute exacerbation of the asthma (Wu *et al*., 2008). In a rodent model of asthma, treatment with donors of H_2S attenuated the pathological remodelling observed in this disease; this included goblet cell hyperplasia (mucus secreting cells), collagen deposition, and infiltration by eosinophils and neutrophils (Chen *et al.*, 2009). It also improved the peak expiratory flow rate (Chen *et al.*, 2009). Furthermore rodent models of asthma have also shown that there is a decrease in amount of plasma H_2S, as well as CSE and CBS messenger RNA in the lung tissues (Li *et al.*, 2010). The latter increased with corticosteroid therapy (Li *et al.*, 2010); this is the mainstay of long-term asthma management through its prevention of disease progression.

1.2.4.1.5 Pulmonary Fibrosis

Pulmonary fibrosis is a respiratory condition characterised by the accumulation of excess fibrous tissue in the lung in response to known or unknown triggers, with the latter referred to as idiopathic pulmonary fibrosis (IPF) (Datta *et al.*, 2011). This causes a distorted alveolar architecture that is associated with a progressive decline in gaseous exchange, as well as pulmonary function, and ultimately culminates with death. The histological hallmark consists of fibrotic foci with excessive collagen deposition and matrix remodelling (Hoo and Whyte, 2012). The pathogenesis of this process is not fully understood, but is thought to involve epithelial micro-injuries which then lead to the development of the fibroblastic foci with the process mediated by cytokines such as platelet-derived growth, epidermal growth factor, insulin-like growth factor-1, fibroblast

growth factor-2, and Transforming growth factor-β1 (Fang *et al*., 2010; Datta *et al*., 2011; Hoo and Whyte, 2012).

There is increasing evidence for the role of H_2S in models of pulmonary inflammation and fibrosis (Yanfei *et al.*, 2006). Fang *et al*. (2009) have published data on the anti-fibrotic effect of H_2S (50 – 500 μM) on the FCS induced migration and proliferation of the foetal lung fibroblast-like cell line MRC-5. Others have shown a pro-apoptotic effect of NaHS/H_2S on the non-primary human fibroblasts (Baskar *et al.*, 2007). The Fang group have also reported that H_2S was shown to prevent the epithelial to mesenchymal transition (EMT) in the human epithelial carcinoma cell line A549 (Fang *et al.*, 2010). EMT is being increasingly realised as another mechanism through which cells from a non-mesenchymal lineage can transition to produce myofibroblasts. In contrast, myofibroblasts have classically been thought to derive from transformed fibroblasts, and are believed to play a major role in the fibrotic process in disorders such as IPF (Hoo and Whyte, 2012). As airway smooth muscle myocytes have been shown to express both CSE and CBS (Perry *et al.*, 2013), it is postulated that they may be capable of modulating local H_2S levels, this would thus prevent the transition of cells to myofibroblasts and inhibit the fibrotic process.

1.2.4.2 Cardiovascular System

This system is closely associated with the respiratory system, and underlies some of the therapeutic effects of H_2S in the sequelae of pulmonary pathologies such as the pulmonary hypertension that can be observed in the latter stages of COPD. However the effects of H_2S on the heart and vessels also have implications in several other disease processes, for example H_2S has been found to be beneficial in ischaemic reperfusion injury (IRI) (Elrod *et al.*, 2007). IRI is a process that can occur during the reperfusion of the cardiac myocardium after a period of ischemia. During this process the reperfusion with blood induces a release of reactive oxygen species (ROS) that subsequently promote cell death; this propagates the tissue injury caused by the initial ischaemia (Elrod *et al*., 2007). The cardioprotective role of H_2S in IRI is thought to involve the activation of K_{ATP} channels and the upregulation of genes encoding antioxidant proteins (Salloum, 2015). Another beneficial effect of H_2S in this circumstance is through the reduction in myocardial work due to its negative inotropic and chronotropic effects (Predmore *et al*., 2012). H_2S has also been shown to have pro-angiogenic effects that are mediated through an elevation in the levels of vascular endothelial growth factor (VEGF), and this was found to mitigate the progression from compensatory cardiac hypertrophy to heart failure (Givvimani *et al*., 2011). The favourable effects of H_2S in the cardiovascular diseases such as atherosclerosis are also thought to occur through the consumption of homocysteine during the production of H_2S. Homocysteine is an amino acid associated with endothelial injury, with raised levels observed in atherosclerosis (McCully, 1996). An additional mechanism involved in the H_2S mediated reduction in homocysteine could be through the ability of H_2S to provide direct vascular endothelial protection from oxidative stress (Mancardi *et al*., 2009).

H_2S has been repeatedly shown to consistently produce vasodilatory effects on both systemic and pulmonary vasculature (Hosoki *et al.*, 1997; Olson, 2011). The predominant mechanism that underpins these vasodilatory effects involve extracellular calcium (Ca^{2+}) as well as K_{ATP} channels, however is independent of the normal vasodilators such as nitric oxide, prostacyclin, superoxide or hydrogen peroxide (Olson, 2011). In addition, H_2S has been found to inhibit the activity of renin, an enzyme which is involved in the production of the potent vasoconstrictor angiotensin II (Lu *et al*., 2010). The reduction in the production of angiotensin II together with the direct

vasodilatory effects of H_2S may in part underlie the profound hypotension observed in patients with septic shock. An indirect effect of H_2S on the vascular system has also been reported in type I diabetes; here an inappropriate H_2S mediated regulation of insulin secretion has been associated with the development of micro- and macrovascular complications (Brancaleone *et al*., 2008).

The beneficial effects of H_2S on the cardiovascular system have led to clinical trials aimed at reducing myocardial injury using the first generation of H_2S donating drugs (ClinicalTrials.gov identifiers: NCT01007461 and NCT00858936). Unfortunately the trials were terminated early without any published explanation or results. It may be postulated that reasons behind an early trial termination was that the first generation of H_2S donors were ineffective and/or toxic as a result of a poorer understanding of their properties *in vivo;* this will be discussed later. Such events do identify a greater need to further explore both the H_2S system as well as the current H_2S donating compounds in order to develop improved H_2S based treatments in the future.

1.2.4.3 Metabolic

The first major publication on the effects of H_2S on a whole organism was presented in Blackstone *et al*. in 2005. This team provided evidence for the role of H_2S in reducing the murine metabolic rate which in effect allowed the mice to enter a state of hibernation. During this state there was a significant reduction in the core body temperature and oxygen consumption (Blackstone *et al*., 2005). Upon removal of the exogenous H_2S the mice returned to their pre-treatment physiological state, and displayed no alterations in their behaviour. This has opened up the possibility of using H_2S based therapies in states of potentially fatal hypoxaemia for example acute respiratory distress syndrome or septic shock. Drugs based on these principles are still undergoing development, however there has been some work investigating the effects of administrating low concentrations (<5 ppm) of H_2S gas in healthy human volunteers. These studies found that the inhalation of H_2S gas caused an increase oxygen uptake, reduction in carbon dioxide excretion and an increase lactate production, which when taken together suggests that H_2S was uncoupling oxidative respiration.(Bhambhani and

Singh, 1991; Bhambhani *et al.*, 1996). It would be anticipated that such an uncoupling would alter the bioenergetics of cells and thus affect their physiological properties including their ability to grow (O'Brien and Vetter, 1990).

1.2.4.4 H_2S concentrations in vivo

One of the major challenges with understanding the physiology of H_2S has been to precisely measure the concentrations of H_2S present *in vivo* as well as in experimental models. Several different methods have been developed to achieve this including assays utilising methylene blue or monobromobimane, ion selective electrodes or gas chromatography (Wang, 2012). All of these can be difficult to perform with precision and accuracy, and dynamic measurements are hampered by destruction of samples during the assays (Nagy *et al*., 2014; Zhao *et al*., 2014). Due to these problems, it is unclear what the exact levels of H_2S are at various sites, however in mammalian blood the concentration of H_2S is estimated to be within the high nanomolar to micromolar range, with this depending on the state of the sulphur atom i.e. gaseous or bound sulfide (Furne *et al*., 2008; Wang, 2012). One reason as to why H_2S is found freely present in blood is due to its increased stability in biological systems compared with other gasotransmitters such as NO (Wallace and Wang, 2015). Furthermore, the tissue concentrations of H_2S are believed to be even higher than those observed in the blood, with a site-specific variability in levels (Olson *et al*., 2014).

1.2.5 Current H_2S Based Therapies

The aforementioned perturbations in the levels of H_2S have been shown to play an important role in many organ systems during normal physiology and disease (Szabó, 2007). This provides the foundation for the development of H_2S based therapies to modulate and/or treat conditions affecting each of these organ systems, as well as systemic disorders such as sepsis (Zhong *et al*., 2003; Mok *et al.*, 2004; Bhatia *et al.*, 2005).

The H_2S based treatments that are known to have been studied so far, include the administration of the gaseous H_2S (Bhambhani and Singh, 1991; Bhambhani *et al*., 1996; Fiedler *et al.*, 2008), simple sulphur salts such as sodium sulfide (Na_2S) to healthy human volunteers (Toombs *et al*., 2010), the simple addition of a H_2S donating moiety to well-known drugs in order to augment the therapeutic profiles (Bhatia *et al.*, 2008; Frantzias *et al.*, 2012), or finally the synthesis of completely novel H_2S donating drugs (Li *et al.*, 2008; Meng *et al.*, 2015).

The simple addition of an H_2S donating moiety to a known medication has led to the development of drugs such as S-aspirin (ACS14), S-diclofenac (ACS15), and naproxen (ATB-346) which are based on aspirin and the non-steroidal anti-inflammatory drugs (NSAIDs) diclofenac and naproxen respectively. The purpose of the added H_2S moiety is to ameliorate the serious gastrointestinal (GI) side effects of NSAIDs which include fatal GI ulceration (Frantzias *et al*., 2012; Wallace *et al*., 2015). NSAID based therapies have been the current focus of pharmaceutical research into H_2S donating drugs, with ATB-346 undergoing development as a treatment for osteoarthritis. This drug has recently completed a Phase I clinical trial with no notable adverse events reported (Wallace and Wang, 2015). Another H_2S donating drug is a derivative of sildenafil resulting in the compound ACS6 which has been postulated to be effective in the treatment of acute respiratory distress syndrome (Kashfi and Olson, 2013; Bos *et al*., 2014). One may speculate that the aforementioned anti-inflammatory together with antioxidant effects of H_2S underlie its therapeutic action in this case. It would be very exciting to see if ACS6 is shown to be beneficial in pulmonary diseases particularly during the more advanced stages when pulmonary hypertension begins to develop. This would be even more fascinating given that sildenafil has been licensed in the treatment of pulmonary hypertension (Channick *et al.*, 2013).

There are other putative H_2S-based therapies on the horizon, for example the novel synthetic compound GYY4137 (morpholin-4-ium 4 methoxyphenyl (morpholino) phosphinodithioate) has shown promise in reducing bacterial lipopolysaccharide (LPS) induced pulmonary inflammation in rodents (Li *et al*., 2009), and has been found to have anti-proliferative properties in various malignancies both *in vitro* and *in vivo* (Szabó, 2007). This compound is of increasing interest due to its ability to slowly

release H_2S (Li *et al*., 2008). Another new group of compounds that have received a patent (WO2013045951 A1) are the H_2S donating drugs that specifically target the mitochondria, these are postulated to have a role in the treatment of disorders such as hypertension, haemorrhagic shock, as well as in conditions characterised by inflammation and oedema (Szczesny *et al.*, 2014).

The range of H_2S based drugs undergoing clinical trials together with the far reaching effects this molecule has on organ systems provides an exciting opportunity for treatments for several condition in the future including those affecting the respiratory and cardiovascular systems. However the fact that H_2S is known to be fatal at higher concentrations necessitates high quality drug development to ensure the compounds can release H_2S in a stable and regulated manner. Moreover, there is an increasing need to explore further the molecular effects of H_2S in biological systems. The therapeutic and toxic roles of H_2S are eloquently summarised by Paracelsus, "Poison is in everything, and no thing is without poison. The dosage makes it either a poison or a remedy".

1.2.6 Putative molecular mechanisms of action of H_2S

As H_2S is studied in greater depth, a more thorough understanding of its putative mechanisms of action are being gained. There are a growing number of receptors that are now thought to be under the direct or indirect influence of H_2S, with many of these proteins belonging to the ion channel receptor superfamily. The K_{ATP} channel was identified as one of the first direct molecular targets for the cellular effects of H_2S (Reiffenstein *et al*., 1992). This receptor is thought to mediates the vasodilatory properties of H_2S in the cardiovascular, respiratory, nervous and GI systems (Chen *et al*., 2012; Fernandes *et al.*, 2013). Other molecular targets include voltage-gated sodium $Na_v1.5$ channels (Wallace and Wang, 2015), calcium channels such as the T-type voltage gated calcium channel $Ca_v3.2$ (Okubo *et al*., 2012), and the Transient Receptor Potential (TRP) channels TRPV1 and TRPA1 (Streng *et al*., 2008; Miyamoto *et al.*, 2011; Andersson *et al.*, 2012; Ogawa *et al.*, 2012).

1.3 Ion Channels

Ion channels are pore-forming membrane proteins that have an intrinsic membrane spanning channel which can be opened and closed in response to different stimuli. They can be activated by a ligand such as glutamate as in the NMDA receptors, or by changes in the transmembrane potential as observed with $Ca_v3.2$. The selectivity of the pore to various ions is determined by the structure of the pore forming domain and the associated protein linker regions, together these form the selectivity filter (Jiang *et al.*, 2003). This selective permeability coupled with the variation in the number and types of ion channels present within the membranes of the cells, allows cells to establish and control the electrochemical gradients across their plasma and intracellular membranes. Upon channel activation, such electrochemical gradients drive the passage of the ions through the pore which then activate intracellular signalling cascades that mediate the ensuing cellular response. The response can range from the secretion of hormones to cell proliferation or death.

1.3.1 Transient Receptor Potential Channels

The TRP channels are a large family of predominantly non-selective cation channels that are found in a variety of species from the common fruit-fly (*Drosophila melanogaster)* where they were first identified, to mammals (Kaneko and Szallasi, 2014). The mammalian TRP family consists of at least 28 members that are divided into six sub-families based on sequence homology; TRPV (vanilloid), TRPM (melastatin), TRPA (ankyrin), TRPC (canonical), TRPP (polycystin) and TRPML (mucolipin). The TRP proteins are predominantly located on the plasma membrane as homomeric tetramers. Each monomer consists of six transmembrane spanning domains (Figure 2), with the pore-forming loop present between the fifth and sixth segments (Wu *et al.*, 2010). These channels are involved in a vast number of physiological processes from sensory receptors to hormone secretion and development (Wu *et al.*, 2010). They can be activated by a variety of stimuli which include ligands such as capsaicin or allyl isothiocyanate which are respectively found in chillies and garlic, changes in temperature or osmolarity, depletion of intracellular Ca^{2+} stores, intracellular secondary messengers, as well as physical stimuli such as stretch and shear stress (Di and Malik, 2010; Pedersen *et al*., 2005).

1.3.2 TRPA1

The distinguishing feature of the TRPA family is the presence of 14–16 N-terminal ankyrin repeats which are postulated to allow mechano-sensation (Wu *et al.*, 2010). The TRPA1 channel itself is unique to the TRPA channels as it is the only one found to be present in mammals, whereas the other members are also present in insects (Wu *et al.*, 2010). The TRPA1 channel is found in the vagal sensory nerves of the airways, trigeminal nerves, and dorsal root ganglion (DRG), which is consistent with the postulated role of the TRPA1 receptor in inflammation and bronchoconstriction (Caceres *et al.,* 2009; Banner *et al.,* 2011). Furthermore, the reported activation of these receptors by the pungent ingredients in wasabi (isothiocyanates), garlic (allicin), cinnamon (cinnamaldehyde), cloves (eugenol), and ginger (gingerol) may explain how these compounds are detected by the human respiratory sensory pathways and thus elicit a physiological response to these ingredients (Jordt *et al*., 2004; Bautista *et al.*, 2006; Hinman *et al.*, 2006; Louhivuori *et al.*, 2009; Geppetti *et al.*, 2010). The detection of such compounds many of which contain sulphur may also play an important role in detecting H_2S and thus underlie the respiratory irritation caused by increasing concentrations of inhaled H_2S. Accordingly, there is accumulating evidence to show that H_2S can directly activate these receptors (Andersson *et al.*, 2012; Ogawa *et al.*, 2012). Consequently it has been postulated that the TRPA1 receptor may serve as an integrator in certain neuro-inflammatory processes found in diseases such as COPD and asthma (Caceres *et al*., 2009; Jha *et al*., 2015; Raemdonck *et al*., 2012).

The aforementioned chemical stimuli of TRPA1 have been shown to interact with the protein at various different sites (Deering-Rice *et al*., 2015; Laursen *et al.*, 2015). A significant number of ligands are believed to activate the receptor through covalent modifications at critical cysteine residues on the N-terminus (Hinman *et al*., 2006; Macpherson *et al*., 2007; Sadofsky *et al.*, 2011). These modifications result in a conformational change in the TRPA1 channel which opens the pore and allows a flux of cations in particular Ca^{2+} through the channel (Wang *et al.*, 2012). Similarly H_2S is also thought to stimulate the TRPA1 receptor through such covalent interactions with critical cysteine residues (Ogawa *et al.*, 2012; Takahashi *et al.*, 2012). However in sensory trigeminal neurones, a novel indirect mechanism has been proposed whereby H_2S first reacts with NO to produce nitrosothiols that then activate TRPA1 (Wild *et al.*, 2015).

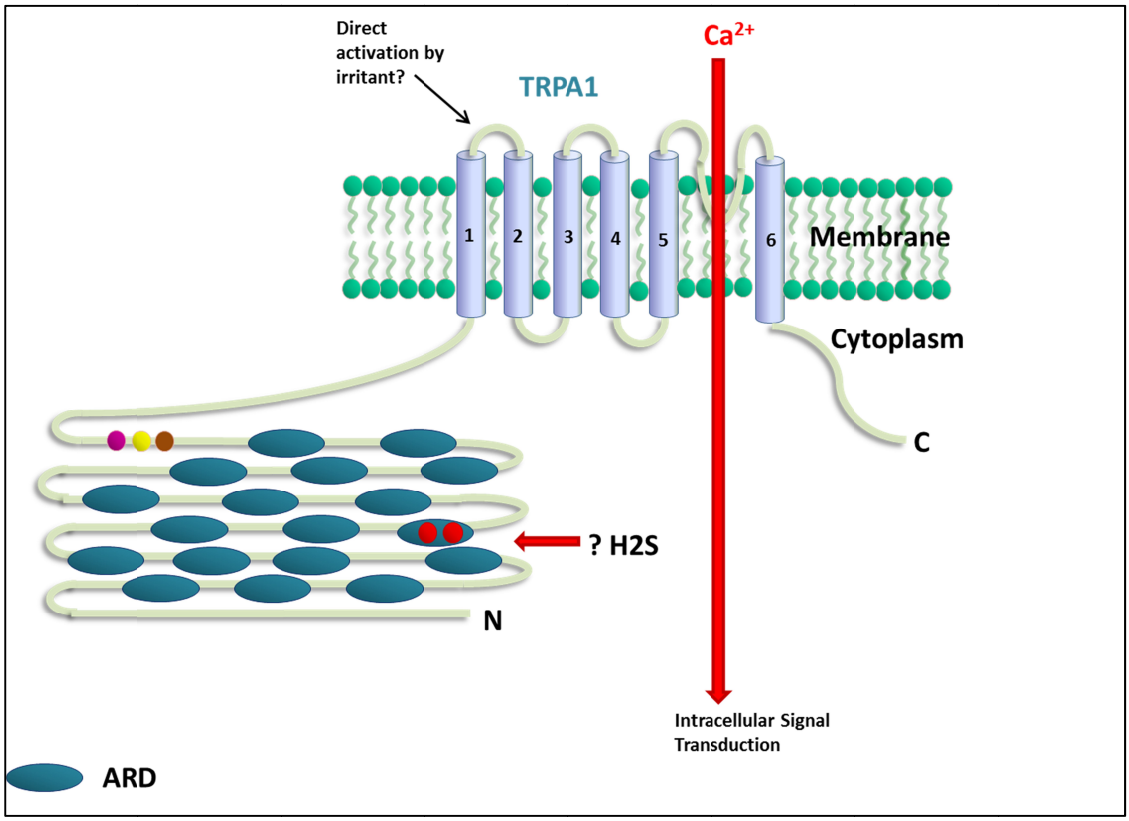

Figure 2: Schematic showing the structure of the TRPA1 receptor together with the typical ankyrin repeat domain (ARD). Also highlighted are the important cysteine residues that are thought to be involved in the channel activation through covalent bonds with sulphurous compounds and may represent the candidate H_2S binding site. Adapted from Macpherson *et al.*, 2007.

1.3.3 TRPV1

The TRPV family of channels has six members that are activated by vanilloids, noxious stimuli, ROS, heat and low pH (Wu *et al.*, 2010; Nishio *et al.*, 2013). Receptor activation results in the opening of the non-selective cation pore which is permeable to Ca^{2+}, Mg^{2+}, Na^{+}, and K^{+} (Geppetti *et al.*, 2006) The response to such stimuli allows these channels to function as nociceptors in the trigeminal and vagal nerves, the dorsal root ganglia, as well as in non-neuronal tissue (Weller *et al.*, 2011; Baxter *et al.*, 2014). The TRPV1 receptors have been implicated in the pathogenesis of chronic cough, pain, and airway inflammation (Geppetti *et al.*, 2006; Sadofsky *et al.*, 2008; Baxter *et al.*, 2014; Ruan *et al.*, 2014). Interestingly, in patients with refractory asthma recent studies suggest there is an upregulation of TRPV1 receptors which may be contributing to the observed airway hyper-responsiveness (McGarvey *et al., 2014*). TRPV1 has also been identified as a molecular target of H_2S and thus could mediate some of the cellular responses of this gasotransmitter (Trevisani *et al.*, 2005; Takahashi *et al.*, 2012).

1.3.4 Inflammation and TRP Channels in Bronchi

As mentioned earlier, pulmonary fibroblasts have been shown to play an important role in the pathophysiology of airway diseases such as asthma, COPD and IPF. However the comprehensive mechanism underlying fibroblast activation in such disorders is not completely understood. It is becoming increasingly evident that human bronchial fibroblasts undergo changes in their membrane receptor repertoire following stimulation by inflammatory mediators such as Tumour Necrosis Factor α (TNFα) and Interleukin-1α (IL-1α) (Sadofsky *et al.*, 2012). These changes include the up-regulation TRPV1 which is subsequently stimulated by noxious stimuli such as capsaicin, protons, and high temperatures; all of these factors that are present during inflammation *(Mitchell et al.*, 2005; Sadofsky *et al*., 2012). Both TRPV1 and TRPA1 receptors that are present on non-neuronal airway cells are then able to facilitate the release of further inflammatory mediators such as prostaglandins and interleukins (Geppetti *et al.*, 2010; Nassini *et al.*, 2012a). Hence TRPA1 and TRPV1 do not only act as sensors of noxious stimuli but also modulate the ensuing inflammatory response (Sadofsky *et al.*, 2012; Baxter *et al.*, 2014; Kichko *et al.*, 2015). As further evidence is emerging, it is becoming evident that TRPA1 may in fact dominate over TRPV1 in mediating the airway hyper-responsiveness, this is achieved through the induction of both neurogenic and non-neurogenic inflammation in the airways in response to airway irritants (Nassini *et al.*, 2012b). The findings of the importance of airway inflammation in the pathogenesis of asthma and COPD, together with the effects of H_2S in these disorders as well as on TRP channels, have led to the hypothesis that TRP channels may mediate some of the effects of H_2S in acute and chronic inflammatory lung conditions including acute lung injury, asthma and COPD (Geppetti *et al*., 2006; Ang *et al*., 2011; Takahashi *et al.*, 2012).

1.4 Cell Growth and Mechanisms Altering Growth

The inflammatory process is a complex active process involving cell recruitment, activation, differentiation and death. Cellular survival is determined by a delicate equilibrium between differentiation, proliferation, and death with a perturbation in any of these processes leading to cellular dysfunction and disease. A more detailed discussion of the normal cell cycle is provided in chapter four.

1.4.1 Hydrogen Sulfide and Cell Survival

There is increasing evidence for the diverse activity of H_2S in cellular function and survival *(*Yang *et al.,* 2004*;* Guang-dong and Wang*,* 2007*;* Baskar *et al.,* 2008*;* Tyagi *et al*., 2009; Yang, 2011). Depending on the circumstances, it can act as a mitogen and inhibitor of cell proliferation or as a promoter of apoptosis (Guang-Dong and Wang, 2007). The effects of H_2S on cell survival appear to be cell-selective with certain malignant cells entering pro-apoptotic stage (Chattopadhyay *et al*., 2012; Frantzias *et al.*, 2012), whereas in other cells a pro-proliferative state is activated (Szabo *et al.*, 2013). These complex effects of H_2S do not appear to only be cell specific but the effects also vary depending on the concentration of H_2S present; low micromolar concentrations (10-20 μM) have been shown to promote angiogenesis whereas at higher concentrations (≥200 μM) such effects are lost (Yang, 2011). Pro-angiogenic effects of H_2S are also witnessed in rodent models of inflammation, where knocking out CSE and thus reducing H_2S delayed wound healing through a mechanism postulated to involve the K_{ATP} channel/MAPK pathway (Papapetropoulos *et al.*, 2009; Szabó and Papapetropoulos, 2011).

The concentration dependent dual effects of H_2S on angiogenesis are also mirrored in models of oxidative stress, where pre-treatment with 50-100 μM NaHS provided cytoprotection, but concentrations above 250 μM caused cytotoxicity (Tyagi *et al*., 2009). Such cytoprotective effects have been observed in cell and tissue types ranging from cardiac myocytes and airway smooth muscle cells to neuroblastoma cell lines (Yang, 2011). The effects get even more complex as the Szabo group have recently

reported a pro-proliferative effect of tumour-derived H_2S which was only evident with H_2S synthesised from CBS rather than CSE (Szabo *et al*., 2013). Thus, the differences in the effects of H_2S on cell survival appear to depend on the concentration applied, the tissue type as well as the environment within which H_2S is added.

1.5 Clinical Relevance of Study

Patients with chronic respiratory conditions such as asthma and COPD routinely undergo surgery; this can either be performed under general, regional or local anaesthesia. A concern when anaesthetising patients with such airway pathologies particularly those with the more severe forms, is the respiratory reserve these patients possess to cope with the effects of a general anaesthetic (GA). This concern is amplified when the surgery is prolonged or if the surgery involves significant lung resection for a pulmonary malignancy. Indeed the latter has a higher incidence in patients with COPD due to smoking which is a common risk factor to both (Brunelli *et al.,* 2008; Decramer *et al.,* 2012; Durham and Adcock, 2015). Moreover there is a concern that patients with minimal respiratory reserve may require a period of post-operative ventilatory support on the intensive care unit (ICU) (Linden *et al*., 2005; Brunelli *et al.*, 2008). Post-operative ventilation brings further risks to the patient including the complication of ventilator associated pneumonia (VAP). These factors increase the morbidity and mortality, prolong the stay of patients in ICU/hospital and significantly increases the cost of the healthcare episode (Nair and Niederman, 2015). Furthermore, those suffering from COPD have an increased risk of developing a VAP during their stay in ICU (Rouzé *et al*., 2014). It is important to highlight that a much more common source of referral of patients with COPD or other chronic respiratory conditions to ICU is during episodes of sepsis. At such times, the ICU clinician is frequently faced with the conundrum of whether it would be in the best interest of the patient to undergo invasive ventilation due to the associated poorer outcomes (Squadrone *et al*., 2004; Rouzé *et al*., 2014). Through studying the role of H_2S at the molecular and cellular level it is hoped that further treatments can be developed that can either retard the disease progression in chronic lung inflammatory conditions, or increase the range of therapies available in ICU for the treatment of significant hypoxia in pathological states such as acute respiratory distress syndrome.

During a GA the airway hyper-responsiveness present in patients with asthma and COPD is also a concern due to the difficulties experienced in ventilating such patients through episodes of severe bronchospasm. There are several acute bronchodilatory agents utilised in current clinical practice, these include beta-adrenergic receptor agonists and muscarinic acetylcholine receptors antagonists, whereas steroids are used to prevent the chronic inflammatory response (Decramer *et al.*, 2012; Martinez and Vercelli, 2013). H_2S is a newer agent that has been reported to have bronchodilatory properties in several different species (Fitzgerald *et al*., 2014; Huang *et al*., 2014; Rashid *et al.*, 2013). Preliminary unpublished experiments performed on human bronchi by the host research group have shown that H_2S also appears to have bronchodilatory effects.

Given the evidence that has been discussed, my hypothesis is that the H_2S mediates part of its effects on the respiratory system through the activation of the TRPA1 channel. One of these effects is the regulation of pulmonary fibroblasts during episodes of pulmonary inflammation. The aim of this project is to investigate the mechanisms of action of H_2S. The medium to long term value of such work would be in the development of novel treatments that could be translated to the clinic,and thus benefit patients with the aforementioned pulmonary conditions.

1.6 Aims

To investigate the effects of hydrogen sulfide on TRP channels as well as on human primary bronchial fibroblasts.

2.1. Materials and Reagents

Dulbeco's modified Eagle's medium (DMEM), foetal calf serum (FCS), trypsin EDTA and amphotericin B were purchased from Gibco (Paisley, UK). The antimicrobials penicillin G sodium and streptomycin sulphate, glutamine and fluo-3 acetoxymethyl ester (fluo-3 AM) were from Life Technologies (Paisley, UK). Fluo-3 pentammonium salt and geneticin were obtained from Santa Cruz biotechnology (Heidelberg, Germany). Sodium hydrosulfide (NaHS) was purchased from Acros Organics (Geel, Belgium). Allyl isothiocyanate (AITC), dimethyl sulphoxide (DMSO), tris(hydroxymethyl)aminomethane base (tris base), acetic acid, hydogren peroxide, and calcium chloride were bought from Fisher Scientific (Loughborough, UK). Basement membrane matrix (Matrigel) was procured from BD biosciences (Oxford, UK). All other reagents were from Sigma-Aldrich (Poole, UK).

2.1.1. Ligand Composition

Calcium Ionophore: The calcium ionophore A23187 dissolved in DMSO was used at a final concentration of 2 M as an experimental standard.

NaHS: A 1M solution of the H_2S donor NaHS was produced by dissolving NaHS (Sigma-Aldrich, UK) in deionised water. Serial dilutions were then performed with the deionised water to give the stock solutions with concentrations of 100 μM- 1 M NaHS. The concentrations utilised ranged from 100 nM to 1 mM of NaHS.

Capsaicin: The TRPV1 agonist capsaicin was used to confirm the presence of this receptor in the cell culture. Stock solutions of 1 and 25 mM capsaicin in DMSO were used to produce a final concentration of 1-25 μM.

Cinnamaldehyde: Stock solution of this TRPA1 agonist was produced using DMSO and applied at a final concentration of 40-400 μM.

Allyl Isothiocyanate (AITC): The stock solution of AITC a potent TRPA1 receptor agonist was produced using DMSO.

Hydrogen Peroxide (H_2O_2): Fresh stock solutions of H_2O_2 were diluted in water and produced on the day of experiment.

2.2. Fluorometric Calcium Assays: Direct NaHS Application

2.2.1. Transfected Human Embryonic Kidney 293 Cells

Human Embryonic Kidney-293 (HEK293) cells that had been previously transfected with human (h) TRP channels (A1 and V1) or with an empty plasmid vector (EV) were used (Morgan *et al.*, 2014). The host group had formerly characterised these transfected cells and channels to determine the presence of the operational TRP channel or EV (Sadofsky et al., 2011; Morgan *et al.*, 2014). Cultures of these cells had been previously frozen in a freezing mix (containing Foetal Calf Serum; FCS) and stored either at -80 °C (short term storage) or -200 °C (longer term storage). When required, frozen cells were rapidly thawed in warm water, washed in phosphate buffered saline (PBS without calcium and magnesium; Gibco, Invitrogen, UK), and placed into Dulbecco's α-MEM (α-modified essential medium) (DMEM; Gibco, UK) with v/v 10% FCS, 1 % penicillin, 1% streptomycin, 1 % L-glutamine, and 100 $\mu g.ml^{-1}$ geneticin (medium-H). Cells were incubated in T75 cell culture flasks (Sigma, UK) at 37°C, in a 5% CO_2:95% air-mix until over 70% confluent.

2.2.2 Cell Harvesting

On the day of experiment, healthy cultures were washed with PBS, and detached using HEPES-buffered saline EDTA (HBSE 10mM HEPES, 150 mM NaCL, 1.7mM EDTA). Cells were washed further with PBS, and quantified using a haemocytometer, following which centrifuged at 500 x relative centrifugal force (RCF) for 5 min. The pellet was re-

suspended in an isotonic buffer containing 10 mg/ml bovine serum albumin to a final concentration of 5 x 10^6 cells per ml. The isotonic buffer consisted of 145 mM NaCl, 5 mM KCl, 1mM $MgCl_2$,1 mM $CaCl_2$, 10 mM HEPES, 10 mM glucose; adapted from (Merritt et al., 1990). Cells were then incubated in the dark for 30 min with 5-10 µM of fluo-3AM (F3AM) at room temperature on an orbital mixer. Following this, cells were centrifuged at 500 RCF for 5 min, washed with PBS and re-suspended in the isotonic buffer to a final concentration of 5 x 10^6 cells per ml.

2.2.3 Fluorescence Assay

Fluorescence measurements were performed on a fluorescence spectrofluorometer (Photon Technology International, US), with an excitation wavelength of 506 nm and emissions recorded at 526 nm, using F3AM or fluo3. These probes were chosen due to the vast experience the host laboratory had of using F3AM for calcium imaging. The AM ester allows the delivery of the probe across the cell membrane and into the cytosol. 100 µl of the aforementioned cell suspension was added to 1900 µl isotonic solution in cuvettes containing a magnetic stirrer. In this experimental model, changes in fluorescence normally relate to variations in the intracellular calcium concentration. During the assays, the cells were allowed to equilibrate to a steady baseline (approximately 50-100s), followed by the addition of the ligand and the fluorescence count recorded. Individual cell lines expressing the particular TRP channels were then exposed to the respective receptor-specific agonist to confirm expression of the functional receptor (e.g cinnamaldehyde for TRPA1, capsaicin for TRPV1), to calcium ionophore, and also to increasing concentrations of the H_2S donor, NaHS (Olson, 2012).

2.2.4 Data Analysis

The baseline fluorescence response was classed as the stable fluorescence count (**A**) immediately prior to addition of the test ligand. The peak fluorescent count (**B)** was recorded following the addition of a test ligand. The change in the fluorescent count was thus **B – A.** The change in the fluorescent count was then standardised as a percentage

of the mean ionophore response. The mean ionophore result was produced by taking the mean of all the responses to the ionophore within that experiment; each ionophore response was calculated using **B – A**. The intensity of the fluorescence was determined using Felix GX 4.2.2 software (Photon Technology International, US). Due to the protracted response pattern seen with NaHS particularly at the higher concentrations, the peak height was taken as the count at 250s post-addition of NaHS; this was a compromise between prolonging the experiment with the associated cellular instability versus a sufficient time for the response to NaHS to develop.

The experiments investigating the autofluoresce of the dye, the % change in the relative fluorescent unit (RFU) was calculated using the formula:

$$\% \Delta RFU = ((\mathbf{B-A})/\mathbf{A}) \times 100\%$$

All results were analysed and graphically represented using either Excel 2010 (Microsoft, US) or Prism 6 (GraphPad, US). Unless otherwise stated all results are mean ± the standard error of the mean (SEM).

2.3. Fluorometric Calcium Assays: NaHS Pre-Treatment

2.3.1 HEK293 Cells

HEK293 cells transfected with hTRPA1 were transferred to T75 flasks as described above (2.2.1) and incubated at 37°C, in a 5% CO_2:95% air-mix until over 70% confluent. Cells were then split into two smaller T25 flasks and kept under the aforementioned conditions. Once approximately 70% confluent, the flask was either treated with 10 µM NaHS or vehicle (sterile distilled water), and left overnight in the incubator. Fluorometric calcium assays were performed on the following day using the same protocol mentioned in 2.2.2 - 2.2.4. The TRPA1 agonist AITC was utilised as a substitute to cinnamaldehyde in assessing TRPA1 activity due to the former having a greater potency (Bandell *et al*., 2004), and to particularly avoid the autofluorescence that is observed with higher concentrations of cinnamaldehyde (data not shown).

2.4 Cell Growth Assays

These assays are based on the Sulforhodamine B (SRB) cell growth assays described by Skehan *et al*. (Skehan *et al.*, 1990).

2.4.1 HEK293 Cell Culturing and NaHS Treatment

HEK293 cells transfected with hTRPA1 or EV were cultured and harvested as in 2.2.1. The cell harvesting protocol was as in 2.2.2 apart from the cells in the pellet were re-suspended in medium-H to a density of 40 x 10^3 cells per ml. The haemocytometer was used to confirm this cell density. One ml of this cell mixture was then added to each well on a twelve-well plate coated with Matrigel (BD biosciences, UK). Cells were incubated overnight at 37°C, in a 5% CO_2:95% air-mix, the following day each well was treated with vehicle control (sterile ddH_2O), medium-H, or the test concentration of NaHS dissolved in the medium. Following treatment of all plates, the day 0 controls were allowed to settle for 2 hours before the medium was removed, and the cells fixed. The rest of the plates were left to grow to allow a time-course experiment.

2.4.2 Pulmonary Fibroblasts Cell Culturing and NaHS Treatment

Human Primary Bronchial Fibroblasts (HPBF) cultures were derived from normal conducting bronchial tissue explants obtained under informed consent from patients undergoing pulmonary surgery. Ethics approval for the collection of tissue had been obtained from the Oxford Central national research and ethics service under the reference 12/SC/0474. The culturing of HPBF was based on modifications of a previously published protocol (Ramachandran *et al*., 2006). The bronchial tissue explants were dissected into pieces of less than 1mm^3 and were placed into individual wells of a 24 well culture plate with 500 µl DMEM containing v/v 20% FCS, 1% L-Glutamine and 1% antibiotic/antimycotic (penicillin G sodium, streptomycin sulphate and amphotericin B) and then grown at 37 °C in humidified 95% air:5% CO_2. The cells were harvested by trypsinisation using TrypLE (Gibco , Paisley) when confluent, split by a 1:3 ratio and transferred into 25cm^2 flasks in 5 ml of fresh fibroblast specific

medium (HPBF medium) which was renewed at least twice weekly. The HPBF medium (medium-F) consisted of DMEM containing v/v 10% FCS, 1% L-Glutamine, 1% non-essential amino acids and 1% antibiotic/antimycotic (penicillin G sodium, streptomycin sulphate and amphotericin B).

Cells were allowed to grow to confluence, with medium changes at least twice weekly. Confluent cells were trypsinised, and passaged with a split ratio of 1:5. Cells were only used between passages 2-8 for all experiments to avoid the spontaneous loss of the fibroblast phenotype through culturing on plastic for extended periods of time (Ramachandran et al., 2006). Cells were characterised through their typical spindle shape morphology with characteristic swirls on full confluence (Ramachandran et al., 2006). After trypsinisation, fibroblasts that were used in each growth assay were managed as the HEK293 cells in 2.4.1, except the fibroblasts were re-suspended at a density of 20 x 10^3 cells per ml (this was found to be the optimal concentration for this cell type, data not shown) in medium-F. A 0.5 ml aliquot of this cell mixture was added to each well in 24-well plate coated with matrigel.

2.4.3 Cell Fixation and Staining.

On each day of the time course, the corresponding control and treatment plates were removed and the cells fixed with 1 ml of cold 25% trichloroacetic acid (TCA) that was gently added to each well and left on ice for one-hour. The mixture was then discarded, followed by four gentle washes with distilled water following which the plates were allowed to air-dry and stored for staining. Fixed cells were stained for 30 minutes using 0.5 ml per well of 0.4% SRB dissolved in 1% acetic acid. This was followed by 4 washes with 1% acetic acid after which plates were left to air dry. Stained cells were then dissolved in 0.75ml of 10mM Tris Base (pH 10) and a 150 µl aliquot of this solution added to a flat bottomed 96-well plate. The optical density of the samples was measured by assessing the absorbance at 492 nm using a mutiwell microplate reader. The volume of SRB, Tris and the dissolved dye solution added to the 96-well plate were determined through preliminary experiments aimed at optimising the signal-to-noise ratio (data not shown).

2.4.4 Data Analysis

Data analysis was performed by comparing the optical density at 492 nm (OD_{492}) and the percentage growth in treatment and control groups, with statistical analysis performed using Prism 6.0 (Graphpad, US) software. Unless otherwise states all results are mean ± the standard error of the mean (SEM). The % cell growth was calculated using the equation:

$$\% \text{ Cell Growth} = \frac{\text{mean } OD_{sample} - \text{mean } OD_{day0}}{\text{mean } OD_{negative\ control} - \text{mean } OD_{day0}} \times 100\%$$

2.5 Flow Cytometry

2.5.1 Cell Plating, treatment and fixation

HEK293 cells transfected with TRPA1 were cultured and harvested as in 2.4.1. Three ml of the cell suspension containing 40 x 10^3 cells.ml^{-1} was then plated onto a matri-gel coated 12 well plate. Cells were then treated for 30 minutes within the class II laminar flow hoods with either vehicle containing medium-H, 100 µM H_2O_2, or NaHS (1 µM - 10 mM), following which the treatments were exchanged for 5 ml fresh medium-H and the plate returned to the incubator. Cells were allowed to grow without interruption, before being processed on the fifth day when both the cells (after dissociation with TrpLE, and quenching with medium-H) and media were centrifuged together at 500 RCF for 5 minutes. The ensuing pellet was re-suspended in PBS and centrifuged again at 500 RCF for 5 minutes. The pellet containing the cells was then fixed in 66% ethanol at a density of 1 x 10^6 cells per ml and stored at 4 ºC.

2.5.2 Flow Cytometry

On the day of flow cytometric analysis, 0.5 ml of the cell solutions mentioned in 2.5.1 were transferred to the bench-top, gently agitated to re-suspend any aggregates and allowed to equilibrate to room temperature. The cells were then centrifuged at 500 RCF for 5 minutes, the ensuing pellet was re-suspended in 100 µL of PBS, and centrifuged at 500 RCF for 5 minutes; this PBS wash step was repeated. The new pellet was then gently re-suspended in 200 µL of a staining solution of PBS containing Propidium Iodide (PI) and RNaseA with a final concentration of 50 µg.ml^{-1} and 200 µg.ml^{-1} respectively; these were found to be optimal for these experiments (data not shown). The cells were incubated in the staining solution for 30 mins at 37 ºC in the dark, after which they were placed on ice in the dark. The samples were analysed on a FACS Calibur flow cytometer (BD Biosciences, US), with the forward scatter and side scatter gates set to exclude debris and large cell aggregates. The FL2-H (height) channel was then used to collect PI fluorescence under 488 nm laser illumination and detection at 585/42 nm. Data was collected using Cell Quest pro software (BD biosciences, US) until at least 10 000 counts were recorded and/or the entire sample had been utilised.

2.5.3 Data Analysis

PI fluorescence collected under FL2 Channel-H was plotted against the cell count on a histogram, the ungated data was then analysed using Mod Fit LT version 4.1.7 (Verity software, USA).

3.1. Introduction

3.1.1. Hydrogen Sulfide and TRPA1

H_2S is emerging as a novel gasotransmitter that has numerous roles in both health and disease. Recently there have been an increasing number of reports suggesting that some of the physiological and pathological effects of H_2S are mediated through the activation of TRPA1 and possibly TRPV1 receptors (Trevisani *et al.*, 2005; Geppetti *et al*., 2006; Streng *et al.*, 2008; Miyamoto *et al.*, 2011; Andersson *et al.*, 2012; Ogawa *et al.*, 2012; Pozsgai *et al*., 2012; Munaron *et al.*, 2013;).

Trevisani *et al.* (2005) were among the first to raise the possibility that TRPV1 mediated the observed intense respiratory tract irritation which follows a toxic exposure to NaHS. They examined the effects of NaHS on guinea-pig airways, and found an elevation in neuropeptide release which could be significantly attenuated using either a TRPV1 antagonist or through capsaicin desensitisation. Furthermore they showed that the NaHS induced contractions in isolated airways were resistant to atropine, but could be prevented in part by capsaicin desensitization or with TRPV1 antagonists. They also found intratracheal administration of NaHS increased the total lung resistance and airway plasma protein extravasation, both of which were reduced with TRPV1 antagonism. The effects of intratracheal administration of NaHS are akin to the pulmonary oedema observed with high concentrations of inhaled H_2S. Other experimental models have also implicated TRPV1 as the mediator of the effects of H_2S (Patacchini *et al.*, 2005).

More recent findings utilising patch-clamp analysis have instead suggested TRPA1 is the predominant receptor mediating the aforementioned effects of H_2S *(Miyamoto et al.*, 2011; Andersson *et al.,* 2012; Ogawa *et al.*, 2012). The data in these studies also demonstrate that TRPV1 itself was not sensitive to H_2S. Additionally, subsequent to the Trevisani study it is now becoming evident that capsaicin sensitive lung vagal (CSLV)

afferents which are known to mediate airway inflammation, express TRPA1 receptors in addition to TRPV1 (Hsu *et al.*, 2013). This finding opens up the possibility that the earlier results implicating TRPV1 as a target of H_2S may have actually been mediated by TRPA1. The Trevisani group were not the only authors to suggest the effects of H_2S were mediated through TRPV1, others have reported this in organs such as the bladder (Patacchini *et al*., 2005). However as with the CSLV afferents, both TRPA1 and TRPV1 have also been shown to be co-expressed in the urinary tract (Streng *et al.*, 2008; Gratzke *et al.,* 2009), thus possibly explaining the findings by Patacchini *et al*, (2005). White *et al.* (2013) have provided data which is consistent with TRPA1 facilitating an indirect action of H_2S, here activation of the TRPA1 receptor induced the release of sensory neurotransmitters in a capsaicin-like action. These results may also explain the findings reported by Trevissani and others whereby antagonsists of TRPV1 together with capsaicin-mediated desensitisation were found to attenuate the effects of H_2S (Patacchini *et al*., 2005; Trevisani *et al*., 2005).

It is well known that thiol containing compounds such as mustard oil induce their effects through the activation TRPA1 (Bautista *et al.,* 2005; Hinman *et al.,* 2006; Macpherson *et al.,* 2007; Sadofsky *et al.*, 2011). Morevoer, at present there are several lines of evidence to support the theory that H_2S itself activates the non-human TRPA1; this includes single channel studies, whole neuronal cells experiments, knock-out models and animal behavioural models (Miyamoto *et al.*, 2011; Andersson *et al.*, 2012; Ogawa *et al*., 2012; Pozsgai *et al*., 2012). Miyamoto *et al*. (2011) using whole cell neurones from rat dorsal root ganglia provided the early data that exposed H_2S as a TRPA1 agonist. This was subsequently elaborated upon by Ogawa *et al.* (2012) and Andersson *et al*. (2012). The former revealed a reduced intracellular calcium response to H_2S in mouse sensory neourones when TRPA1 was knocked-out. This was also mimicked in naïve DRG cells via TPRA1 selective antagonists, as well as in HEK293 cells transfected with mouse TRPA1. In contrast such findings were not observed in $TPV1^{-/-}$ DRG cells. Andersson *et al*. (2012) provided further evidence for this using chinese hamster ovary (CHO) cells together with behavioural mouse models of chemical and cold hypersensitivities.

It is pertinent to note that none of the above studies utilised human TRPA1 receptors. This is particulalry important as TRPA1 channels are known to have species-specific variations in their response to certain chemical ligands and temperature stimuli (Bianchi *et al.*, 2012; Laursen *et al.*, 2015). These differences are especially significant when the ligands concerened act through the modification of cysteine residues on the N-terminal of the receptor, as is postulated with H_2S (Chen *et al.,* 2008; Laursen *et al.*, 2015). Therefore it is essential to investigate the effects of H_2S on human TRPA1 channels.

3.1.2. H_2S Donors

H_2S is a gas at room temperature which makes the safe use of H_2S in the laboratory more difficult due to the requirement of specific equipment to both store and apply it as well as extract its waste. Moreover, for prolonged experiments additional specialist equipment such as H_2S delivering incubators would be required to provide a controlled and safe supply of H_2S. Nevertheless, it has been previously utilised in its gaseous state in experiments (Blackstone *et al.,* 2005), as the administration of gaseous H_2S avoids the reliance on the unpredictable release of H_2S from donor compounds, this has been previously discussed in section 1.2.1.

In spite of these advantages, the practical problems and expense of using gaseous H_2S have led researchers in the field to utilise H_2S donating compounds such as the inorganic sulfide salts NaHS and Na_2S (Olson, 2012; Wang, 2012). Although these salts have been shown to have a similar biological effect to that seen with H_2S, a disadvantage is that they tend to release H_2S spontaneously upon solvation (Zhao *et al*., 2014). This renders it difficult to precisely control the release of H_2S. Nevertheless, NaHS appears to be the favoured salt in the literature due to its familiarity from the early studies on H_2S, cost, and availability. Furthermore NaHS has a reduced propensity to affect the pH of the vehicle solution relative to Na_2S as it requires fewer protons from the solvent during the solvation process (Dombkowski *et al*., 2005).

3.1.3. HEK293 Cell Line

The HEK293 cell line has been a commonly used expression tool for recombinant proteins since its inception around 40 years ago (Graham *et al.*, 1977). It was produced through the permanent immortalisation of human embryonic kidney cells with type 5 adenovirus DNA, and is thus regarded to have an epithelial lineage (Graham *et al.*, 1977). Due to this lineage, there is a lack of the complex cellular architecture, subcellular organization or the biochemistry associated with native neuronal preparations thus bringing into question the utility of these cells as a model of sensory neurones (see Thomas and Smart, 2005). However HEK293 cells do contain many of the intracellular signalling pathways present in neuronal tissue (Thomas and Smart, 2005). Furthermore, studies have revealed that immortalised HEK293 cells do show an even greater similarity to neuronal cells through the presence of certain neurofilamental proteins and neurone specific mRNAs (Shaw *et al*., 2002). This latter observation maybe the product of the adenovirus immortalisation inducing a neuronal gene expression profile (Graham *et al.*, 1977; Thomas and Smart, 2005).

The relative high proportions of neuronal elements observed in HEK293 cells do provide an advantage when utilised as a neuronal model when it is compared against other commonly used transformed cell-lines such as CHO cells. On the other hand, HEK293 cells also provide an advantage over the use of primary neuronal cells as they are easier to work with and more amenable to stable transfection with plasmids thus allowing the overexpression of a protein of interest. Another advantage is that these cells have been shown to possess certain elements that are required for the action of ligand gated ion channels (such as TRP receptors) in their native environment (Thomas and Smart, 2005). Conversely, the disadvantages of studying ion channels in such cell lines include the presence of endogenous receptors/channels which may confound the results. However, this can be partly overcome through comparisons with control HEK293 cells which have undergone transfection with a plasmid lacking the DNA encoding the receptor of interest. In addition the overexpression of the transfected receptor also helps to mitigate the effects of endogenous receptors which may confound the results. In conclusion, models such as the HEK293 cells provide a foundation on which initial studies can be performed in order to understand the core features of a receptor. This knowledge can then be built upon in more complex models.

3.1.4. IMR-32 Cells

This cell line was originally derived from a 13-month old boy diagnosed with a neuroblastoma (Tumilowicz *et al.*, 1970). IMR-32 cells have been used as an *in vitro* model to study sensory pathways such as those found in the lung (Carbone *et al.*, 1990). The sensory receptors TRPA1 and TRPV1 are found upregulated in these cells (Louhivuori *et al.,* 2009; Raemdonck *et al.*, 2012; Abdullah *et al.*, 2014), consequently these cells provide a neuronal model within which the effects of H_2S on TRPA1 channels can be examined. This also allows further verification of any results obtained in the experiments examining the effects of H_2S on hTRPA1 and hTRPV1 in the HEK293 cells.

3.2 Aim

Chapter one has discussed the relevance of TRP receptors such as TRPA1 in pulmonary inflammation and the role that H_2S may play in this. The aim of this part of the project is to:

I. Assess whether H_2S interacts with the hTRPA1 receptor protein.
II. Examine if H_2S affects hTRPV1
III. Investigate whether any of the effects of H_2S are also reproduced in the IMR-32 neuronal model.

3.3 Methods

Fluorometric calcium assays and NaHS were utilised to examine the direct interaction of H_2S and TRP channels.

3.3.1 Cell Preparation

HEK293 cells previously transfected with TRPA1, TRPV1 and EV, were thawed, cultured and harvested as described in 2.2.1-2.2.3. A similar protocol was used for the IMR-32 cell line.

3.3.2 Cell Treatment

In all experiments utilising HEK293 or IMR-32 cells, ligands were applied as described in section 2.2.3. The cells were then either directly treated with NaHS during the experiment, or had already undergone an overnight pre-treatment with NaHS as described in section 2.3.1.

3.3.3 Autofluorescence Assays

3.3.3.1 NaHS Autofluorescence

A cell free system was used to determine the presence of any inherent fluorescence within NaHS. 1998 µl of the isotonic buffer solution with 1mM $CaCl_2$ was added to a cuvette containing a magnetic stirrer. The fluorescence of the solution was then measured using a spectrofluorometer with an excitation wavelength of 506 nm and the emissions recorded at 526 nm. Changes in fluorescence were recorded following the addition of NaHS (final concentrations between 1 µM to 10 mM), followed by 100 mM $CaCl_2$. In a parallel set of experiments, the isotonic solution was produced without the addition of 1 mM $CaCl_2$ to investigate whether the initial calcium in the solution had an effect on any autofluorescence observed with NaHS.

3.3.3.2 Fluo-3 and F3AM fluorescence

A cell free system was used to assess the change in fluorescence upon the addition of NaHS to either F3AM or fluo-3. These experiments were performed by adding 1950 µl of double distilled deionised water to cuvettes, the fluorescent count was recorded at baseline and after the addition of 10 nM of either F3AM or fluo-3. Next the response to the addition of 1 mM of $CaCl_2$ was recorded, followed by responses to different concentrations of NaHS (100 nm – 1mM). Data analysis was performed as described in 2.2.4, however in these experiments, the change in fluorescence was recorded as a percentage of the fluorescence before the ligand was added (i.e. **(B-A)/B x 100%**; please see methods section). The use of a cell-free system negated the need to use the ionophore.

3.4 Results

3.4.1 The Effect of NaHS in HEK293 Cells

The initial experiments examined the effects of NaHS on cells that had been transfected with TRPA1. The cells displayed a concentration-dependent increase in the F3AM fluorescence; this response was found to be relatively rapid in onset, although this was slower in comparison to the other ligands such as the calcium ionophore (Figure 3). In contrast the response was much larger in magnitude and duration. The RFU did not return to the baseline in the majority of experiments, although in some experiments there was a trend towards the original baseline fluorescence (Figure 3). The response was sustained at concentrations of NaHS >50 µM, with little reversibility even with the use of receptor antagonists (data not shown).

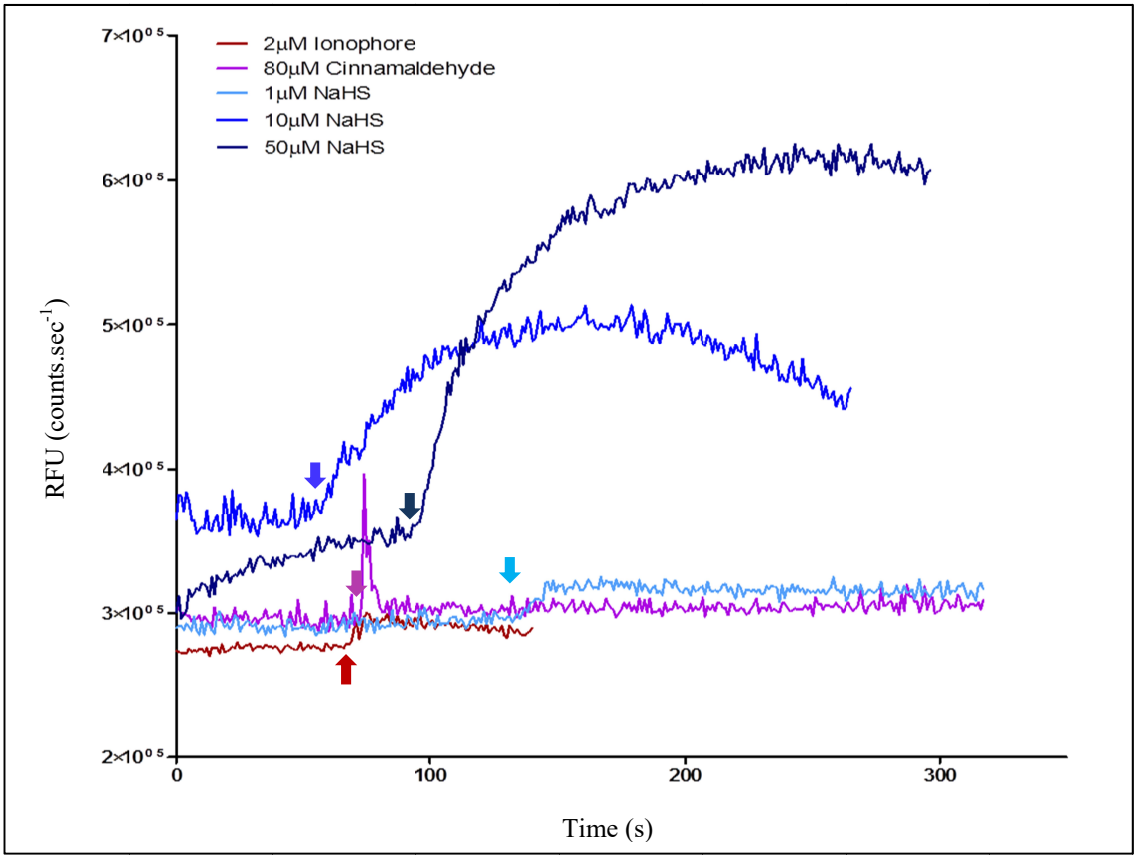

Figure 3 An example of a recording from the *in vitro* cell suspension based fluorometric calcium assay. This recording shows the response of HEK293-hTRPA1 cells following the application of the calcium ionophore (2 µM), TRPA1 agonist cinnamaldehyde (80 µM), and NaHS. Each graph represents a new sample of cells which is then treated with the ligand of interest (arrows indicate the addition of the ligand after the cells had reached a stable baseline reading). NaHS induced an increase in the fluorescence; this was slower in onset but larger and more sustained than seen with the other ligands applied. NaHS also had a variable response depending on the concentration applied with the increase in fluorescence with 10 µM reaching a peak before it starts to return back to the baseline, in contrast with 50 µM NaHS the increase in fluorescence is much larger and continues for longer.

3.4.2 The Stability of NaHS

The majority of ligands used in the host laboratory remain stable after freeze-thaw cycles at -20 °C and are thus stored and utilised in this manner. An examination of the literature did not reveal whether stock solutions of NaHS were stable when frozen, and given that NaHS produces a volatile H_2S gas upon solvation, it was deemed necessary to assess the stability of the NaHS solution. Stock solutions of 1 mM and 1 M NaHS were placed in a freezer at -20 °C for between one day and two weeks. These preliminary experiments revealed that freezing of the 1 mM NaHS stock solutions caused a large reduction in the response observed in HEK293 cells when compared with fresh stock solutions (Figure 4). This reduction was proportional to the duration the stock solutions had been frozen for. In contrast, freezing of the 1 M NaHS stock solution did not result in a reduced response (Figure 4).

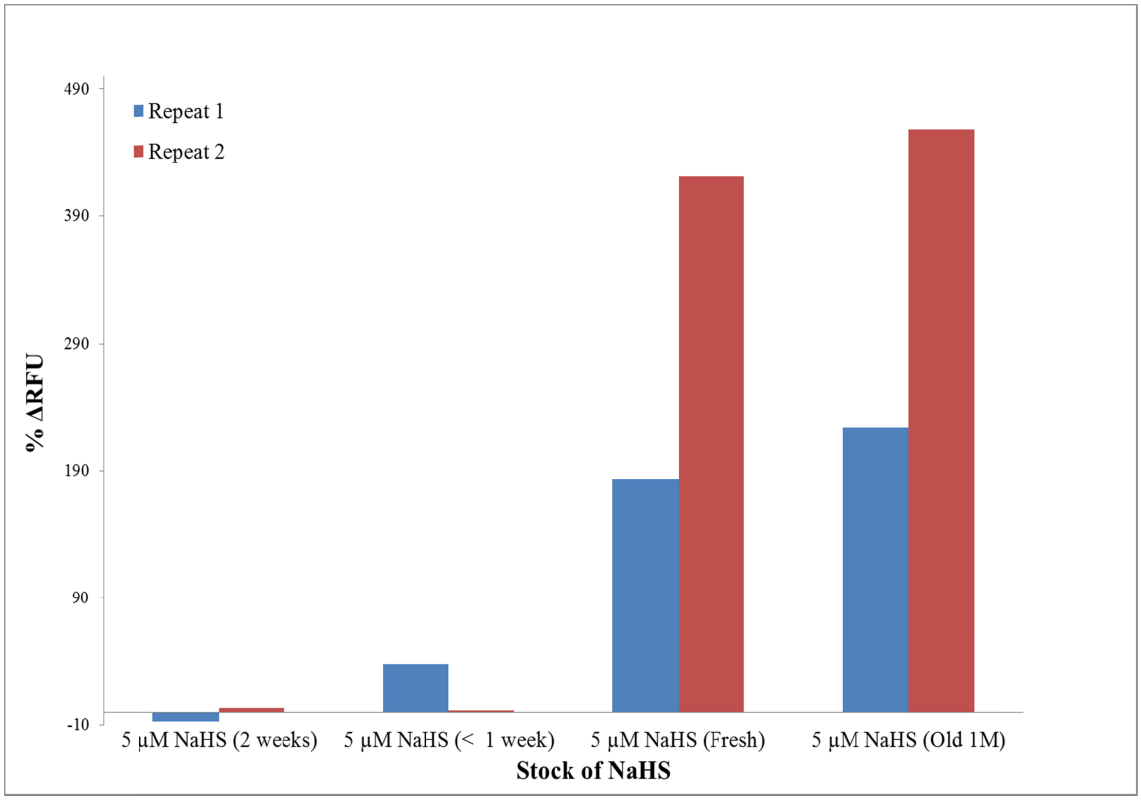

Figure 4 Bar charts with the results from two independent experiments examining the response of HEK293 cells to 5 µM NaHS. The 5 µM NaHS test solutions (unless otherwise stated) were produced using stock 1 mM stock solutions that had been stored at -20°C for various durations of time. A progressive reduction in the NaHS mediated response was observed with stock solutions of 1 mM NaHS that had been stored for longer. Freezing of the 1 M stock solution did not produce such as variable response.

3.4.3 The Effect of NaHS on the pH of the Solution

Alterations in the pH of a solution can affect cellular physiology and this confounding factor may explain any observed responses. Consequently assays were performed to investigate the effect of different NaHS concentrations on the pH of the isotonic solution. The results (Figure 5) revealed there was a significant change in the pH of the isotonic solution upon the addition of NaHS $P < 0.0001$ (One-way ANOVA, n=3 experiments). However Dunnett's post-hoc analysis indicated the effect of 10 mM NaHS appeared to skew the data, with this concentration inducing an increase in the pH from 7.0 to 7.4. As a result, 10 mM NaHS was not used in any of the experiments in this chapter. Removal of this concentration from the statistical model revealed that 100 nM to 1mM NaHS did not cause a significant change in pH of the isotonic solution ($P > 0.40$, One-way ANOVA, n=3).

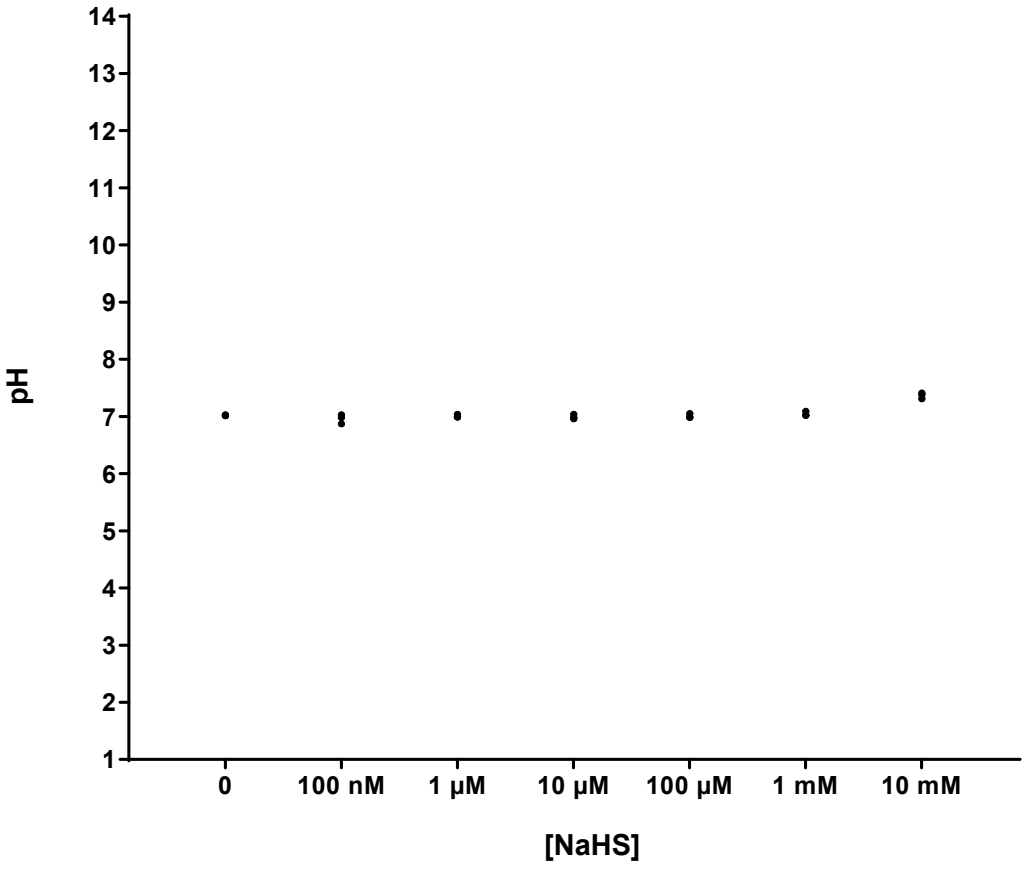

Figure 5 The effect of NaHS (100 nM – 10 mM) on the pH of the isotonic solution. The point 0 on the horizontal axis represents the native pH of the isotonic buffer with no NaHS added. Each individual data point has been plotted on the chart. There was a significant change in the pH of the isotonic solution upon the addition of NaHS $P < 0.0001$ (One-way ANOVA, n=3 experiments).

3.4.4 The Effects of NaHS on hTRPA1, hTRPV1 & EV

The application of NaHS (1 µM – 1 mM) induced a concentration dependent increase in the fluorescence observed in HEK293 cell transfected with hTRPA1, hTRPV1 and EV (Figures 6-8). The concentration response curves indicate that cells transfected with hTRPV1 (EC_{50}= 20.0 µM) were more sensitive to the effects of NaHS relative to hTRPA1 (EC_{50} = 32.0 µM) and EV (EC_{50} = 21.4 µM). However, the hTRPA1 response to NaHS displayed the greatest increase in fluorescence relative to the mean ionophore response; however the replicates in these graphs show large deviations from one another (Figures 6 - 8). There are several possible reasons that could account for these results including errors in the calculations, inconsistencies in the experimental repeats or there may be another factor that will be further discussed later. The calculations were reviewed several times with errors not detected, plus the conditions for the experimental repeats were as homogenous as possible.

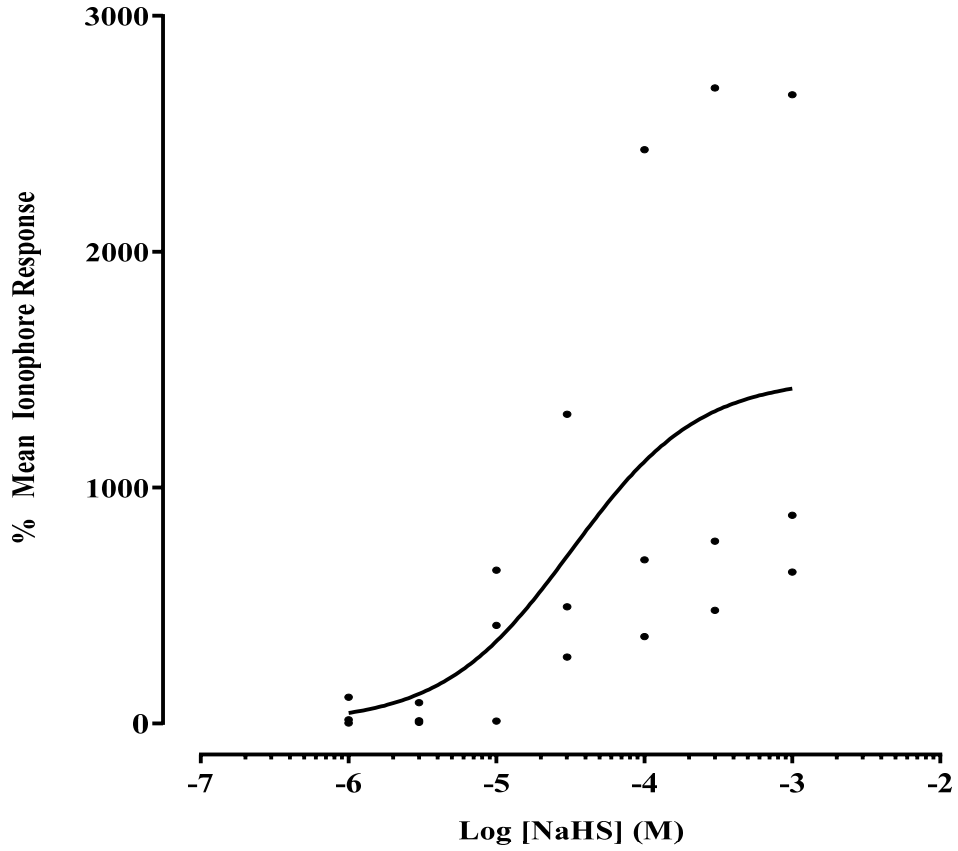

Figure 6 Concentration response curve showing the peak responses (standardised as the % of the mean Ionophore response) of HEK293-hTRPA1 to NaHS (1 µM – 1 mM). Data are plotted from three independent experiments each with two repeats. EC_{50}=32.0 µM calculated with Prism 6; Y= 1465 / $(1+10^{(-4.55-X)})$, three-parameter log agonist versus response curve.

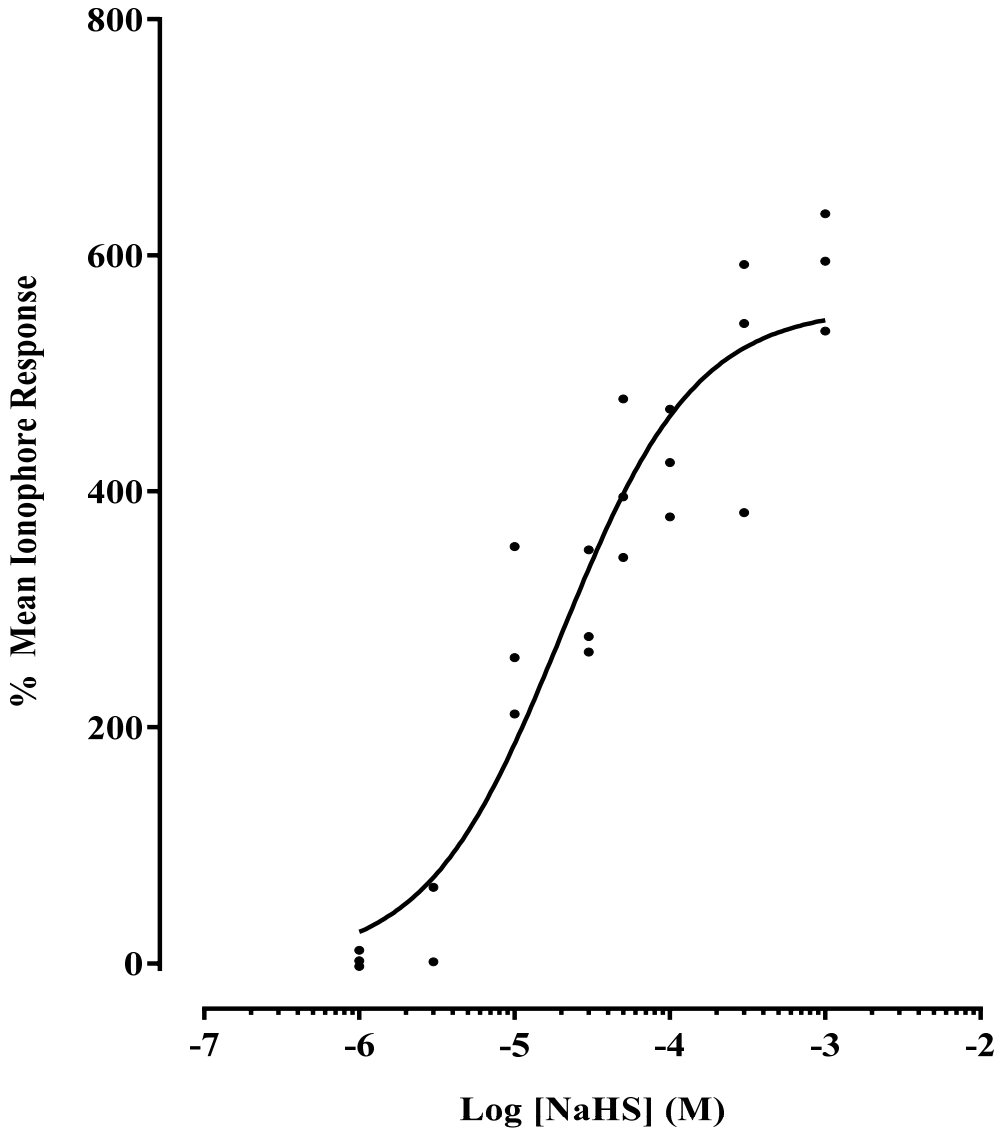

Figure 7 Concentration response curve showing the peak response (standardised to the mean response to 2 µM Ionophore) of HEK293-hTRPV1 to NaHS (1 µM – 1 mM). Data are plotted from three independent experiments each with two repeats. EC_{50}=20.0 µM calculated with Prism 6; $Y= 556 / (1+10^{(-4.70-X)})$, three-parameter log agonist versus response curve.

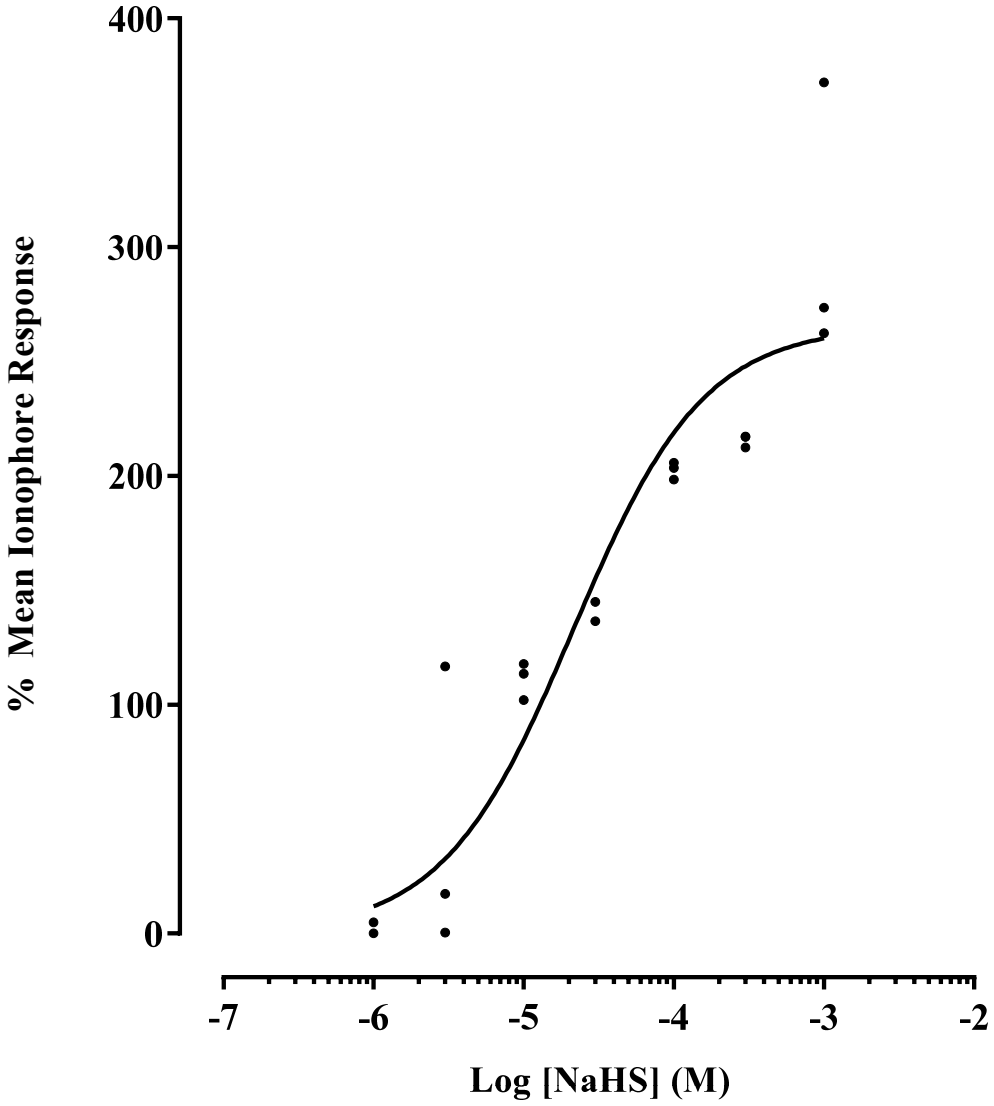

Figure 8 Concentration response curve showing the peak response (standardised to the mean response to 2 μM Ionophore) to NaHS (1 μM – 1 mM) in HEK293-EV cells. Data are plotted from three independent experiments each with two repeats. EC_{50}=21.4 μM calculated with Prism 6; Y= 266 / $(1+10^{(-4.67-X)}$, three-parameter log agonist versus response curve.

3.4.5 The Effect of NaHS on IMR-32 Cells

This cell line has been shown to express TRPA1 and TRPV1 receptors following treatment with Bromodeoxyuridine (BrdU) (Louhivuori *et al.*, 2009; Abdullah *et al.*, 2014). However, in order to assess whether NaHS has a non-TRPA1/V1 mediated response in this cell line, the experiments were initially performed in non-BrdU treated IMR-32 cells. NaHS treatment triggered an increased in the RFU; the characteristics of this response was very similar to that seen in the HEK293 cells, with an EC_{50} of 14.8 µM (n=3, Figure 9). This EC_{50} is even lower than that observed in HEK293 cells transfected with hTRPV1. This result together with those reported in 3.4.5 meant that further experiments to examine the effects of BrdU treatment and/or further studies on HEK293 cells were not performed until the dye had undergone further investigations.

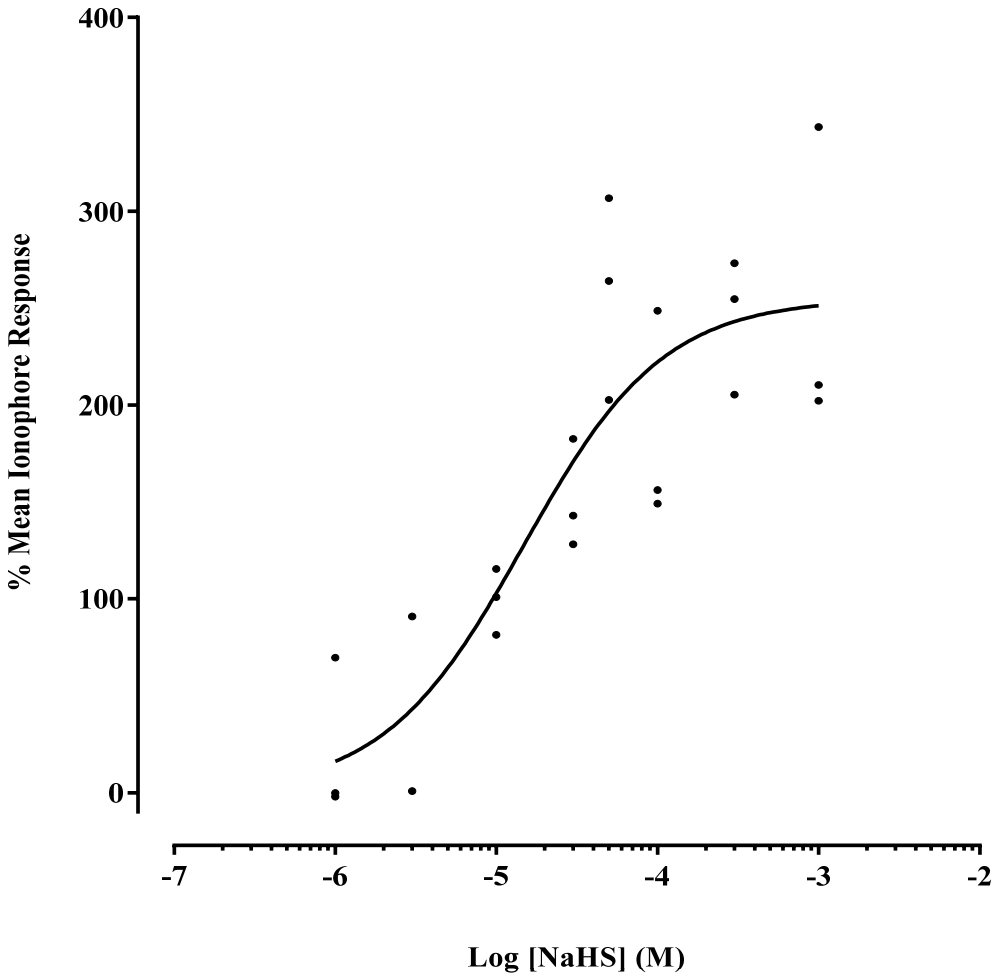

Figure 9 Concentration response curve displaying the peak response (standardised to the mean response from 2 µM Ionophore) of wild-type IMR32 cells to NaHS. Data are plotted from three independent experiments each with two repeats. EC_{50}=14.8 µM calculated with Prism 6; Y= 255 / (1+$10^{(-4.83-X)}$, three-parameter log agonist versus response curve.

3.4.6 Autofluorescence with NaHS

The investigations into the effects of NaHS on TRPA1 provided some evidence of large amounts of fluorescence at the higher concentrations of NaHS (Figure 10). This appeared to plateau at around 1 x 10^6 RFU. The plateauing effect indicates the saturation of an element within the measuring apparatus. Experiments were performed to assess whether NaHS exhibited an inherent degree of fluorescence as this could confound the results. These experiments were performed with the isotonic buffer solution in the absence and presence of Ca^{2+}, the latter was at the working concentration (1mM $CaCl_2$) as well as at a saturating concentration (100 mM $CaCl_2$). These three different parameters were chosen in order to simulate the effects of no, high (333 µM) and extremely high (33.3 mM) concentrations of Ca^{2+}. In the absence of F3AM there was no significant difference in the fluorescence intensity following the addition of NaHS (1 µM - 10mM) or $CaCl_2$ (0 – 100 mM) to the isotonic solution P= 0.62 and P= 0.44, respectively (two-way repeated measures (RM) ANOVA, n=3 per group) (Figures 11 and 12). These results suggest that within the concentrations of NaHS utilised in these experiments, the compound itself does not exhibit an inherent fluorescent activity when applied to a cell free system both in the absence and presence of calcium.

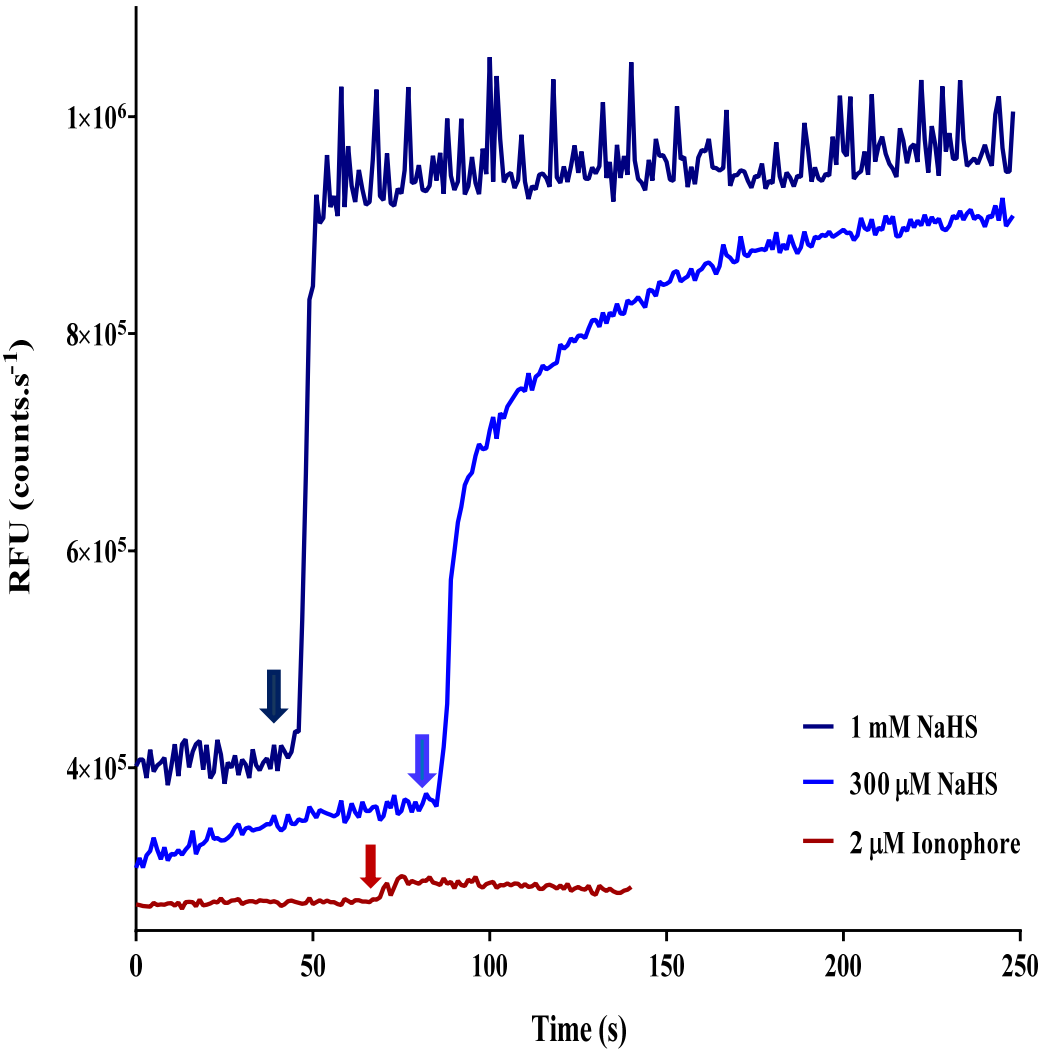

Figure 10 A recording indicating the effects of high concentrations NaHS on HEK-hTRPA1 cells. The graph displays a trace from an experiment whereby the effects of an increasing concentration of NaHS were compared against the response to 2 µM Ionophore. Cells were allowed to equilibrate to provide a baseline tracing, following which the test compounds were added (arrows). Note after treatment with 1 mM NaHS, there is a rapid increase in the fluorescent signal which appears to plateau at approximately 9 x 10^5 RFU.

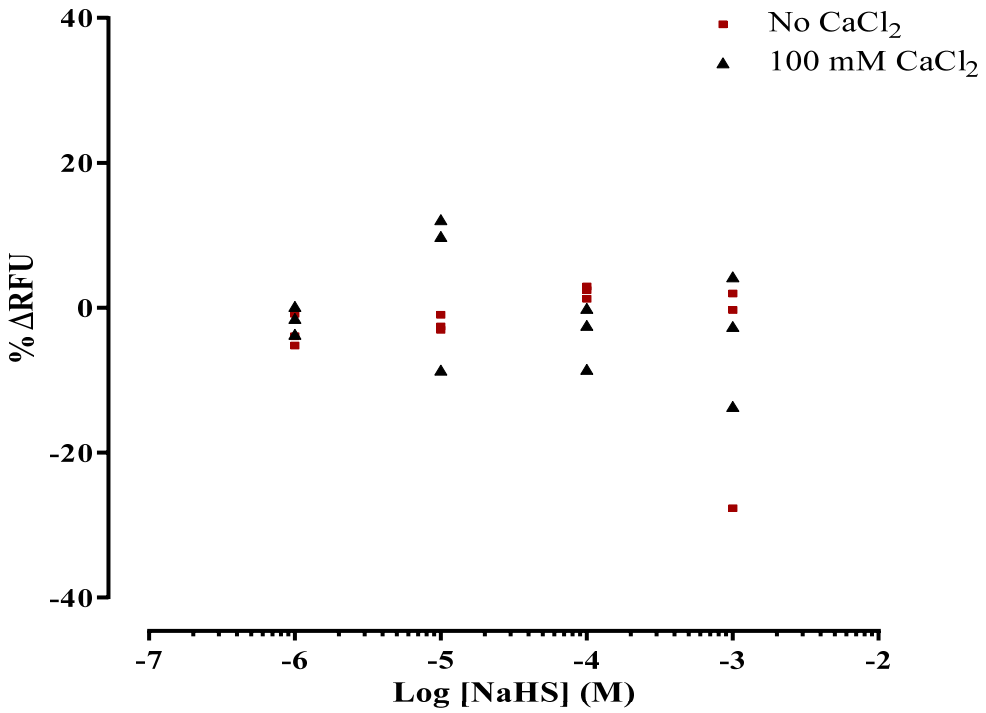

Figure 11 The effects of NaHS concentrations on fluorescence (expressed as a % change in baseline fluorescence) in a cell free system containing the isotonic buffer in the presence of no or 100 mM $CaCl_2$. In this system, NaHS was added to the isotonic solution containing no calcium followed by the addition 100 mM $CaCl_2$. Both the concentration of NaHS and the presence of $CaCl_2$ had no significant effect on the change in fluorescence; P= 0.62 and P =0.44 respectively (two-way repeated measures ANOVA, n = 3).

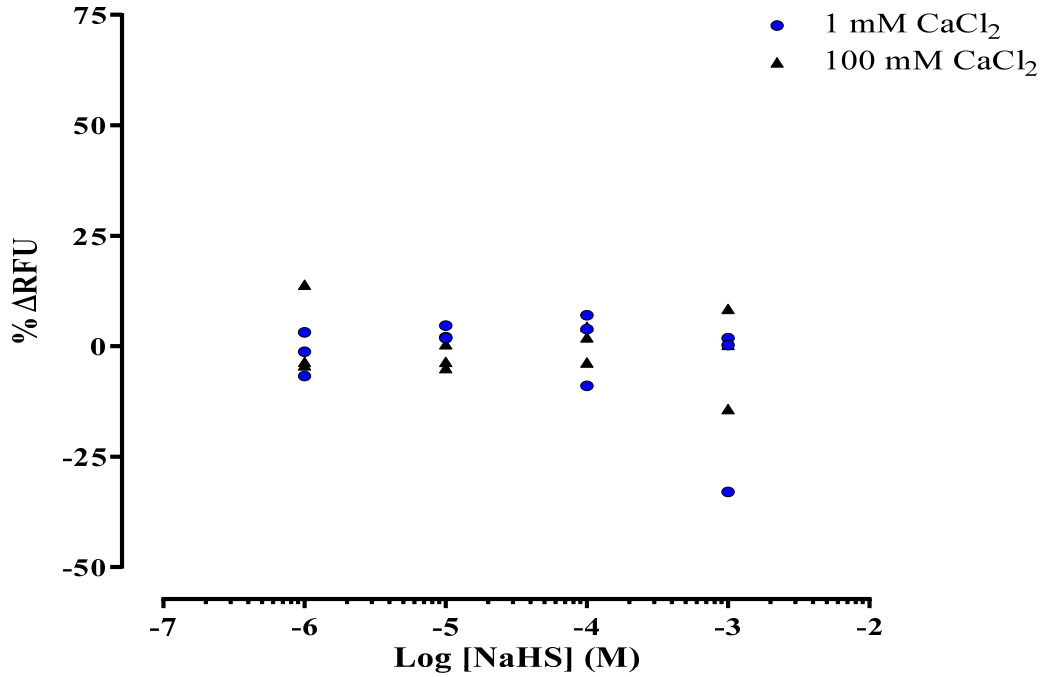

Figure 12 The effects of NaHS concentration on the fluorescence in a cell free system similar to that described in Figure 11. On this occasion, 1mM of $CaCl_2$ was added to the isotonic solution, following which NaHS was applied, and then finally 100 mM $CaCl_2$ to examine the effects of saturating the system with a supra-normal calcium concentration. Once more, both the concentrations of NaHS and the presence of $CaCl_2$ even at a very high concentration had no significant effect on the change in fluorescence; P= 0.74 and P =0.53 respectively (two-way repeated measures ANOVA, n = 3).

3.4.7 The Effects of NaHS on F3AM

The observations that treatment with NaHS induced an increase in the fluorescence intensity in two different cell types (HEK293 and IMR-32) regardless of the presence of TRP receptors highlighted the possibility that the results may be due to autofluorescence. This could be from a direct interaction between NaHS and the F3AM dye. The experiments were performed in double-distilled water (ddH_2O) to avoid any interference from the solutes present in the isotonic solution, thus enabling a pure assessment of any interactions between the dye and NaHS. Preliminary assays were used to identify the lowest concentration of F3AM which would allow detection of a fluorescent signal upon binding to calcium (data not shown). Consequently 10 nM F3AM was established as the ideal concentration in this experimental model. The addition of 10 nM F3AM to ddH_2O induced a minor increase in fluorescence of 7.27 ± 2.32 % from baseline (Figure 13A and B), followed by an increase of 1.96 ± 0.90 % after the addition of $CaCl_2$. A small rise in fluorescence was detected after the addition of 1 μM and 1mM NaHS of 5.16 ± 1.80% and 3.38 ± 2.89%, respectively. The changes in the fluorescence within the four treatment groups was not statistically significant, P = 0.470 (repeated measures one-way ANOVA with Tukey's multiple comparison test, n= 3 per group). The data from experiments examining the effects of NaHS on F3AM (figure 13A shows the trace from one experiment) were used to produce the data in figure 13B. The fluorescence was recorded before (A) and after the addition of F3AM (B), with the post-F3AM fluorescence expressed as a percent of the fluorescence prior to the addition of the drug (% ΔRFU = ((B-A)/A) x 100%). These calculations were also performed following the addition of 1mM $CaCl_2$, 1 μM and 1mM NaHS, with the whole experiment repeated a further two times on different days, the data point from each drug within each experimental repeat have been plotted in figure 13B.

A

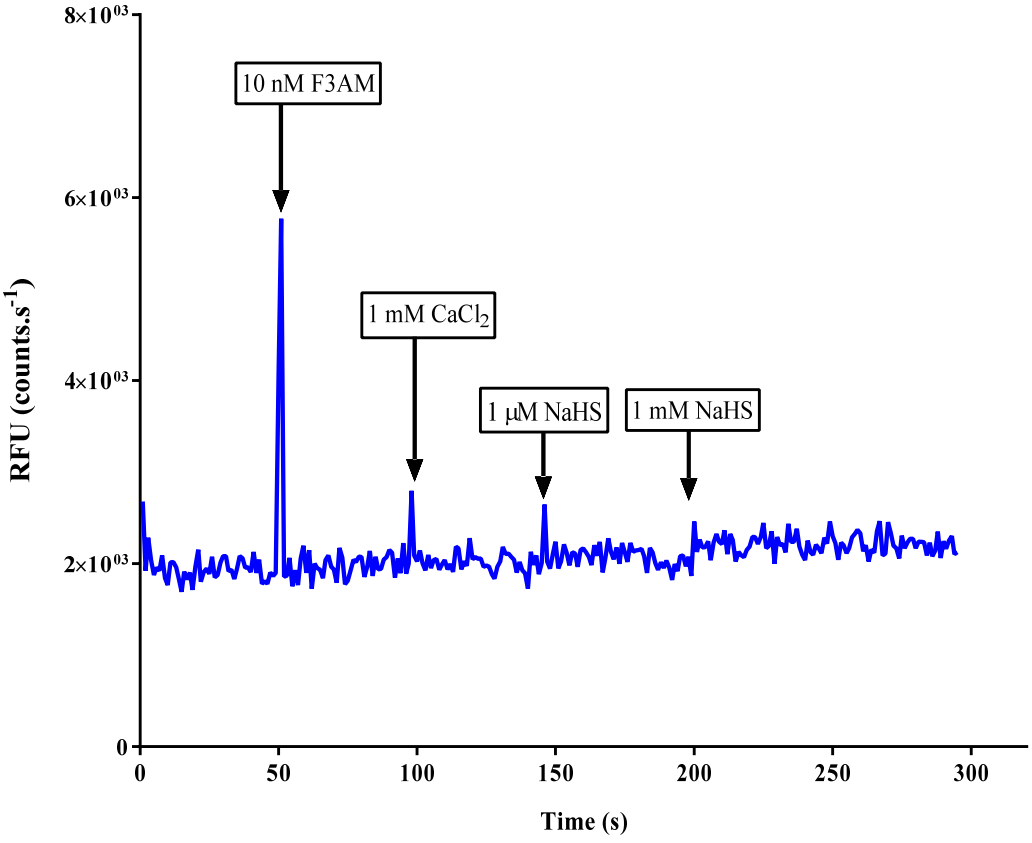

B

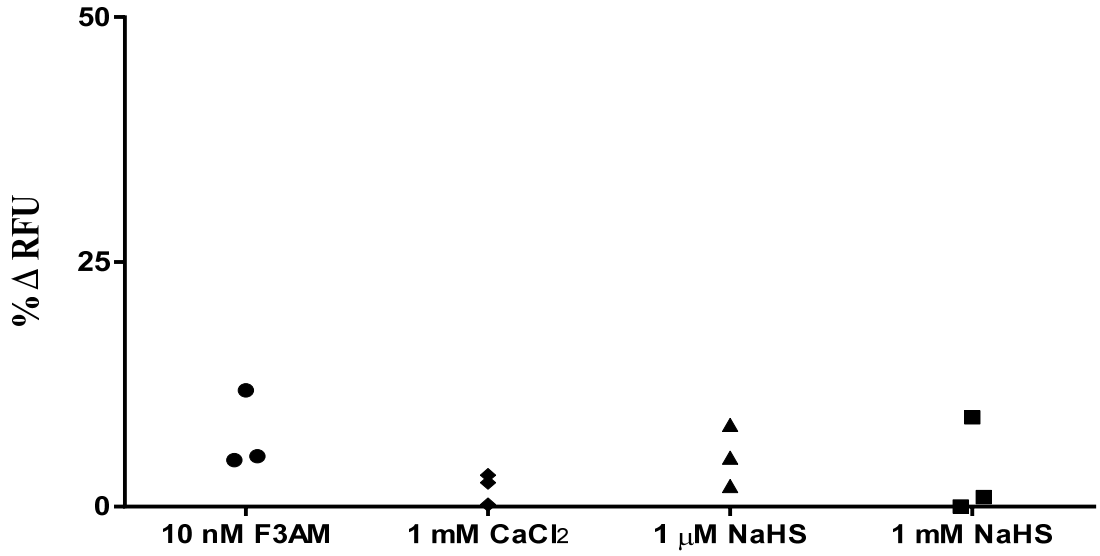

Figure 13A The effects of adding 10 nM F3AM, 1 mM $CaCl_2$, 1 µM NaHS and 1mM NaHS on the fluorescent count at 526 nm in a cell free system using only ddH_2O. The observed spikes on adding each drug are caused by tip of the pipette interfering with the spectrofluorometric detection system. **B** The % change in the baseline fluorescent count at 526 nm upon addition of 10 nM F3AM, 1 mM $CaCl_2$, and NaHS at 1 µM or 1 mM. There was no significant difference observed in the fluorescent responses between the four treatment groups; P= 0.470, one-way RM ANOVA with Tukey's multiple comparisons, n =3.

3.4.8 The Effects of NaHS on Fluo-3

The hydrolysis of F3AM by cellular esterases produces the fluo-3 species intracellularly. The following experiments were performed in order to assess whether this form of the dye was interacting directly with NaHS. The same 10 nM concentration of fluo-3 was used as had been for F3AM. The addition of fluo-3 induced an increase in fluorescence from 1500-3000 RFU seen with water, to 4000-6000 RFU (Figure 14A and B) and most likely signifies the inherent fluorescence of the dye. This change is minimal when placed in the context of the experiments with TRP channels in a cell based system (Figure 3); on that occasion the baseline RFU was over 200 000 RFU and would increase to over 1 000 000 RFU following the application of NaHS.

The addition of 1mM $CaCl_2$ to the fluo-3 induced a 55% increase in the RFU; this is in keeping with a fluorescent dye that is sensitive to calcium (Figure 14A). However, the application of NaHS at concentrations ≥ 1 μM induced an exceedingly large increase in the RFU which plateaued at 200 000 - 250 000 RFU (Figure 14A). 1 μM NaHS initiated a mean % increase of 1738% ± 398.7% in the RFU (n=3 independent experiments each with 1-2 repeats), and 1mM NaHS produced a further elevation in the fluorescence of 1472% ± 571.5% (Figure 15B). The 1 mM NaHS treatment group was excluded from the repeated-measures ANOVA to avoid the violation of circularity that would be observed in the statistical model if there was a ceiling effect observed after treatment with 1 μM NaHS. In this statistical model, there was a significant difference between the three treatments groups of 10 nM fluo-3, 1 mM $CaCl_2$ and 1 μM NaHS, with the latter inducing a significant increase in the fluorescence when compared to the former treatment ($P = 0.013$, one-way repeated measures ANOVA with Tukey's multiple comparison test , n=3).

A

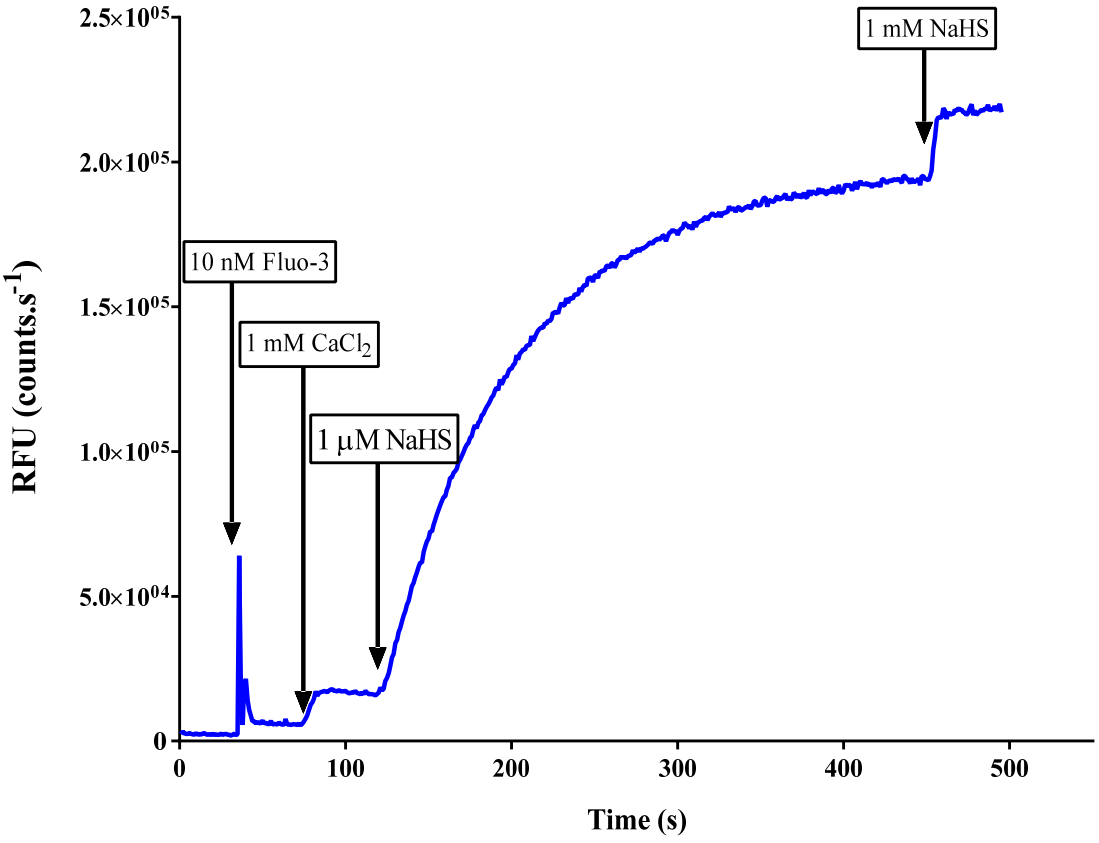

B

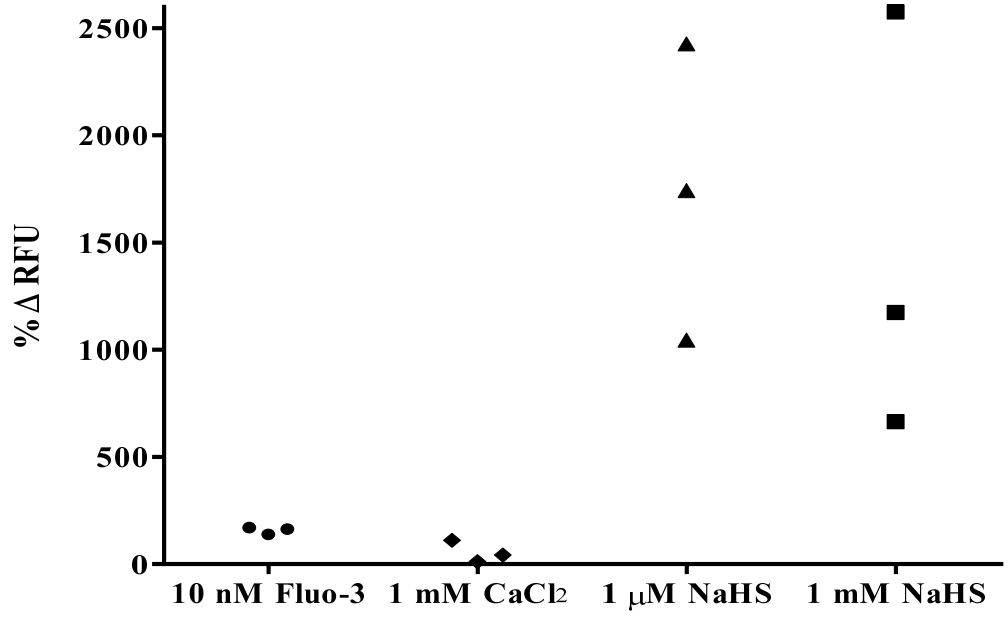

Figure 14A A recording highlighting the effects of adding 10 nM fluo-3, 1 mM $CaCl_2$, 1 µM NaHS and 1mM NaHS on the fluorescent count at 526 nm in a cell free system using only ddH_2O. The addition of fluo-3 did result in a sustained increase in the fluorescence, this was also observed following the addition of $CaCl_2$, and was even more pertinent when 1 µM NaHS was added. **B** Results from 3 independent experiments each with 1-2 repeats in the cell-free system. There was a significant effect of the different treatments on the % change in fluorescence (P = 0.03, repeated measures one-way ANOVA, n=3). Both 1 µM and 1mM NaHS induced an increase in the fluorescence.

Comparisons were made between the changes in RFU observed with fluo-3 and F3AM following treatment with 1 µM NaHS (Figure 15). In the presence of 1 mM $CaCl_2$ there was a significant increase in fluorescence in fluo-3 but not F3AM upon exposure to 1 µM NaHS (P = 0.049, two-tailed t-test, n=3 in each group).

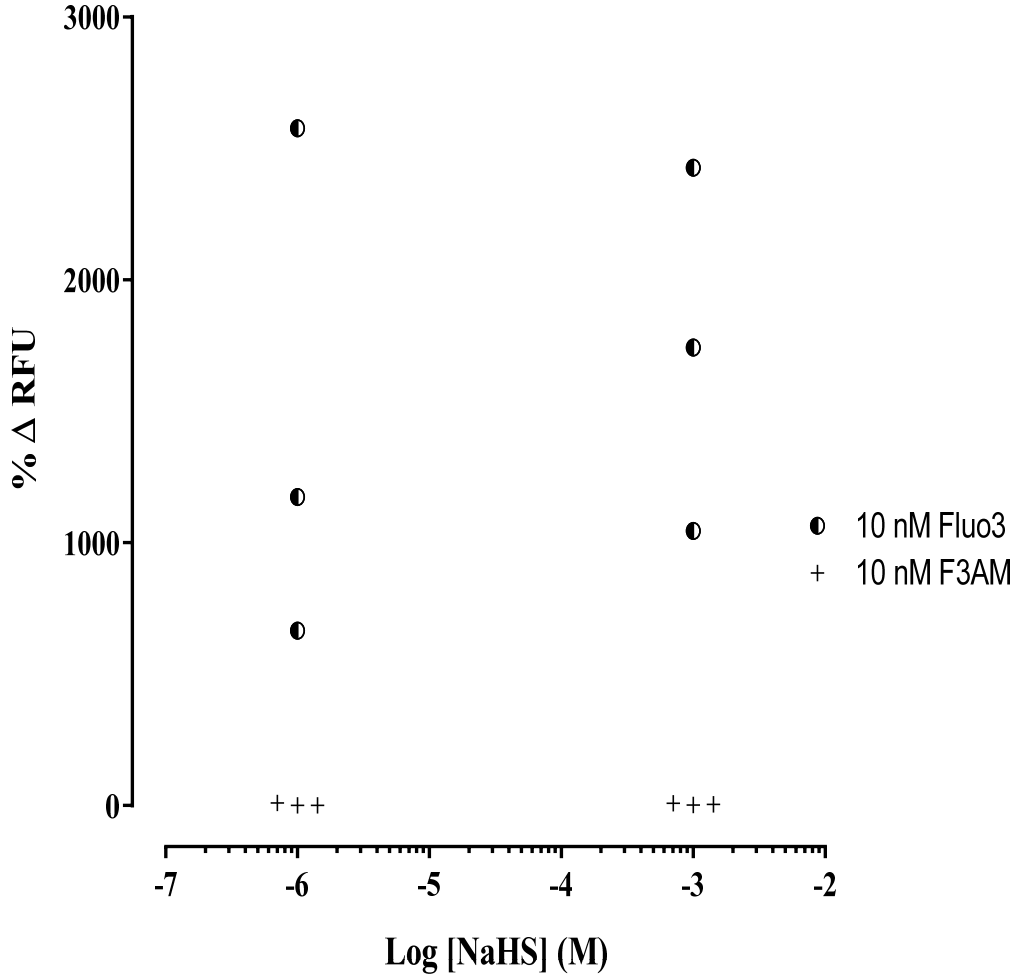

Figure 15 The % change in the RFU of both 10 nM fluo-3 and 10 nM F3AM upon addition of 1 µM and 1mM NaHS in a cell-free system containing 1 mM $CaCl_2$ in ddH_2O. There was a significant difference in the response observed with fluo-3 versus F3AM after the addition of 1 µM NaHS (P = 0.049, two-tailed t-test, n=3 in each group)..

3.4.9 NaHS Pre-treatment

In this experiment the effects of H_2S on the TRPA1 receptors were examined by an overnight pre-treatment of HEK293-hTRPA1 cells with NaHS. TRPA1 receptor activity was assessed using AITC. The overnight pre-treatment with 10 µM NaHS did not result in a significant difference in the response to AITC (EC_{50} of 5.3 µM) when compared with control cells pre-treated with vehicle (AITC EC_{50} of 2.4 µM) (Figure 16; P = 0.752, two-tailed unpaired t-test; n=3)

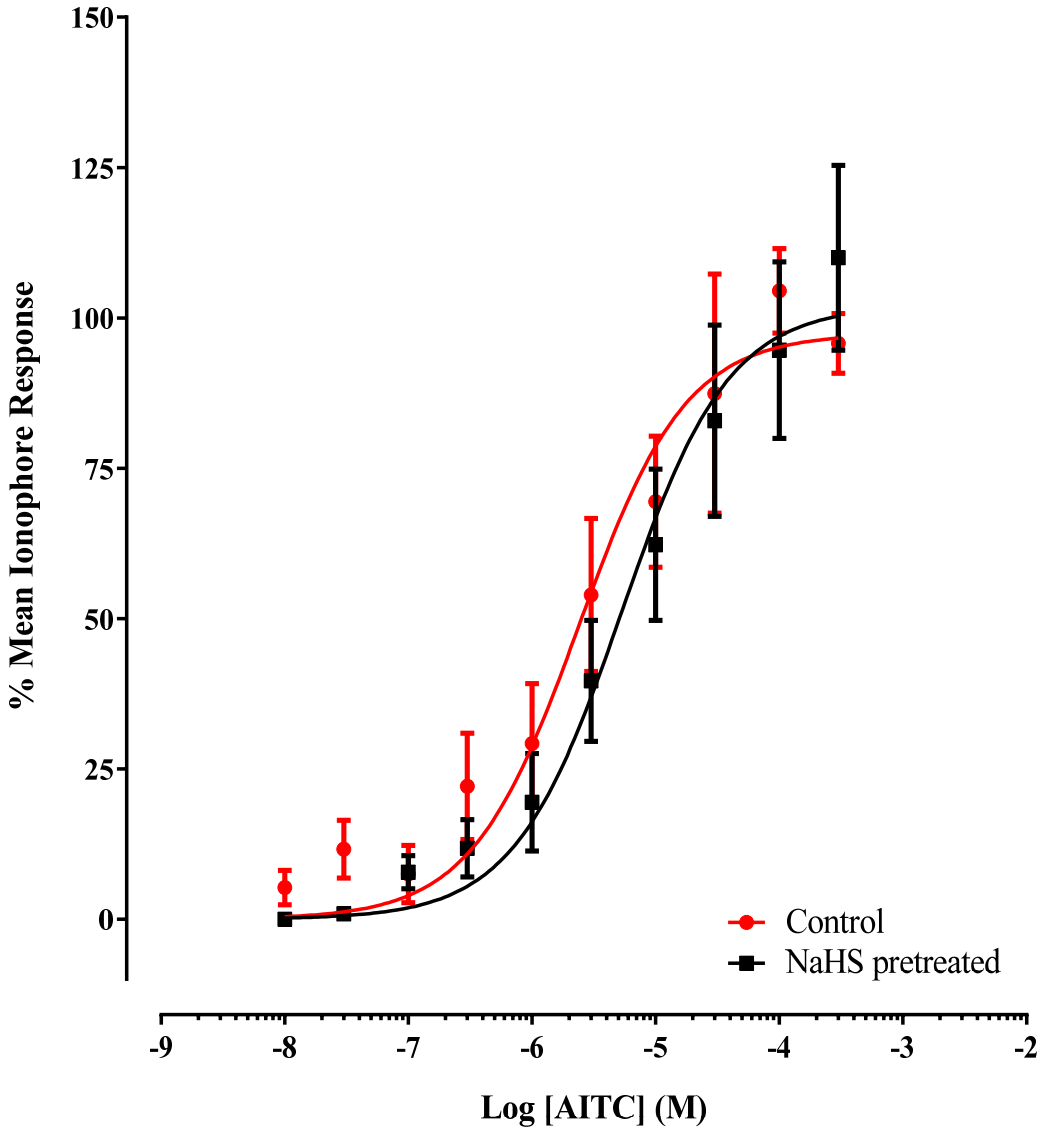

Figure 16 Dose response curves to AITC following an overnight pre-treatment of HEK293-hTRPA1 cells with 10 µM NaHS or vehicle control. Responses shown are peak responses to AITC (standardised to the mean response from 2 µM Ionophore). EC_{50}= 2.4 µM (Y= 97.4 / $(1+10^{(-.5.62-X)})$, and 5.3 µM (Y= 102.1 / $(1+10^{(-5.28-X)})$ for vehicle and NaHS pre-treated cells, respectively, calculated with Prism 6 using a three-parameter log agonist versus response curve. P = 0.752, two-tailed t-test, n = 3 independent experiments each with up to 3 repeats per data point.

3.5 Discussion

3.5.1 The Stability of NaHS

The initial investigations sought to examine the effects of NaHS on HEK293 cells, as well as explore the characteristics of NaHS in a cell-free system. It was shown that older preparations of NaHS particularly those at a lower concentrations, displayed a much greater variability in the fluorescence response observed. This effect is likely to be due to the volatility of H_2S with the effects of its loss from solutions more evident at the lower concentration of NaHS. As a result of that experiment, all NaHS stock solutions were freshly made for each set of experiments and discarded after three hours. These solutions were kept in air-tight containers and shielded from direct light. This approach was further vindicated following the results of a recent publication that highlighted a great deal of variation in the amount of H_2S that is released, and this partly depended on the conditions within which the NaHS was stored (Nagy *et al*., 2014). A potential criticism for this set of experiments was the lack of repeats to allow statistical analysis. However given the strength of the variability in my preliminary results together with the data from Nagy *et al.* (2014) it was deemed the two repeats were sufficient to allow the aforementioned approach for managing the NaHS stock solutions. Nagy *et al.* (2014) found that in their stock solutions, there was a reduction in the sulfide content of approximately 20% after three hours.

These authors also reported that in addition to a temporal-dependence in the stability of NaHS stock solutions, temperature also had an effect. They described a 30% reduction in the amount of H_2S present if the experiment was performed at lower temperatures due to a shift in pK_{a1}. However, they did suggest that stock solutions should be stored on ice and in the dark to help retard the volatilisation and loss of H_2S. Although my experiments were performed in the dark, the samples were not stored on ice because their paper was published after the majority of my experiments had been performed. Furthermore, my experiments were performed at room temperature as it was not feasible to adapt the equipment to function at the temperature of 37 °C. Working at body temperature would render the experiments more characteristic of physiological conditions and avoid temperature acting as a confounding factor. The latter is highly

relevant as TRP receptors including TRPA1 are known to be temperature sensitive (Gracheva *et al*., 2010). Consequently, the advantage of not storing my stock solutions on ice was that this avoided a further reduction in the working temperature of my assay. This reduction would have occurred as the apparatus in the experiment did not have a heating element to help maintain a constant working temperature.

The paper by Nagy *et al*. (2014) has also highlighted other important features of working with H_2S releasing salts which include the lower purity of NaHS available from Sigma-Aldrich (the vendor of the NaHS that was utilised in these experiments), and the presence of polysulfides which may be confounding the results. Unfortunately the recent publication date of this paper meant that the findings could not be implemented in the experiments within this thesis given the majority of the experiments had already been performed. There is a case for the use of a more stable and pure sulfide solution suggested by Nagy *et al*. which is produced via dissolving $Na_2S \times 9H_2O$ crystals that have had their surface washed in double distilled argon saturated water; this apparently produces a solution with low volatilisation and slow oxidation (Nagy *et al*., 2014). However as mentioned in 3.1.2 this has to be balanced with the increased propensity that Na_2S has to affect the pH of the solution (Dombkowski *et al*., 2005). As changes in pH can affect cellular physiology, it was important to rule out the effect of different concentrations of NaHS on the pH of the solution. The experiments in section 3.4.3 provide evidence against NaHS (within the concentration range used) affecting the pH of the isotonic solution.

3.5.2 The Effects of NaHS on TRPA1/EV/V1/IMR-32

The initial results in our model system appeared to support the findings of others that NaHS did have an effect on TRPA1 (3.4.1 and 3.4.4). Although this effect was consistent with the literature, the EC_{50} of 32.0 µM NaHS on hTRPA1 expressed in HEK293 cells was considerably lower than that reported by others who described it to be in the mM range (Andersson *et al*., 2012). The mM range for the EC_{50} of NaHS on TRPA1 receptors suggested by Andersson *et al.*(2012) does appear to be supra-physiological particularly as older estimates place the *in vivo* H_2S concentrations in a range that peaks around a few hundred micromolar (Olson, 2011), whereas the newer

analytical methods suggest peak H_2S concentrations might be much lower (Stein and Bailey, 2013). However there may be areas within the cell where pools with a higher concentration of H_2S exist.

In my experiments, the magnitude and universal nature of the NaHS mediated increase in fluorescence observed in all HEK293 cells transfected with the different TRP receptors as well as in EV (also observed in HEK293 cells transfected with hTRPM8, data not shown), was suspicious of being artefact from a confounding variable and needed further investigation. Accordingly the response to NaHS was assessed in a different cell line to rule out a non-specific response in HEK293 cells. The IMR-32 cells were used as these are known to express TRPA1 and TRPV1 receptors (Louhivuori *et al*., 2009; Raemdonck *et al*., 2012; Abdullah *et al*., 2014). In line with the aforementioned results with HEK293 cells, NaHS treatment initiated a significant increase in the RFU in the IMR-32 cell line (Figure 9). Taken together these results suggested that either the signal was due to autofluorescence of NaHS and/or a non-specific reaction was occurring between the dye and another factor in the experiments which was most likely NaHS. The potential for such confounding factors would explain the large variation in the data in 3.4.4-5. Accordingly, the next set of experiments were performed to examine the autofluorescence of the dye instead of further repeats of the experiments in 3.4.4-5. The autofluorescence that was subsequently detected in 3.4.8 partly explains the relatively poor fit of the data in figures 6-9 and the likelihood that the maximal response has not been determined for hTRPA1,V1 and M8. Furthermore, the results of the autofluorescence experiments mean that the true responses of the TRP receptors could not be determined within this experimental set-up; this renders the data in figure 6-9 invalid for determining the EC_{50} of NaHS on these receptors.

3.5.3 NaHS Autofluorescence

NaHS did not appear to result in autofluorescence at concentrations between 1 µM - 10mM in my cell-free experimental system. As 10 mM NaHS did appear to significantly affect the pH of the isotonic solution (Figure 5), it was deemed important to avoid using NaHS at concentrations above 1 mM whilst performing concentration-response curves. It is notable that others have reported that NaHS within the 1 - 10 mM

range has an effect on TRPA1 (Andersson *et al*., 2012), however their experiments did involve buffering their solutions to maintain a constant pH regardless of the concentration of NaHS utilised. By ensuring my experiments were performed at concentrations ≤ 1 mM avoided the effects of changes in pH of the solution and ensured that physiologically relevant concentrations of H_2S were being investigated.

3.5.4 The Effects of NaHS on Fluo-3 and F3AM

The results discussed in the section 3.5.3 made it less likely that NaHS autofluorescence was the reason behind the universal increase in fluorescence observed in all cells examined. Instead the interaction between NaHS with the calcium dye F3AM and fluo-3 its intracellular de-esterified form was investigated. The results in sections 3.4.7 and 3.4.8 demonstrate that NaHS was indeed reacting with fluo-3. This thus explains the unexpected initial universal observations that NaHS was inducing a large increase in fluorescence (i.e. a marker of intracellular calcium) in all cell types tested regardless of the receptor repertoire. The mechanisms behind the results with the HEK293 and IMR-32 cells would involve the F3AM dye permeating into the cell through its hydrophobic AM group, cellular esterases would catalyse the conversion to fluo-3. This hydrophilic variant is then trapped and can bind to free intracellular calcium. Subsequently $NaHS/H_2S/S^{2-}$ then directly reacts with fluo-3/Ca^{2+} complex to produce a large increase in the fluorescence signal. The results in sections 3.4.7 and 3.4.8 provide evidence for this hypothesis in a cell-free system, but to further confirm this theory, additional assays could be performed where cells are allowed to incubate with fluo-3 and the cells then treated with NaHS as in section 3.3.2. It would be anticipated that there would be a minimal increase in the fluorescence as fluo-3 would not be able to permeate into the cell, and with the excess dye already washed off from the cells, there would be insufficient intracellular concentrations of fluo-3 to react with NaHS.

In addition it would be useful to repeat the experiments with the application of 1 mM NaHS without the preceding application of 1 µM NaHS. This would allow a more accurate comparison to be performed between the effects of 1 µM and 1 mM NaHS by avoiding the cumulative effect observed when adding these concentrations in a serial

manner. Nevertheless such experiments may still be confounded by fluo-3 becoming saturated with micromolar concentrations of NaHS. The lack of a significant difference between the two NaHS treatments groups together with the relatively small change in RFU observed when 1 mM NaHS was added (Figure 14A and B), suggest that upon the addition of 1 μM NaHS, the system is close to reaching the upper limit of detection in this assay thus further increases in NaHS do not proportionately increase the RFU. Furthermore, in the cell based system the maximum RFU detected was over 1 000 000 compared to the 3 000 000 detected in the cell-free system, this thus may suggest that the upper limit of detection may be a consequence of the dye itself becoming saturated, rather than representing the ceiling of the measuring apparatus.

As other authors have used techniques such as patch-clamp electrophysiology or the Fura-2 dye in their calcium imaging experiments, their results are less likely to have been affected by a direct reaction between NaHS and the analytical technique they employed (Miyamoto *et al*., 2011; Andersson *et al*., 2012; Ogawa *et al*., 2012). Nevertheless, it would be useful to explore whether Fura-2 and its AM ester are also directly reacting with NaHS. Furthermore, it should be highlighted that Andersson *et al*. (2012), Miyamoto *et al*. (2011), and Ogawa *et al*. (2012), have all used non-human TRPA1 receptors in their experiments. This raises the question of whether their data is relevant in humans particularly as there is a degree of heterogeneity in the physiological properties of TRPA1 receptors observed within different species (Bianchi *et al*., 2012; Laursen *et al*., 2015). The discrepancies between the levels of NaHS is compounded by some authors assuming that the concentration of NaHS applied is the same as the concentration of H_2S, as is the case by Ogawa *et al.* (2012) who use NaHS but then state the results as the direct response to H_2S. This is not strictly correct, as mentioned in section 1.2.2, NaHS dissolves to produce H_2S as well as S^{2-} and the equilibria for the generation of these species are affected by various factors including temperature (Olson, 2012; Nagy *et al*., 2014).

The large increase in fluorescence seen upon the addition of ≥ 1 μM NaHS to 10 nM F3 is very interesting for several reasons. The first being it explains the aforementioned universal increase in the fluorescence observed regardless of the cell-lineage or the presence and type of TRP channels. Furthermore researchers wanting to study the

effects of H_2S on cellular calcium signalling should not use F3AM/fluo-3 as a calcium indicator. Additionally, scientists who are investigating intracellular calcium signalling using F3AM/fluo-3 in cells which possess large pools of intracellular H_2S should be mindful of this confounding factor (although the active species that is reacting with the fluo-3 in my experiments could also be NaHS/HS^-, however there was insufficient time to perform further experiments to determine the exact species that is reacting with the dye). Therefore, such work should also be complemented and/or replaced by other methods of studying surges in intracellular calcium. Conversely, the results of previous experiments examining intracellular calcium flux using fluo-3AM/fluo-3 may be inaccurate due to the effects of cellular pools of H_2S (if this is the active species which has reacted with fluo-3 in my experiments).

To the best of my knowledge this is the first report of a dye from this family of fluorescent probes being shown to react directly with NaHS/H_2S/S^{2-}. This in itself is a significant finding given that there has been a substantial recent drive to identifying a sensitive and specific intracellular H_2S detector (Lippert, 2014; Guo *et al*., 2015). None of these probes have been found to be appropriately sensitive, specific and or with a feasibly low toxic profile allowing them to be used in live cellular imaging of H_2S. The exact nature of the reaction between H_2S and the dye is beyond the scope of this thesis. However, there is a need for further research to study this unique finding in order to help understand the molecular mechanism of the reaction between NaHS/H_2S and fluo-3. Research is also required to assess whether this well studied dye that has been previously used in live cells (Merritt *et al*., 1990; Dubaj *et al*., 2007), could now also have the appropriate characteristics to make it a successful cellular H_2S probe.

3.5.5 The Effects of NaHS Pre-treatment on TRPA1 Receptor Activity

In this experiment the goal was to determine the effects of pre-treating HEK293-hTRPA1 cells with NaHS in order to overcome the direct interaction between NaHS and fluo-3. Overnight treatment with 10 μM NaHS did not significantly affect the TRPA1 receptor pharmacology as assessed with AITC in HEK293-hTRPA1 cells. There are several putative reasons for the lack of effect, it could be that the results are indeed correct and within this model NaHS does not affect the responses of the

hTRPA1 receptor. Although this is unlikely as others have shown that NaHS/H_2S has been found to affect TRPA1 receptors (Miyamoto *et al*., 2011; Andersson *et al*., 2012; Ogawa *et al*., 2012). In contrast there may be several reasons why the results could not be presenting an accurate picture, for example it might be that the duration of pre-treatment was too long and this allowed for the activation of adaptive mechanisms in the cells to overcome the effects of the NaHS pre-treatment. Furthermore the NaHS may have escaped into the environment soon after the application and thus does not represent a prolonged pre-treatment. To overcome this problem in the experimental model it would be useful to only apply NaHS for a brief period then, wash it off and examine the effects on hTRPA1 activity. Moreover it would be valuable to study the effects of different NaHS pre-treatment durations on TRPA1 activity. On the other hand it may be that the concentration of NaHS used was too low, particularly given the EC_{50} of NaHS on TRPA1 channels that has been described in the literature to be in the millimolar range ((Miyamoto *et al*., 2011; Andersson *et al*., 2012; Ogawa *et al*., 2012). Therefore it would also be beneficial to examine the effects of different concentrations of NaHS used for the pre-treatment. Such experiments would have utility in modelling the effects of H_2S on TRPA1 during different inflammatory episodes for example acute versus chronic inflammation where levels of H_2S may be altered (Banner *et al*., 2011; Chen and Wang, 2012; Kaneko and Szallasi, 2014).

3.5.6 Conclusion

The overall conclusions that can be drawn from this chapter are that fluo-3 directly reacts with NaHS/H_2S/S^{2-}. This renders this calcium indicator inappropriate for experiments investigating intracellular calcium concentrations in response to direct NaHS treatment. Furthermore when working with NaHS several precautions need to be taken, it should be freshly made for each experiment with maximum use of three hours, maintained cool on ice as well as in the dark, and kept in air tight containers. However, overnight pre-treatment with 10 μM NaHS did not have a significant effect on the TRPA1 receptor pharmacology. Further research is required to investigate the utility of fluo-3 as an H_2S probe as well as the effects of the effects of H_2S on human TRPA1 receptors. The reaction between NaHS and fluo-3 does not allow for any conclusions to be drawn from these experiments on the effects of H_2S on TRP channels in HEK293 or IMR-32 cells.

4.1. Introduction

4.1.1. The effect of H_2S on Cellular Proliferation

4.1.1.1. Cell Growth

The growth and replication of eukaryotic cells is a complex process which is governed by multiple, interrelated signalling pathways involving cell cycle regulatory molecules (Campisi, 2005; Pasparakis and Vandenabeele, 2015; Rubin, 1997). In order to maintain cellular homeostasis on a background of normal development and cell turnover, it is essential to coordinate cell proliferation and death (Pasparakis and Vandenabeele, 2015). Such systems are particularly important during times of high cellular activity such as observed during an inflammatory process, whereby to maintain the physiological response to injury, cells need to be rapidly recruited to the site of injury, proliferate and/or differentiate swiftly, then allow healing through resolution of the response by the cells involved either dying or migrating to other sites (Medzhitov, 2008). Uncontrolled excessive and/or prolonged inflammatory responses cause tissue damage and contribute to the pathogenesis of acute and chronic inflammatory diseases.

4.1.1.2. Cell Death

Classically cell death follows two routes; programmed cell death (apoptosis) or unregulated death (necrosis). Apoptosis is an evolutionarily conserved system which is regulated by a complex interaction between cell surface receptors and intracellular proteins, and is the usual mechanism through which inflammatory cells die at the end of an inflammatory response (Medzhitov, 2008). However, it is now becoming evident that the reality is a lot more complex with necrosis also amenable to partial regulation in processes such as necroptosis (Pasparakis and Vandenabeele, 2015). There is increasing evidence that H_2S plays an active role in cell proliferation as well as death (Baskar *et al*., 2007; Guang-dong and Rui, 2007; Baskar and Bian, 2011), for example H_2S has been shown to induce a serum-independent proliferation of non-transformed rat

intestinal epithelial cells (Deplancke and Gaskins, 2003), in contrast it can promote apoptosis in human aorta smooth muscle cells by activating the mitogen-activated protein kinases and caspase 3 (Yang *et al*., 2004b).

4.1.1.3. The Cell Cycle

At the molecular level, the process of cellular growth and proliferation is dependent on the cell cycle (Figure 17). This is the sequence of events through which a cell duplicates its genome, grows, and divides (Alberts *et al*., 2002). Under normal conditions it is a highly regulated process involving checkpoints that can prevent the progression of the cycle in order to mitigate the propagation of errors in the DNA (Kastan and Bartek, 2004; Morgan, 1997). In eukaryotes the cell cycle can be divided into 3 major phases interphase, mitosis and cytokinesis. Interphase can be further separated into three stages, Gap 1 (G1), Synthesis (S), and Gap 2 (G2); following this the cell enters mitosis and cytokinesis which together can be referred to as the Mitotic phase (M) (Scholey *et al*., 2003). During G1 the cells increase in size but the amount of DNA remains constant, and progression to the next stage depends on passing the G_1 checkpoint (Morgan, 1997; Alberts *et al*., 2002). The subsequent stage is the S phase during which DNA replication occurs resulting in the process whereby there is a doubling of the DNA content. The cell then enters the G_2 phase by which point the entire DNA has been replicated, the cell continues to grow, is assessed at the G_2 checkpoint to ensure the cell is appropriately prepared and the environment favourable for the M phase. Progressions through the G_1 and G_2 stages are delayed at the respective checkpoints if the DNA is damaged for example by radiation or chemicals; these interruptions provide time for any potential DNA repair to be completed.

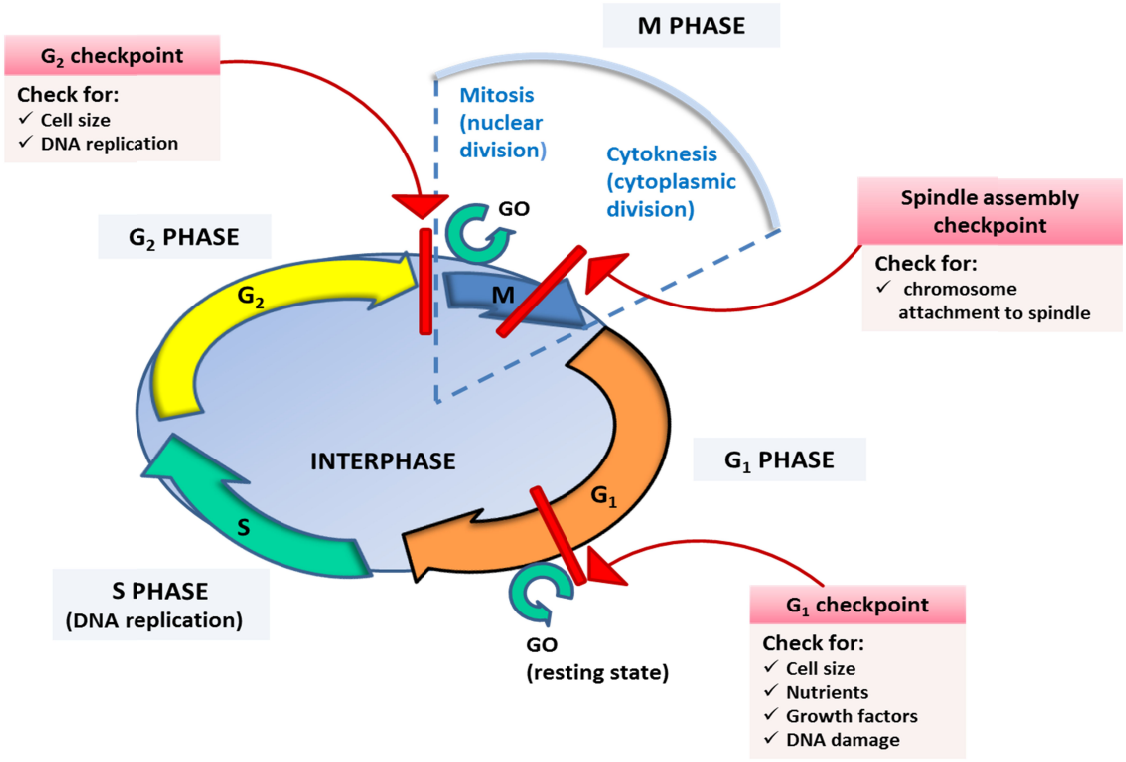

Figure 17 Diagram indicating the phases of the cell cycle together with the location of the major cell cycle check points and what factors are assessed at each of these points. Phases: synthesis (S), Growth 1(G_1), Growth 2 (G_2), Mitosis (M). Adapted from (Alberts *et al*., 2002).

Cell growth then stops within the M-phase as the cell starts to divide, this process is regulated by the metaphase checkpoint in mid-mitosis which ensures all the chromosomes have been attached to the spindle before the completion of the M-phase (Scholey *et al*., 2003). Cells may also enter a quiescent or senescent stage referred to as G_0, within which further cellular division does not occur temporarily or permanently. This entry into G_0 is through a cell cycle checkpoint in the G_1 phase (Alberts *et al*., 2002; Campisi, 2005). The aforementioned major checkpoints in the cell cycle are dependent on cyclins, cyclin-dependent kinases as well as other kinases; an elaborate control system which becomes more complex with higher order organisms (Morgan, 1997). The key proteins involved in the cell-cycle control system are themselves regulated through the actions of ubiquitin-dependent proteolysis (Diehl and Ponugoti, 2010). Such regulatory mechanisms are crucial in ensuring the cellular homeostasis of an organism is maintained and prevent the aberrant cell reproduction which can lead to various diseased states including chronic inflammation, autoimmune disorders and cancers (Medzhitov, 2008; Diehl and Ponugoti, 2010; Pasparakis and Vandenabeele, 2015).

4.1.2. Pulmonary Fibroblasts in Chronic Disease

4.1.2.1. Fibroblasts in Inflammation

Fibroblasts are cells that originate from the primitive mesenchyme and play a major role in providing a supporting framework for the extracellular matrix (ECM) (Flavell *et al*., 2008). They have a characteristic spindle shape with an elliptical nucleus and are highly adapted to synthesise and secrete components of the ECM which includes collagen, elastin, proteoglycans, and glycoproteins (Chang *et al*., 2002; Camelliti *et al*., 2005). In addition to a structural role, fibroblasts are also becoming increasingly recognised for the important part they actively play in both normal and pathological wound healing following tissue injury (Chang *et al*., 2002).

Normal wound healing involves three major phases; inflammatory, proliferative and finally a remodelling phase (Medzhitov, 2008). The inflammatory phase involves vasoconstriction, platelet aggregation, and leucocytosis (Hall, 2010). This is followed by the proliferative stage, where fibroblasts increase in number, lay down collagen and attempt to fill tissue defects in the tissue (Steffensen *et al*., 2001). The wound then starts to gradually contract though the action of smooth muscle cells and also undergoes epithelialisation. The final stage involves the maturation and remodelling of the new tissue; a process that may last years, depending on the severity of the insult (Steffensen *et al*., 2001).

The role of fibroblasts in inflammation and cellular proliferation is in part mediated through intricate communication with leukocytes and other inflammatory cells (Duffield *et al*., 2013; Chrysanthopoulou *et al*., 2014). This process involves the secretion of cytokines and prostanoids, as well as altering the expression profile of cellular adhesion molecules which thus promote leukocyte recruitment, activation and survival (Flavell *et al*., 2008; Kendall and Feghali-Bostwick, 2014). However aberrations in the regulation of fibroblast proliferation can lead to the development of pathological states which are implicated in certain disease conditions such as atherosclerosis, COPD, and pulmonary fibrosis (Libby, 2002; Garantziotis *et al*., 2004; Ojo *et al*., 2014).

4.1.2.2. The Effects of H_2S on Pulmonary Fibroblasts

As described in chapter 1, there is mounting evidence for the role of H_2S in models of pulmonary inflammation and fibrosis (Yanfei *et al*., 2006). The data for the effects of H_2S on pulmonary fibroblasts is mixed with some providing evidence for an anti-fibrotic effect of H_2S in the immortalised cell line MRC-5 (Fang *et al*., 2009), whilst others have shown a pro-apoptotic effect in non-primary human fibroblasts (Baskar *et al*., 2007). Such effects were found to involve different ion channels depending on the tissue studied. In the MRC-5 line it was found not to involve potassium channels (Fang *et al*., 2009), whereas in human atrial fibroblasts the $K_v4.3$ potassium channel was shown to mediate the inhibition of fibroblast proliferation by NaHS (Sheng *et al*., 2013).

4.1.2.3. The Role of TRPA1 in Pulmonary Fibroblasts

TRPA1 is also a viable candidate for the pro- and anti-proliferative effects of H_2S due to several reasons; it is expressed in pulmonary fibroblasts, in fact it was originally cloned from human lung fibroblasts (Jaquemar *et al*., 1999). Other reasons include the wide tissue distribution of this channel which is found in the pulmonary, cardiovascular, gastrointestinal, haematological systems as well as in the brain which would explain the different effects on different regions of the body (Takahashi *et al*., 2012). TRPA1 has also been shown to promote cell survival in small cell lung cancer (Schaefer *et al*., 2013), and regulates local tissue inflammation (Okada *et al*., 2011). The latter may be achieved through TRPA1 functioning as a component of the transduction machinery through which environmental irritants are detected. Consistent with this theory, these receptors are found to be present on several different pulmonary cell types in addition to the aforementioned pulmonary fibroblasts (Bautista *et al*., 2006, 2005; Jaquemar *et al*., 1999; Nassini *et al*., 2012). Finally as already discussed, H_2S has been reported to activate TRPA1 receptors (Miyamoto *et al*., 2011; Andersson *et al*., 2012; Ogawa *et al*., 2012), furthermore both the lung and pulmonary artery tissues are rich in active CSE thus providing an endogenous source of H_2S (Hosoki *et al*., 1997).

These findings have led to the hypothesis that the perturbations in the H_2S-TRPA1 interaction is involved in pulmonary inflammation which may then progress to produce disorders such as COPD, asthma and pulmonary fibrosis. Despite this evidence, there have not been any studies that investigate the effects of NaHS/H_2S on the growth of primary pulmonary fibroblasts.

4.1.2.4. N-Acetylcysteine and Fibrotic Conditions

Several different therapies have been investigated for the treatment of the pulmonary fibrotic condition IPF. N-Acetylcysteine (NAC) is one such treatment, and has shown promise in experimentally-induced fibrosis both in animal models as well as in some early clinical trials. Although the mechanisms underlying its action are not fully understood, it is believed that the benefit of this cysteine derivative is through the synthesis of glutathione and thus the potentiation of the cellular antioxidant reserves (Datta *et al*., 2011). This together with the beneficial effect of NAC in the treatment of toxicity from sulphurous compounds (Shohrati *et al*., 2014), opens up the possibility that NAC is able to modulate the effect of H_2S, and thus this will be studied in this chapter.

4.2. Aims

The aim of this chapter is to investigate the effects of H_2S on cellular growth in both HEK293 cells and HPBF by:

I. Assessing whether the hTRPA1 receptor protein mediates any effects of H_2S on cell growth in HEK293 cells.
II. Examining the effects of a brief exposure to H_2S in both the immortalised cell line (HEK293) and primary pulmonary fibroblasts (HPBF).
III. Assessing whether NAC modulates the effects of H_2S.

4.3. Methods: Cell Growth Assays

4.3.1. Chronic NaHS Treatment in HEK-hTRPA1 cells

These sets of experiments were performed to examine the effects of chronic treatment with NaHS on the growth of HEK293-hTRPA1 cells. The 'chronic' term was used as NaHS was added to the medium and left until the end of the experiment. Unless otherwise stated all experiments in section 4.3.1 utilised HEK- hTRPA1 cells that were cultured, harvested, treated and stained as described in 2.4.1, 2.4.3-2.4.4.

4.3.1.1. The effect of vehicle on HEK293 cell growth

Cells were treated with either medium alone or medium containing the sterile ddH_2O vehicle (1% v/v) (Figure 18A).

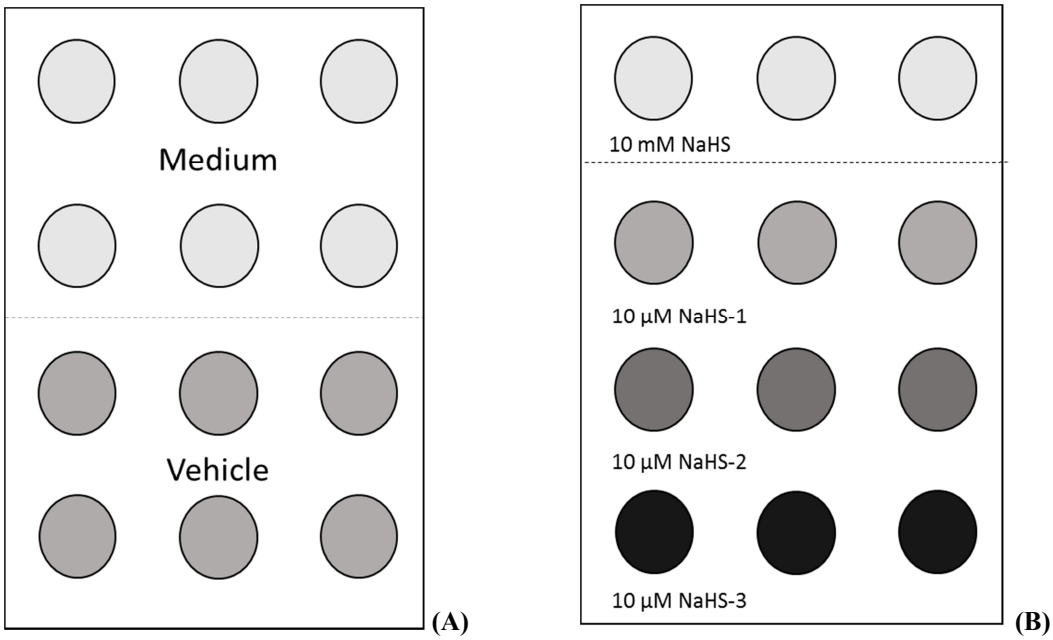

Figure 18 Schematic diagrams indicating how the plates for the cell growth assay were arranged. (**A**) Control plates (treatment and incubator) were split into two six well halves half contained cells with either medium alone or vehicle (sterile water) and medium. (**B**) NaHS treated plates were organised to assess the effects of a very high (mM) and low (µM) concentration of NaHS. Three rows of 10 µM NaHS were used at varying distances from the 10 mM NaHS to assess whether the presence of a high concentration of H_2S affects neighbouring cells.

4.3.1.2. The effect of NaHS on the pH of the medium

The pH of the medium was measured before and after the addition of NaHS (100 nm – 10 mM) using a calibrated pH meter (FiveEasy, Mettler Toledo; UK).

4.3.1.3. The effect of NaHS within the incubator on control cell growth

As H_2S is a volatile gas it could potentially escape from the NaHS treated wells and affect the growth of neighbouring controls. To address this, two control plates were placed in two separate incubators under the same conditions (temperature, humidity and air mix). One of the incubators contained both vehicle treated control cells and cells treated with NaHS, whereas the other only contained vehicle treated cells ('incubator control').

4.3.1.4. The effect of high concentrations of NaHS on adjacent cell growth

This experiment was used to compare the effects of the location of the 10 M NaHS treated cells (relative to 10 mM NaHS) on growth. Plates were arranged as indicated in Figure 18B. One row of cells were treated with 10 mM NaHS and the other three rows of cells were treated with 10 μM NaHS; each successive row of 10 μM NaHS treated cell was thus at an increased distance from the 10 mM NaHS.

4.3.1.5. Concentration dependent effects of chronic NaHS treatment

Cells were treated with increasing concentrations of NaHS (1 μM – 10 mM).

4.3.2. Chronic NaHS Treatment of HEK293-EV Cells

HEK293-EV cells previously were cultured, harvested and plated as described in 2.4.1, 2.4.3-2.4.4. The cells were then treated with increasing concentrations of NaHS (1 μM – 10 mM) that was left on as part of the 'chronic' treatment paradigm.

4.3.3. Acute NaHS treatment of HEK293-hTRPA1 cells

These sets of experiments were performed to examine the effects of acute NaHS treatment on the growth of HEK293-hTRPA1 cells. The 'acute' term was used as NaHS was applied to the cells for 30 minutes and then replaced with fresh media. The HEK293-hTRPA1 were cultured and harvested as described in 2.4.1. However, in contrast to the chronic experiments, these experiments were performed in 24-well plates, 0.5 ml of the 40 x 10^3 cells.ml^{-1} cell solution added to each well. The plates were left overnight in the incubator at 37 °C in a 95%:5% air-CO_2 mix. The following day ('Day 0') cells were either treated with medium only, medium containing vehicle, or NaHS (1 μM – 10 mM) for 30 minutes within the class II laminar flow hoods. The solution was then exchanged for 1.5 ml of fresh medium, and the plates returned to the incubator to allow cell growth.

On each day of this growth assay, the appropriate plate was removed and the cells fixed, stained and analysed as per 2.4.3 and 2.4.4 with some modifications. These changes were due to the use of 24-well instead of 12-well plates and involved using 0.75 ml of cold 25% TCA per well, 0.25ml per well of 0.4% Sulforhodamine B, and 0.3 ml per well of 10mM Tris Base (pH 10). The volume of TCA, SRB, Tris Base and the dissolved dye solution, were determined through preliminary experiments (data not shown).

4.3.4. Acute NaHS treatment of HPBF

The effects of a 30 minute acute treatment with NaHS on the growth of HPBF was assessed using the SRB growth assay as described in 2.4.2. The plates were left overnight in the incubator at 37 °C in a 95%:5% air-CO_2 mix in medium-F. The next day, HPBF cells were either treated with medium-F, medium-F containing vehicle, or NaHS dissolved in medium-F (1 μM – 10 mM) for 30 minutes within class II laminar flow hoods. Cells were allowed to grow for 0-5 days and the SRB assay performed as described for HEK cells in section 4.3.3.

4.3.5. Application of NAC on HEK293-hTRPA1 and HPBF cells

In these sets of assays, growth was assessed on days 0 and 5, instead of a detailed time-course. The growth was standardised as a % of the vehicle (ddH_2O) treated controls using the formula described in 2.4.4.

4.3.5.1. The effects of NAC on HEK293-hTRPA1 cells

Cells were plated as described in 4.3.3, allowed to settle overnight, then treated for 1.5 hours with either medium, medium with vehicle or NAC (100 nM – 10 mM) dissolved in medium (Figure 19A). The NAC was then exchanged for 1.5 ml of medium and returned to the incubator. Plates were then fixed on each consecutive day as per the SRB assay.

In a parallel set of experiments, the above was repeated however after 1 hour of NAC treatment, 10 mM of NaHS was also applied for 30 minutes to all wells except the vehicle and medium controls (Figure 19B). Hence, the total NAC exposure time was 1.5 hours and total NaHS exposure 0.5 hours. The drugs were then exchanged with 1.5 ml of medium, returned to the incubator, and processed as per the SRB assay.

4.3.5.2. The effect of NAC on HPBF

Cells were plated as described in 4.3.4 and allowed to settle overnight. The following day they were treated for 1.5 hours with either medium-F, medium-F with vehicle or NAC (100 nM – 10 mM) in medium-F (Figure 19A). The NAC was then exchanged for 1.5 ml of medium-F, returned to the incubator and processed as per the SRB assay.

As with the HEK-hTRPA1 cells in 4.3.5.1, HPBF cells were treated with NAC and NaHS, however 1 mM of NaHS was used (Figure 19B).

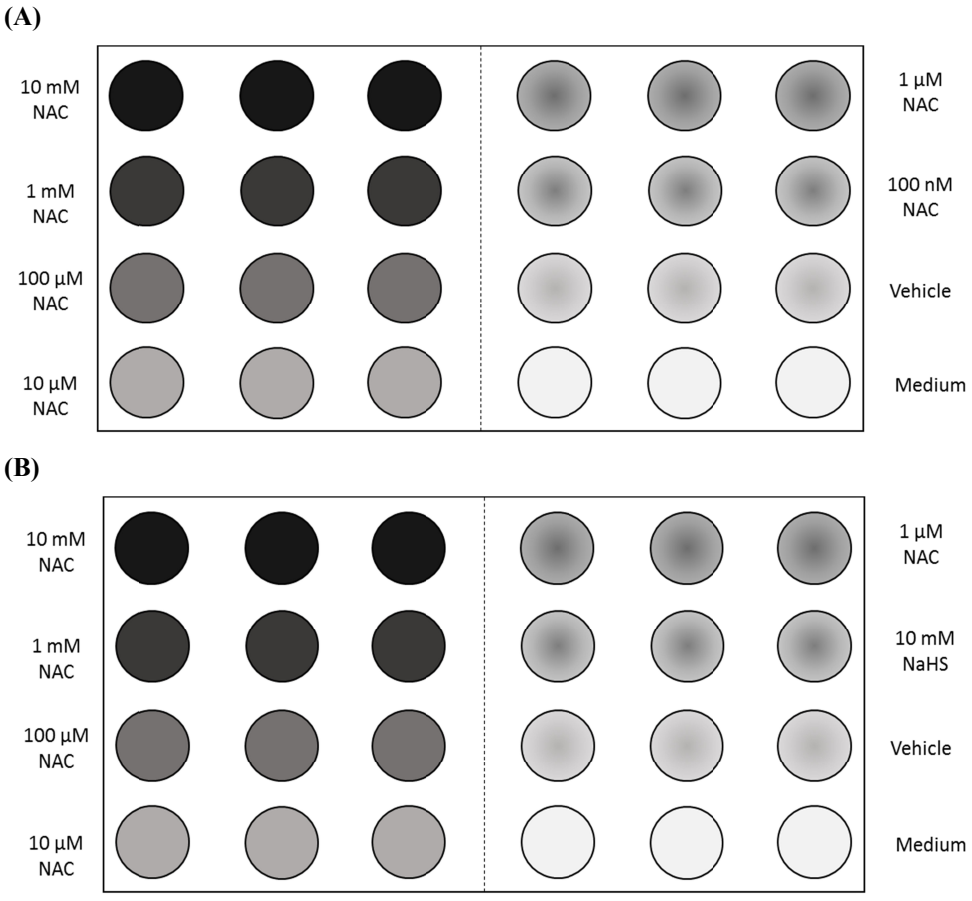

Figure 19 Schematic diagrams to indicating how plates for the cell growth assay were arranged. HEK-hTRPA1 or HPBF cells cultured on 24-well plates were treated. (**A**). Cells were treated with 1.5 hours of NAC (100nM-10mM). (**B**).Cells were treated with 1.5 hours of NAC (1 µM-10mM) and 30 mins of either 10mM (HEK) or 1mM (HPBF) NaHS.

4.4. Methods: Flow Cytometry

4.4.1. HEK293-hTRPA1 Cells

HEK293-hTRPA1 cells were cultured, harvested, treated and analysed as in section 2.5

4.4.2. HPBF Cells

HPBF cells were cultured and harvested as discussed in 2.4.2, followed by plating and treatment as described in section 2.5 for HEK293 cells. In contrast to HEK293 cells, the density of the HPBF cells used was 20 x 10^3 cells per ml of medium-F. Furthermore, an extra 1mM NaHS treatment group was also added.

4.5. Results: Cell Growth Assays

4.5.1. Chronic NaHS treatment in HEK-hTRPA1 cells

4.5.1.1. The effect of vehicle on HEK293 cell growth

These experiments were performed to compare the effects of vehicle versus medium alone on the growth of HEK293-hTRPA1 cells. In both groups there was an increase in the OD at 492 nm with time; in the SRB assay this represents an increase in the number of cells present on the plate. The mean OD on day 0 was 0.119 ± 0.018 (± SEM) and 0.108 ± 0.011 for medium and vehicle respectively (Figure 20). The greatest staining was seen on the day five of the assay where the OD had significantly increased to 1.909 ± 0.276 and 1.795 ± 0.215 in the medium and vehicle groups, respectively ($P<0.0001$ two-way ANOVA, n = 3). This increase in OD was also evident in the expected greater numbers of cells visible under light microscopy on day 5. There was no significant difference found in the rate of cell growth observed between the two groups $P=0.68$ (two-way ANOVA, n=3). Hence treatment with 1% v/v ddH_2O vehicle does not significantly affect cell growth in this assay.

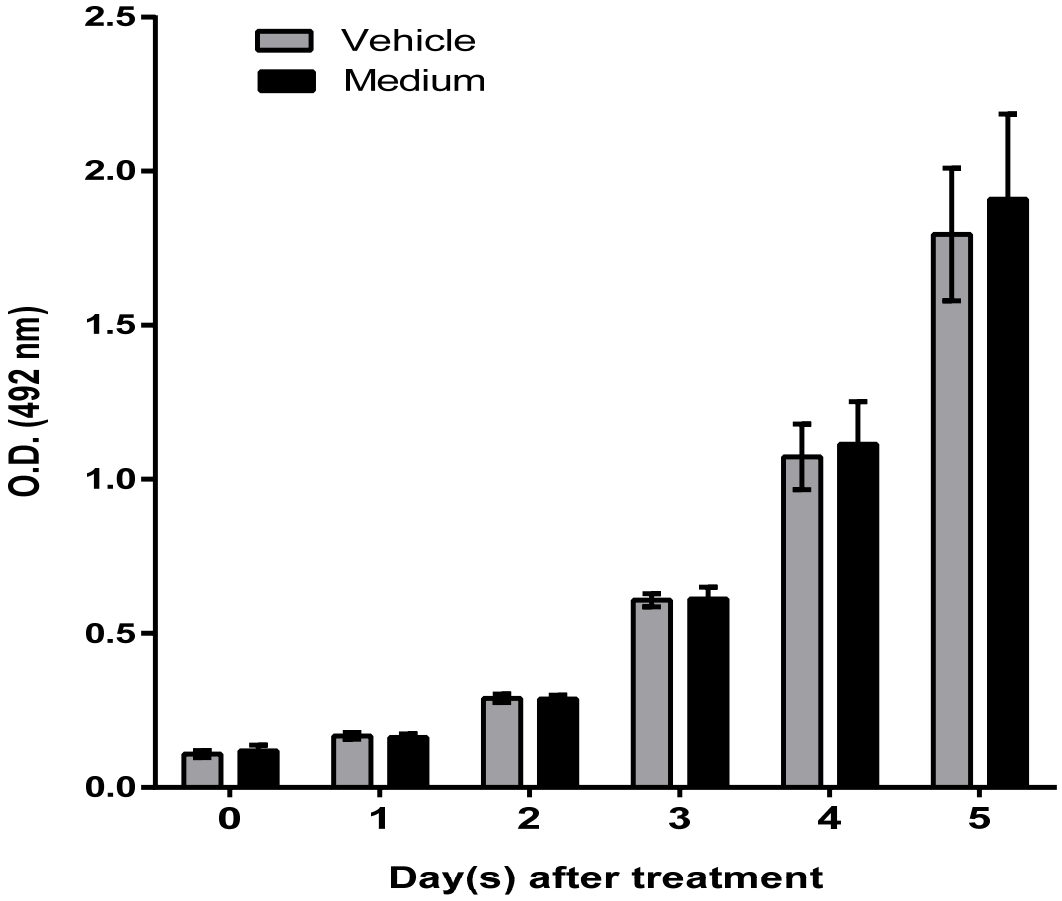

Figure 20 The SRB calorimetric assay was utilised to examine the density of cells present on the growth plates. Day 0 consists of the growth present on the day of treatment; the reference start of the assay. The graph shows the mean OD at 492 nm ± SEM for each group on each day. As growth increases, a greater number of cells become adherent, which when fixed and stained causes a greater amount of SRB staining which relates to an increased OD in the sample. There was no statistically significant difference between growth in medium containing vehicle (1% v/v sterile ddH_2O) and medium alone; P= 0.68, two-way ANOVA, n=3 separate experiments (each experiment contained 6 wells for each group on each day). In both groups there was a significant ($P < 0.0001$) increase in OD, and hence cell growth with time.

4.5.1.2. Does the Addition of NaHS Change the pH of the Medium?

These experiments were performed in order to rule out changes in pH as the determinant of any observed effects, particularly since NaHS can alter the pH of the solvent (Figure 21). There was no significant difference in the hydrogen ion (H^+) concentration (P =0.594, one-way ANOVA, n = 3) or the pH of the medium when 100 nM – 10mM NaHS was added (P = 0.534; one-way ANOVA, Dunnett's multiple comparison, n=3).

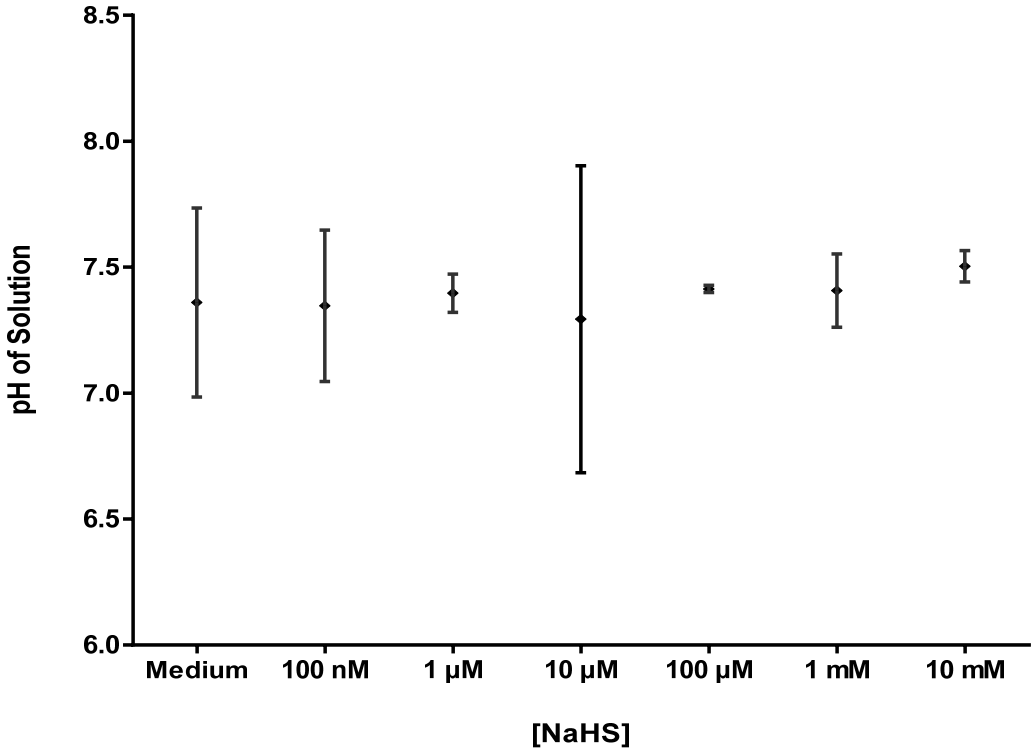

Figure 21 The effect of adding different concentrations of NaHS to the pH of the medium. Data are shown as the mean ± 95% confidence intervals (CI). There was no significant difference in the pH of the medium before and after the addition of NaHS (100nM – 10mM); P=0.492, one-way ANOVA with Dunnett's multiple comparisons, n=3.

4.5.1.3. The effect of NaHS within the incubator on control cell growth

On day five, control cells that were in the same incubator as NaHS/H_2S treated cells had a mean OD of 1.816 ± 0.226 compared with 2.156 ± 0.184 in those cells in a NaHS/H_2S-free incubator (Figure 22). Hence the growth in two groups was not significantly different, P = 0.31 (unpaired two-tailed t-test, n=3 experiments with 12 wells in each group per experiment).

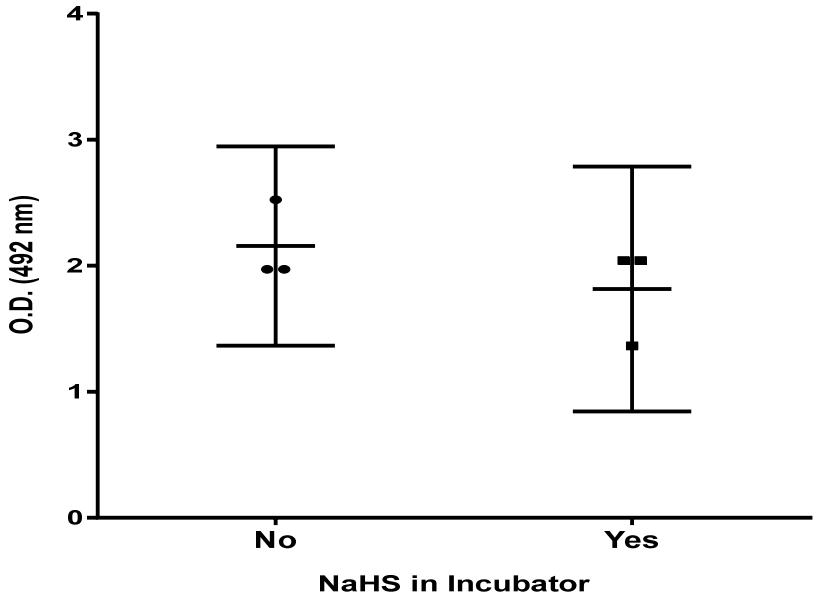

Figure 22 The OD at 492 nm observed on day five in the controls cells exposed to NaHS treated cells in their incubator, and those in an incubator devoid of NaHS. Data presented as the mean ± 95% CI. There was no statistically significant difference in the OD and thus growth between the two groups, P = 0.31 (unpaired two-tailed t-test, n=3 experiments with 12 wells in each group).

4.5.1.4. The effect of high concentrations of NaHS on adjacent cell growth

The volatile nature of H_2S could allow it to diffuse from wells with a high concentration of NaHS to those with low/no NaHS thus affecting those cells. This would create a concentration gradient with those cells closest to the 10 mM NaHS treatment group encountering a greater perturbation in their growth. Figure 23 shows the effect on cell growth of the proximity of the 10 μM NaHS treatment groups on each day of the SRB

assay. The mean % growth observed in the 10 µM NaHS treated cells adjacent to wells exposed to 10 mM NaHS was 74.6 % ± 14.8%, this was 90.5 ± 7.3% for cells one row of wells away, and 58.8 ± 22.3% for cells furthest away. Although it appears that the cells further away from the 10 mM NaHS (i.e. '2 rows away') had a reduced growth particularly on days 3 - 5, the considerable variability in the repeats rendered statistically insignificant. The location of 10 µM NaHS treated cells had no significant effect on cell growth (P = 1.00, two-way ANOVA with Tukey's multiple comparison test, n = 3 experiments each with 3 wells per group per day), only the number of days after treatment resulted in a significant change in the % growth of cells (P = 0.01).

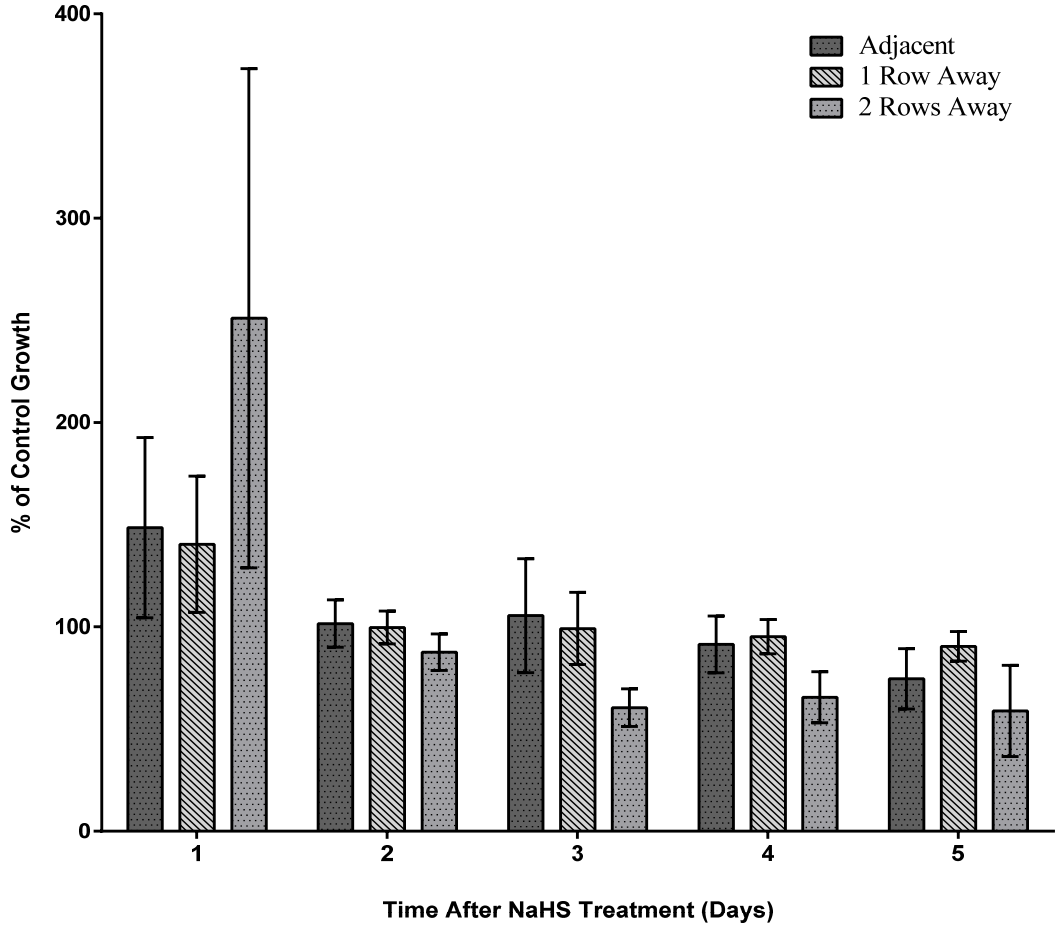

Figure 23 Bar Chart displaying the mean % cell growth ± SEM relative to controls in HEK293-hTRPA1 cells treated with 10 µM NaHS. The cells treated with 10 µM NaHS were either adjacent to, one row away, or two rows away from cells treated with 10 mM NaHS. Although the number of days after treatment had a significant effect on cell growth (P = 0.01, two-way ANOVA), the relative location of the 10 µM NaHS treated cells had no effect on growth of cells (P = 1.00, two-way ANOVA with Tukey's multiple comparison test, n = 3 experiments each with 3 wells per group per day).

4.5.1.5. The effects of chronic NaHS treatment on HEK293-hTRPA1 cells

The growth of control cells increased from a mean OD ± SEM of 0.077 ± 0.0139 (day 0) to 0.904 ± 0.600 (day 5; Figure 24A). All other treatment groups also exhibited a significant increase in growth with time (P = 0.0003) though not with NaHS treatment (P = 0.730; two-way ANOVA with Tukey's multiple comparison test, n = 3). The mean OD ± SEM following 10 mM NaHS increased from 0.099 ± 0.042 on day 1 to 0.153 ± 0.074 on day 5 post treatment. This rate of growth was much less than that observed in the other groups.

On further analysis of the data on day five (Figure 24B), it was observed that NaHS treatment caused a significant difference in growth (P = 0.043, one-way ANOVA, n=3), with only 10 mM NaHS inducing a significant reduction in the growth to 11% ± 3.4% of control (P < 0.01; Tukey's multiple comparisons). This reduction in growth is evident in Figure 24C which shows a photo of a plate from the experiment. Also shown in Figure 24B is the fitting of a log inhibitor versus a response curve with an IC_{50} of 2.6 mM (1.2 mM – 5.5 mM; 95% CI) and a R^2 0.83. There is a steep decline in the % growth at concentrations greater than 100 M NaHS; however, the variation in the data does mean the fit is not very accurate. To obtain a better fit, further repeats are required to help narrow the confidence intervals and there is a need for several more concentrations of NaHS to be assessed between 100 M – 10 mM.

(A)

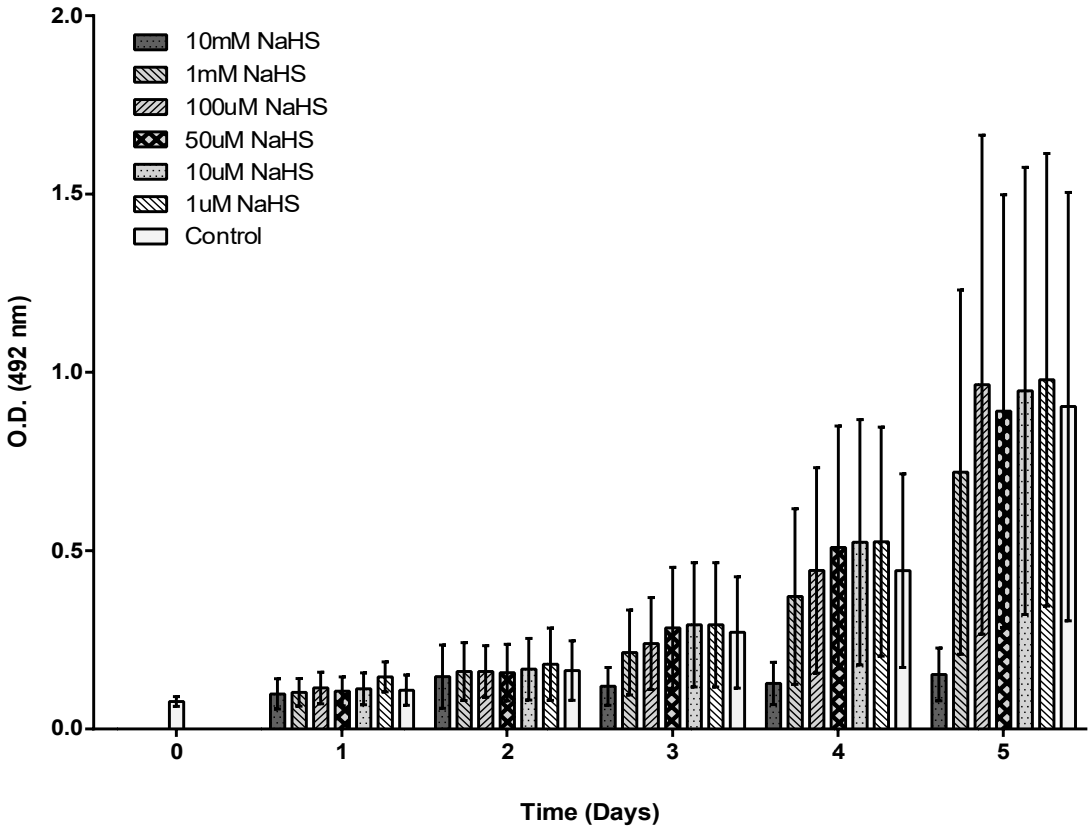

(B)

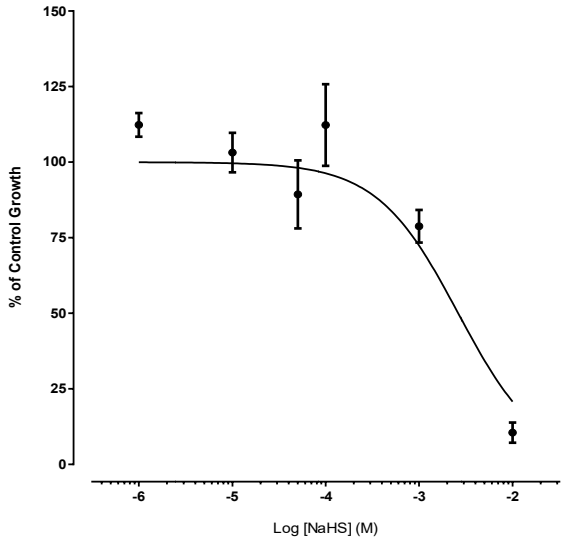

(C)

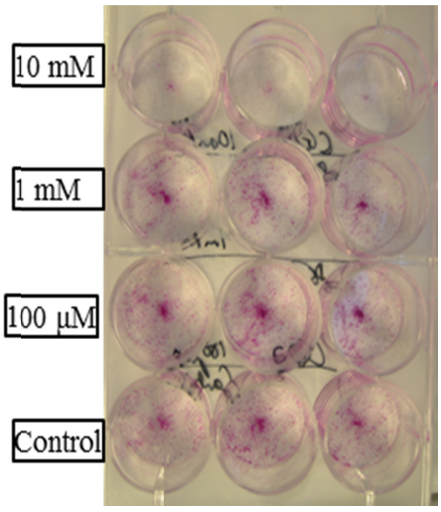

Figure 24 (A) The mean OD at 492 nM ± SEM observed in the cell growth assay on each day following chronic NaHS treatment of HEK293-TRPA1. Two-way ANOVA revealed a significant effect of day ($P<0.001$), but not NaHS concentration on cell growth ($P=0.730$, n=3 independent experiments each with up to 3 observations). **(B)** The mean % growth ± SEM of control cell growth on Day 5 following chronic treatment of HEK293-TRPA1 with 1 M – 10 mM NaHS. One-way ANOVA with Tukey's multiple comparison revealed a significant reduction in growth on day 5 following 10 mM NaHS treatment ($P<0.05$, n=3 independent experiments each with up to 3 observations). Superimposed is the log inhibitor versus normalised response curve; IC_{50} is 2.6 mM (1.2 mM – 5.5 mM; 95% CI), $R^2 = 0.83$, calculated using Prism 6.0, % Control Growth=$100/(1+10^{([NaHS]+2.58)})$ **(C)** Inset a photograph of a plate from this experiment on day 5 post treatment with NaHS.

4.5.2. The effect of chronic NaHS treatment on HEK293-EV cells

HEK293-EV cells were treated similarly to the HEK-hTRPA1 (Figure 25). There was a significant effect of time ($P < 0.0001$) but not NaHS treatment on the OD of the groups (i.e. growth, $P = 0.055$; two-way ANOVA, n=3). Tukey's multiple comparison test revealed 10 mM NaHS treatment caused a significant reduction in the OD ($P < 0.05$) relative to control cells on day 5. The % growth of HEK-EV cells on day 5 was significantly affected by 1 M – 10 mM NaHS (Figure 25B, $P<0.0001$, one-way ANOVA, n=3). Tukey's multiple comparison tests revealed that in fact only 10 mM NaHS induced a significant reduction in the growth, with the mean cell growth 16% ± 4.6% of control ($P < 0.001$). Figure 25B also shows the fit of a log inhibitor versus response curve to the data, this has an IC_{50} of 2.3 mM (1.1 mM – 5.0 mM; 95% CI) with a R^2 0.76. Interestingly, as observed with HEK-TRPA1, 100 M NaHS tends to buck the dose-dependent trend of reduced cell growth on day 5 following NaHS treatment. This could represent a true observation with a partial stimulatory effect occurring at this concentration following a complex interaction of NaHS with cell systems, or it could simply just arise from the error margins in this assay.

(A)

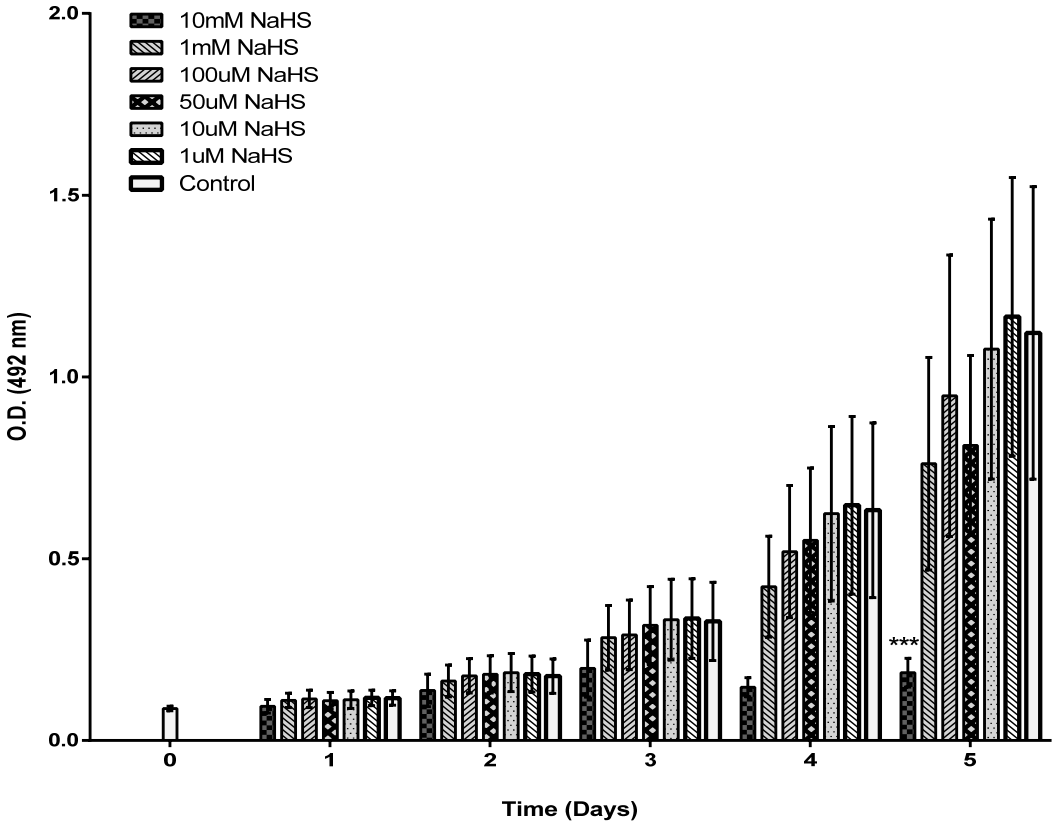

(B)

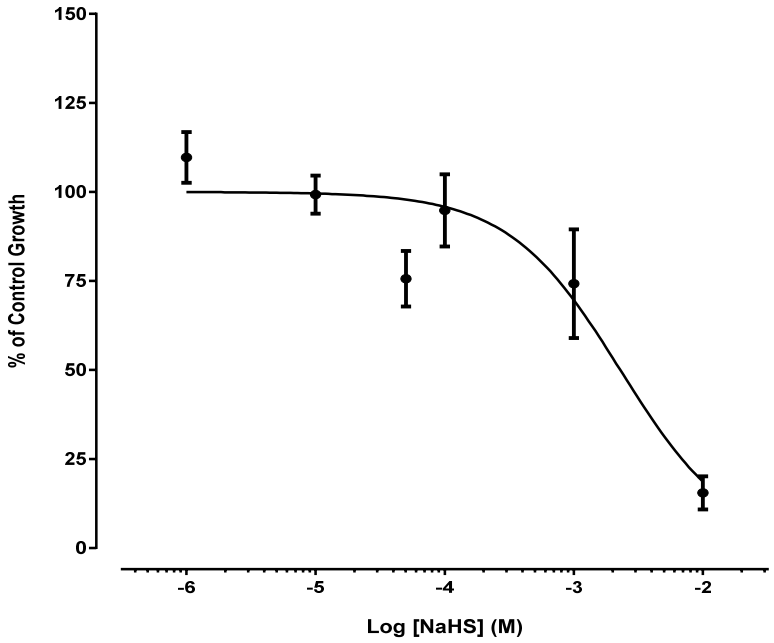

Figure 25 (A) The mean OD ± SEM observed in the cell growth assay on each day following chronic treatment of HEK-EV with NaHS. Two-way ANOVA revealed a significant effect of day ($P<0.0001$), but not the NaHS concentration on cell growth ($P=0.055$, n=3 independent experiments each with up to 3 observations). **(B)** The mean % growth ± SEM of control cell growth on Day 5 following chronic treatment of HEK-EV with 1 M – 10 mM NaHS. One-way ANOVA with Tukey's multiple comparison revealed a significant reduction in growth on day 5 following 10 mM NaHS treatment ($P<0.001$, n=3 independent experiments each with up to 3 observations). Superimposed is the fitting of a log inhibitor versus normalised response curve; IC_{50} is 2.3 mM (1.1 mM – 5.0 mM; 95% CI), R^2 = 0.76, calculated using Prism 6.0, % Control Growth=$100/(1+10^{([NaHS]+2.64)})$.

4.5.3. The effects of acute NaHS on HEK-hTRPA1 cells

In the acute experiments cells were treated with NaHS for 30 minutes only. Initially, screening experiments were performed to identify the optimal NaHS concentrations to use in the formal experiments (Figure 26). Acute treatment with 1 M – 10 mM NaHS caused a significant difference in the growth of cells (P=0.001, one-way ANOVA, n= 3 experiments). Tukey's multiple comparisons test revealed the effect was primarily due to the 10 mM NaHS treatment, with growth at 38 % ± 11.4% of controls (mean ± SEM). This matches the results observed with chronic NaHS treatment and suggests that the inhibition in growth observed with chronic NaHS treatment may in fact be occurring during the early stages of the application. This effect is long-lasting and continues even after the NaHS is removed. The preliminary experiments did highlight a need for a 3 mM NaHS treatment group to help improve the resolution in the data between 1 mM NaHS and 10 mM NaHS.

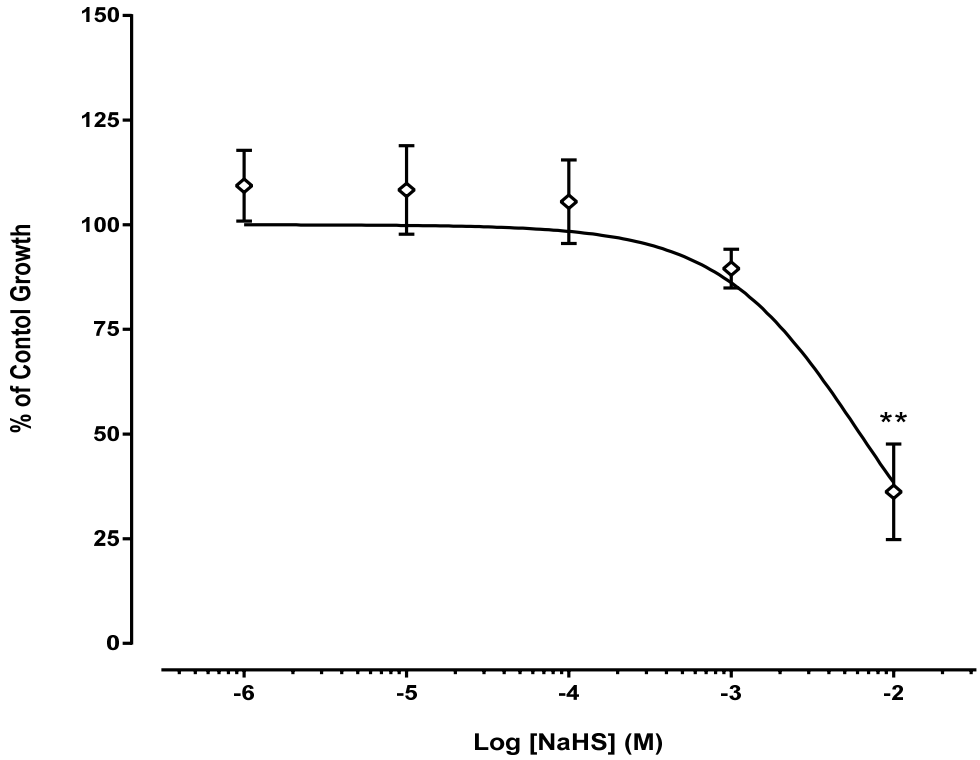

Figure 26 The growth of HEK293-TRPA1 cells on day 6 following an acute 30 minute treatment with NaHS (1 M – 10 mM). Data is expressed as the mean ± SEM % of control growth. There was a significant reduction in growth following acute treatment with 10 mM NaHS relative to vehicle and other NaHS treatment groups ($P < 0.05$; one-way ANOVA with Tukey's multiple comparison, n=3 experiments with up to 4 repeats per experiment). Also shown is a log inhibitor versus normalised response curve with an IC_{50} is 6.2 mM (3.0 mM – 12.8 mM; 95% CI), $R^2 = 0.77$, calculated using Prism 6.0, % Control Growth=$100/(1+10^{([NaHS]+2.21)})$.

The main experiments were then performed to assess when the effects of 10 mM NaHS became evident on the standard 5 day cell growth assay (Figure 27A). These experiments indicated that both day ($P < 0.0001$) as well as 30 minute NaHS treatment ($P < 0.001$) caused a significant difference in the OD (two-way ANOVA, n=3). Tukey's multiple comparisons test revealed that this significant effect on growth was predominantly due to 10 mM NaHS ($P < 0.01$). This effect on growth was only apparent on day 5 post-acute NaHS treatment and is consistent with the data from the chronic treatment group (section 4.5.1.5). When the results are assessed in terms of the % of control growth (Figure 27B), acute 10 mM NaHS treatment caused a significant reduction in growth to 65.8% ± 4.7% ($P<0.01$, one-way ANOVA with Tukey's multiple comparisons test, n =3). This appears to indicate that acute treatment with 10 mM NaHS has a smaller effect on cell growth relative to chronic treatment where growth was 11% of control on day 5. An explanation may be that the greater duration of NaHS exposure during chronic treatment allows it to hamper cell growth further.

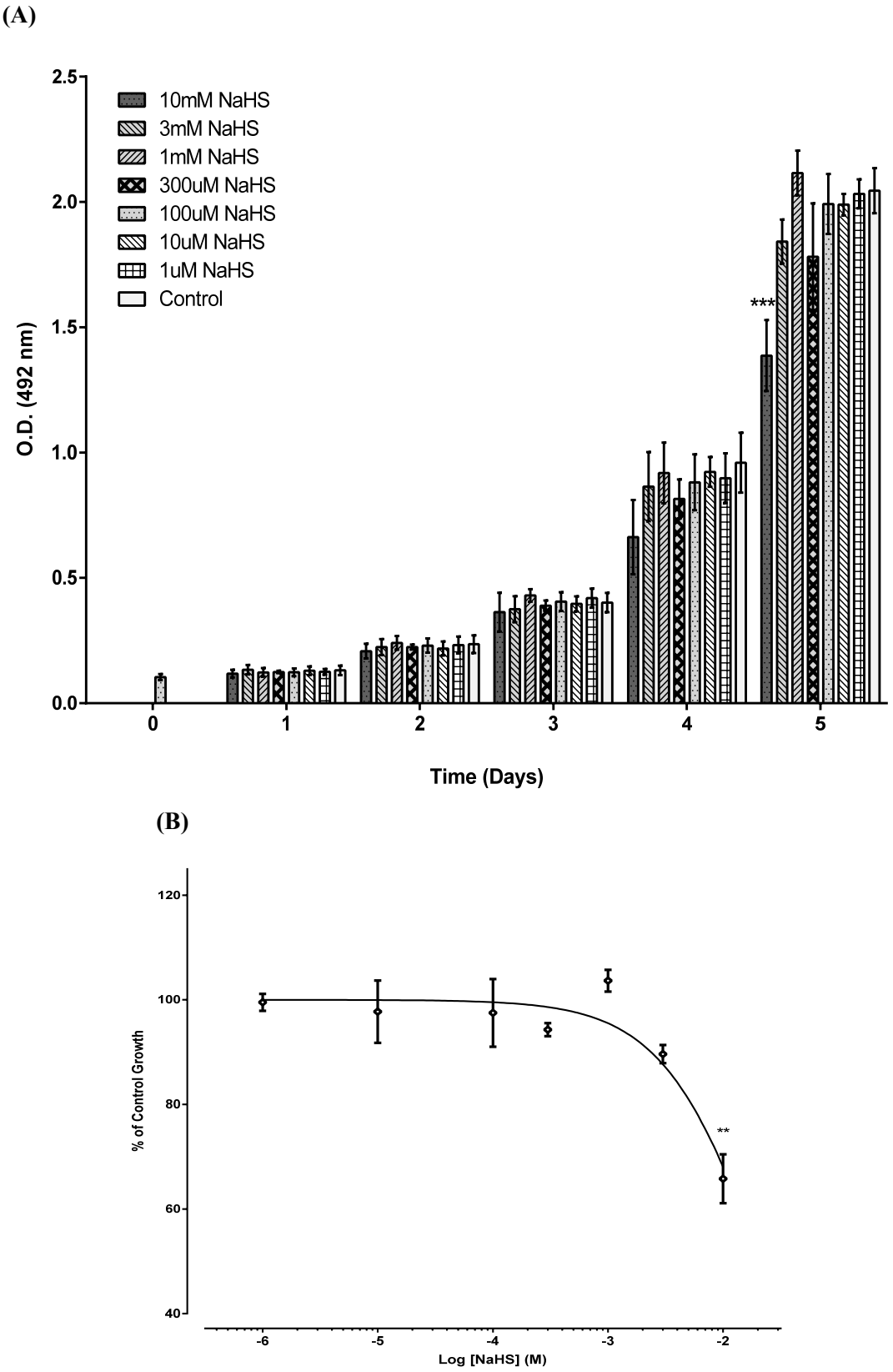

Figure 27 (A) The mean OD ± SEM observed in the cell growth assay on each day following acute treatment of HEK293-TRPA1 with NaHS. Two-way ANOVA revealed a significant effect of day ($P<0.0001$), and the acute 30 minute NaHS treatment on cell growth ($P=0.001$, n=3 independent experiments each with up to 3 observations). **(B)** The data from **A** on day 5 expressed as a mean ± SEM % growth. One-way ANOVA with Tukey's multiple comparison revealed a significant reduction in growth on day 5 following 10 mM NaHS treatment ($P<0.001$-0.001, n=3 independent experiments each with up to 3 observations). Superimposed is a fitted log inhibitor versus normalised response curve; IC_{50} is 21 mM (15 mM – 30 mM; 95% CI), R^2 = 0.72, calculated using Prism 6.0, % Control Growth=$100/(1+10^{([NaHS]+1.67)})$.

4.5.4. The effects of acute NaHS treatment on HPBF cells

These experiments sought to investigate the effects of NaHS on cultured primary cells from the lung (HPBF). This was performed in order to examine if a similar effect on growth is observed as had been with the immortalised HEK293-hTRPA1 cells. The HPBF were plated at a lower density relative to the HEK293 cells as preliminary experiments (data not shown) found they have a propensity to form layers as they grow in close proximity to each other. Preliminary experiments examined the effect of vehicle versus medium on the growth of HPBF and found there was no significant difference in growth between medium or vehicle treated HPBF cells ($P = 0.51$, 2-tailed unpaired t-test, n=3; data not shown). What was evident was a lower OD in this assay, this is attributable to the lower density of plated cells together with a tendency of the fibroblasts to stain weakly in the SRB assay (Figures 24 and 28).

However, there was a significant effect of both day ($P < 0.0001$) as well as a 30 minute NaHS treatment ($P < 0.001$) on the OD (two-way ANOVA, n=3). Tukey's multiple comparisons test revealed further that both 3 mM and 10 mM NaHS had a significant effect on the OD relative to the vehicle control on day 5 ($P = 0.01$ for both; Figures 28A and 29). This was also evident when analysed as % of cell growth ($P < 0.0001$, one-way ANOVA, n=5; Figure 28B). Growth on day 5 after 3 and 10 mM NaHS treatments was 30% ± 10.7 and 23% ± 6.6% respectively, relative to the vehicle controls ($P < 0.05$; Tukey's multiple comparisons). The reduced growth following 10 mM NaHS and the significant effect of 3 mM NaHS suggests HPBF have an increased susceptibility to NaHS relative to HEK-TRPA1 cells; this is emphasised by the lower IC_{50} of 1.2 mM NaHS (Figure 28B). This IC_{50} has a narrower 95% confidence interval (0.3 mM -4.3 mM) and thus provides a more accurate estimation of the IC_{50} in the HPBF population.

The concentration-response curve also appears to have a much more recognisable curve than that seen with the HEK-TRPA1 cells; this may be due to the increased sensitivity allowing the determination of the peak inhibitory response in this assay. However, the R^2 value is lower compared to the HEK cells at 0.62. Although a higher R^2 value does

normally suggest the regression line forms a good fit of the data, this is not a universal feature as sometimes a regression line with a lower R^2 value may provide a more accurate model of the interaction between the independent and dependent variables. Figure 29 provides photographs of an actual experimental plate of HPBF on day 5 post-acute NaHS treatment. As can be seen, there is a reduction in the SRB colour in the wells when moving from the vehicle treatment to 10 mM NaHS group of wells. Microscopically the reduced number of cells is evident at 40 times magnification.

(A)

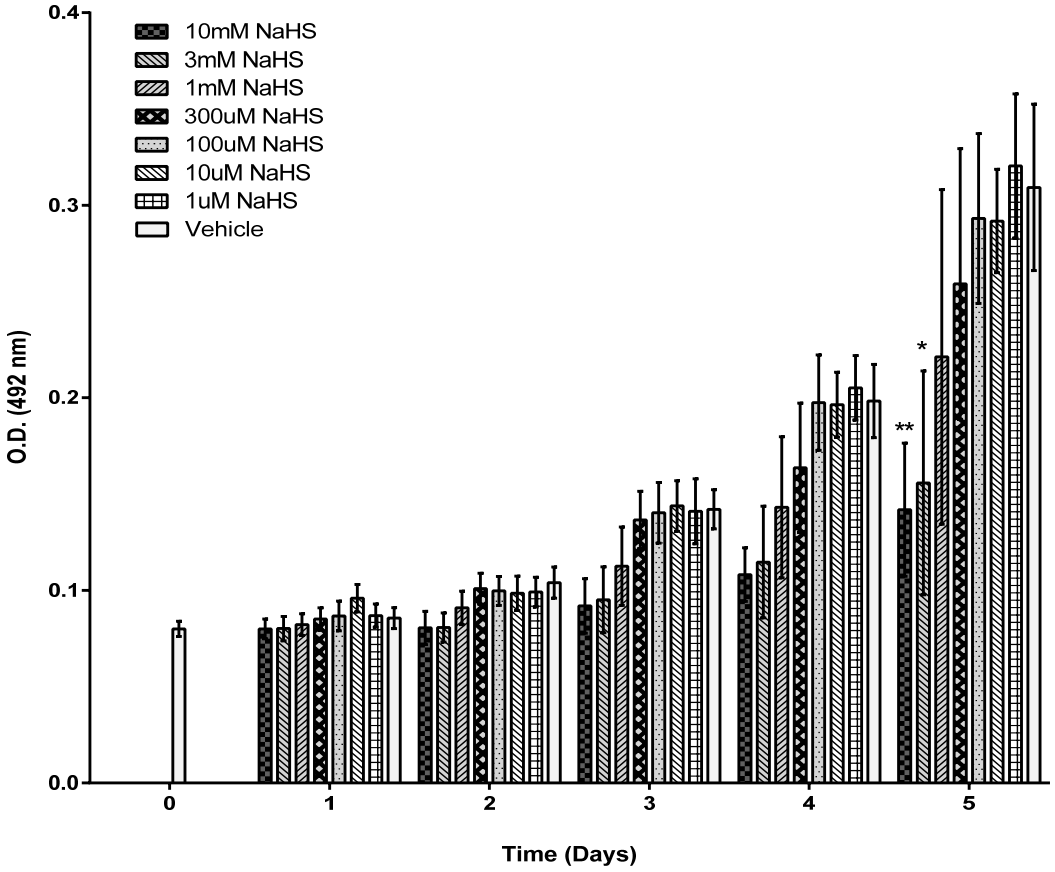

(B)

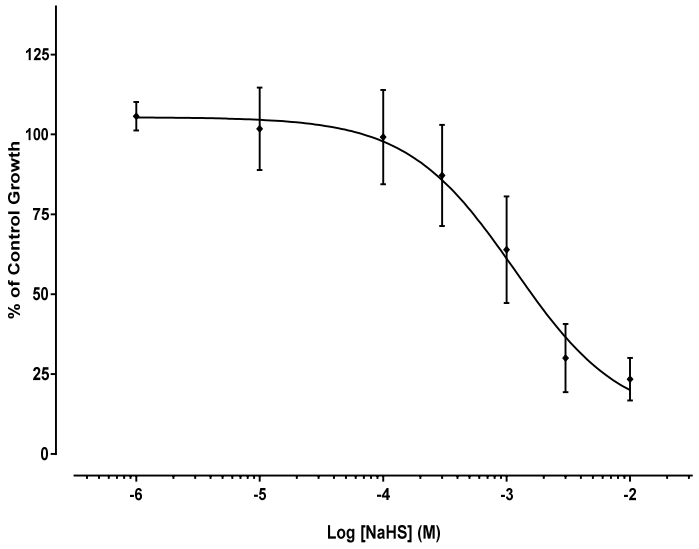

Figure 28: **(A)** The mean OD ± SEM observed in HPBF following acute NaHS treatment (1 µM – 10mM). Two-way ANOVA revealed a significant effect of day ($P<0.0001$) and the acute NaHS treatment on OD i.e. cell growth ($P<0.0001$, n=3 independent experiments each with up to 3 observations). Both 3 mM and 10 mM NaHS induced a significant reduction in OD relative to vehicle treatment ($P=0.01$, Tukey's multiple comparison). **(B)** The data from day 5 in **A** expressed as the mean ± SEM % cell growth. One-way ANOVA with Tukey's multiple comparison revealed a significant reduction in growth on day 5 following both 3 mM and 10 mM NaHS treatment ($P<0.001$-0.05, n=5 independent experiments each with up to 3 observations). Also shown is the fitted log inhibitor versus response curve; IC_{50} is 1.2 mM (0.3 mM – 4.3 mM; 95% CI), $R^2 = 0.62$, calculated using Prism 6.0, % Control Growth= $10.1 + \{95.3/(1+10^{([NaHS]+2.94)})\}$.

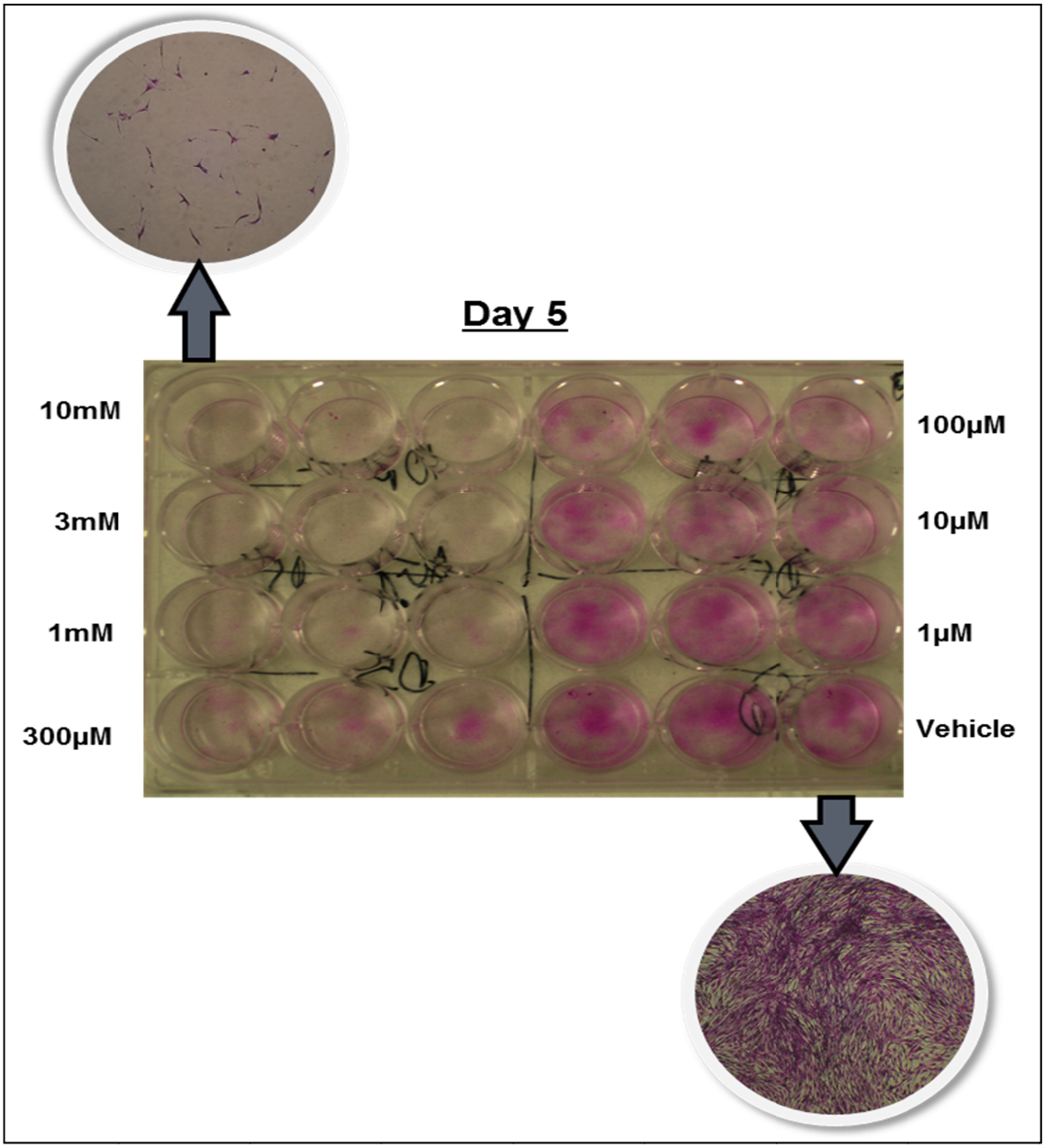

Figure 29: Pictures of a plate of HPBF at day 5 following acute treatment with 1 M – 10 mM NaHS, fixation and staining. The pictures in the circle represent a 40 fold magnification of a well in the vehicle and 10 mM NaHS treatment groups. It can be seen that the growth in the control group is significantly greater than with 10 mM NaHS.

4.5.5. Application of NAC on HEK-TRPA1 and HPBF cells

These experiments sought to examine the role of NAC in HEK and HPBF cells in the presence as well as absence of NaHS; this was at the IC_{50} concentrations of each cell line.

4.5.5.1. The effect of NAC and NaHS on HEK-TRPA1 cells

An acute NAC treatment did not induce a significant effect on growth of HEK-hTRPA1 cells (P = 0.63, one-way ANOVA, n=3; Figure 30A). However, as seen in figure 30A there does appear to be a trend of NAC inhibiting growth. Treatment with 10 mM NAC reduced growth to 42% ± 11.4% of control cells; in contrast this was 61% ± 26.7% after 100 nM NAC.

Next the effects of NAC pre-treatment on the NaHS induced inhibition of cell growth were examined. The addition of 10 mM NaHS reduced the mean growth to 86 ± 21% of the control response, whereas in the presence of 10mM NAC pre-treatment, the growth was 84 ± 6% (Figure 30B). Therefore 10mM NaHS alone did not have a significant effect on growth relative to vehicle treatment (P=0.536, unpaired two-tail t-test, n=3); this result is inconsistent with those observed in section 4.5.3. This difference may be due to an underpowered study and thus further repeats would be beneficial. However in order to examine the overall effects of NaHS on HEK-hTRPA1 cells treated with NAC, the data from figure 30A and B were pooled (Figure 31). It was subsequently evident that 10 mM NaHS induced a significant effect on growth (P=0.015, two-way ANOVA, n=3 independent experiments). This growth was in fact greater in the presence rather than absence of 10 mM NaHS. Furthermore the aforementioned trend of reduced cell growth with increasing NAC concentrations appears to have been attenuated in the presence of 10 mM NaHS (Figure 31).

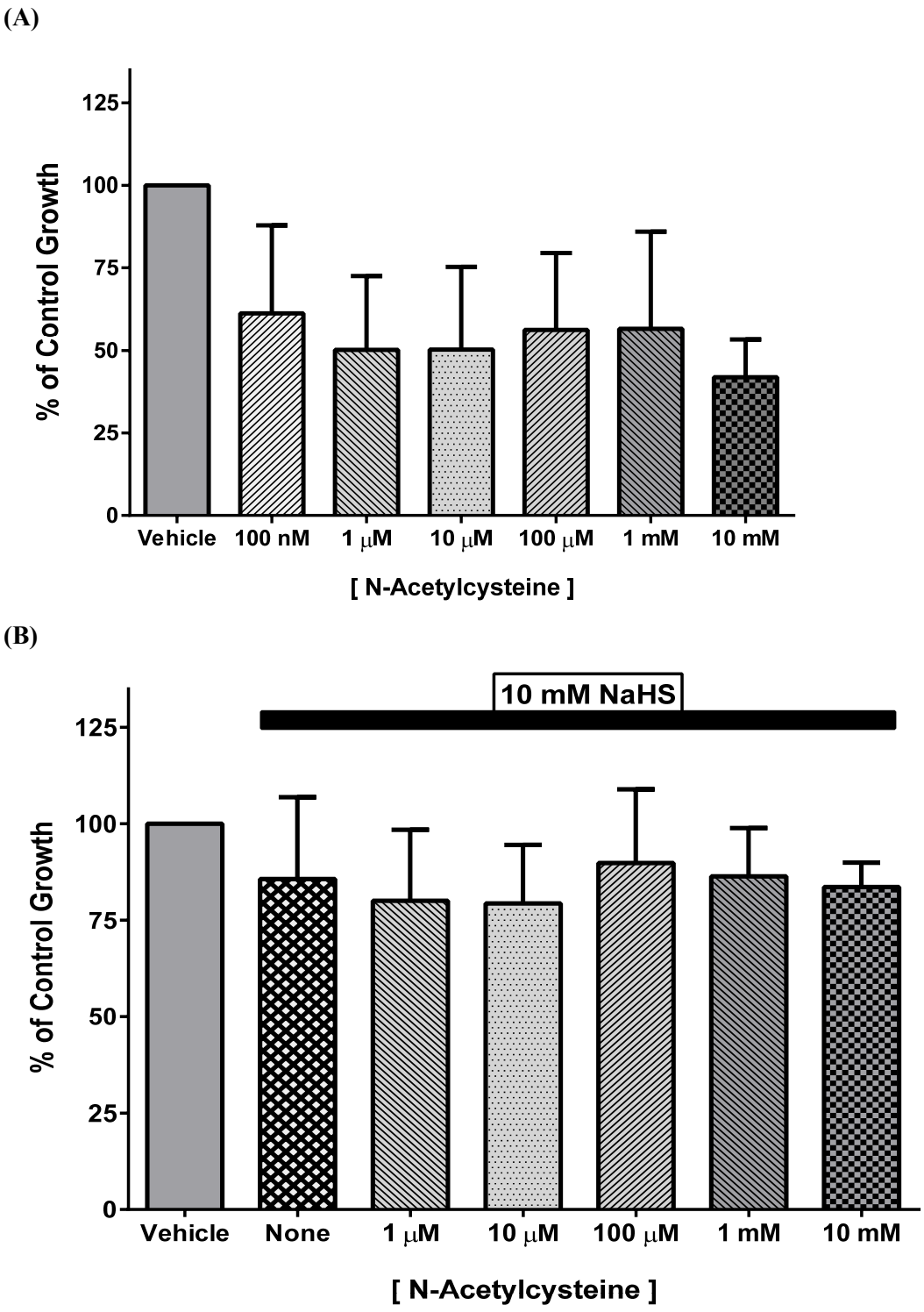

Figure 30: (A) The mean % cell growth ± SEM observed on day 5 following acute treatment (1.5 hours) of HEK293-TRPA1 cells with 100 nM – 10 mM NAC. One-way ANOVA with Dunnett's multiple comparison, revealed there was no significant reduction in growth P=0.63 (n=3 independent experiments each with up to 3 repeats). **(B)** The mean % cell growth ± SEM observed on day 5 following acute treatment (1.5 hours) of HEK293-TRPA1 cells with 1 M – 10 mM NAC and 10 mM NaHS. One-way ANOVA with Dunnett's multiple comparison revealed there was no significant reduction in growth P=0.959 (n=3 independent experiments each with up to 3 repeats).

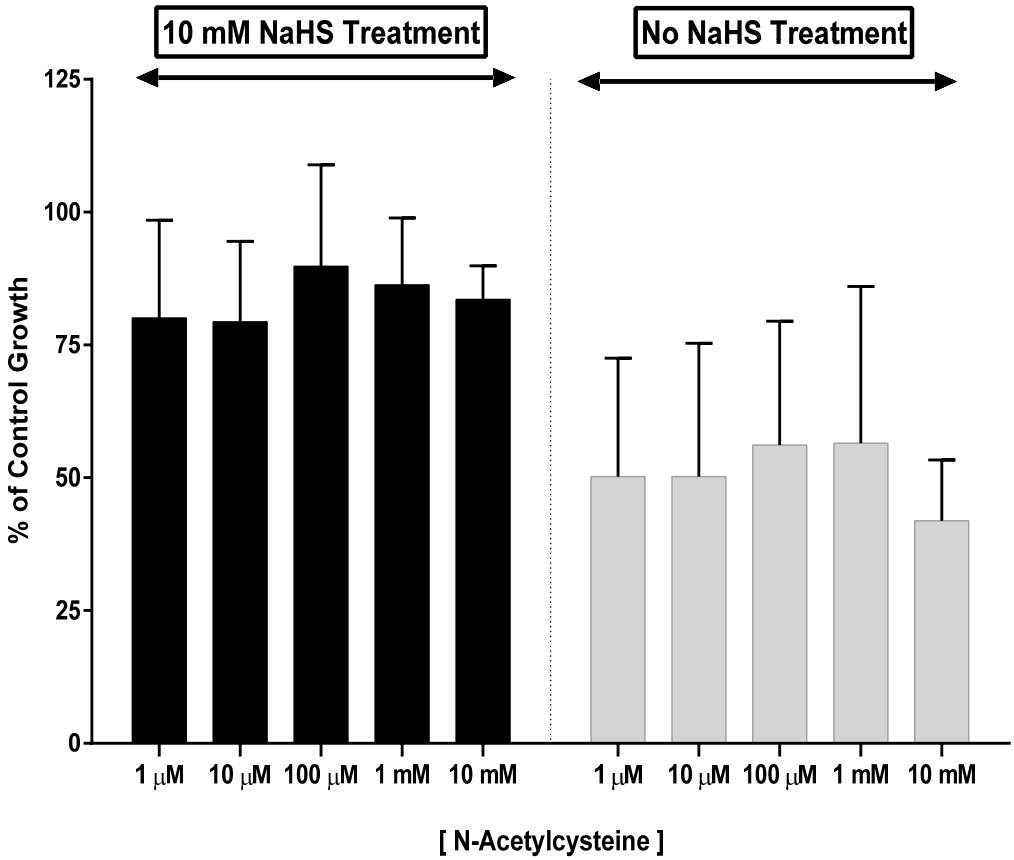

Figure 31: The mean % cell growth ± SEM observed on day 5 following a 1.5 hr treatment of HEK293-TRPA1 cells with 1 M – 10 mM NAC with or without a 0.5 hr of 10 mM NaHS. Two-way ANOVA revealed the concentration of NAC had no significant effect on growth (P=0.979), however the presence of NaHS significantly affected growth P=0.015 (n=3 independent experiments each with up to 3 repeats).

4.5.5.2. The effect of NAC and NaHS on HPBF cells

These experiments were performed in a similar manner to those is 4.5.5.1, with HEK-TRPA1 substituted with HPBF. Acute 1.5 hour application of NAC caused a significant reduction in HPBF growth on day 5 (P=0.017; one-way ANOVA, n=3); this was particularly evident following 1 mM and 10 mM NAC treatment with growth at 44% ± 11.2% and 53% ± 9.1% respectively (Figure 32A). However, Dunnett's multiple comparisons test revealed that only 1 mM NAC had a statistically significant effect on growth relative to the vehicle treated controls. This initially appears to show that HPBF have a greater sensitivity to NAC compared with HEK293-TRPA1.

In the next group of experiments, HPBF were treated with NAC in a similar manner to the HEK293 cells in 4.5.5.1 (Figure 32B). On this occasion a 1 mM NaHS concentration was utilised due to the lower IC_{50} of 1.2 mM identified in section 4.5.4. There was a significant reduction in cell growth following treatment with 1 mM NaHS (76 ± 1.8%) in the absence of NAC (P=0.0002, unpaired two-tailed t-test, n = 3); this was consistent with the inhibitory effects observed in 4.5.4. Pre-treatment with NAC (1 M – 10 mM) in the presence of NaHS did not have a significant effect on growth (P = 0.160, one-way ANOVA with Dunnett's multiple comparison corrections, n=3, figure 32B). However when pooled comparisons were made between HPBF treated with NAC (1 M – 10 mM) in the presence and absence of 1 mM NaHS (Figure 33), NAC was found to have a significant effect on cell growth (P=0.004), in contrast 1 mM NaHS did not (P=0.339, two-way ANOVA, n=3). These results are very interesting as what they appear to initially suggest is that although the 1 mM NaHS independently induced a significant reduction in growth relative to controls, this effect was mitigated in the presence of NAC.

A more thorough examination of the graphs in figures 32B and 33 suggest that 1 mM NaHS did result in an inhibition of growth, this inhibition was greater with 1 µM NAC pre-treatment, however 10 -100 µM NAC (mean growth 92 ± 11%) reversed these effects. Finally 1 mM and 10 mM NAC (52% ± 21.5% and 49% ± 15.4% respectively) in the presence of NaHS induced a similar level of growth inhibition to that observed with these concentrations of NAC in the absence of NaHS. The results suggest a biphasic process occurring with NAC in the presence of NaHS; at the high micromolar concentrations NAC is able to reverse the inhibitory effects of 1mM NaHS but this is then lost as NAC enters the mM concentrations as it begins to inhibit cell growth. This theory is supported by the results of a one-way ANOVA with Dunnett's multiple comparisons; there was a significant effect of 1 mM NaHS in the absence ($P \leq 0.05$) and presence of 1 M NAC ($P \leq 0.01$) in comparison with vehicle, however 10 and 100 M NAC were not significantly different ($P \geq 0.05$) from vehicle (n=3; in these comparisons 1mM and 10mM NAC data was excluded). Although it is fully appreciated that repeating such statistical tests with the exclusion of data can result in false positive results.

(A)

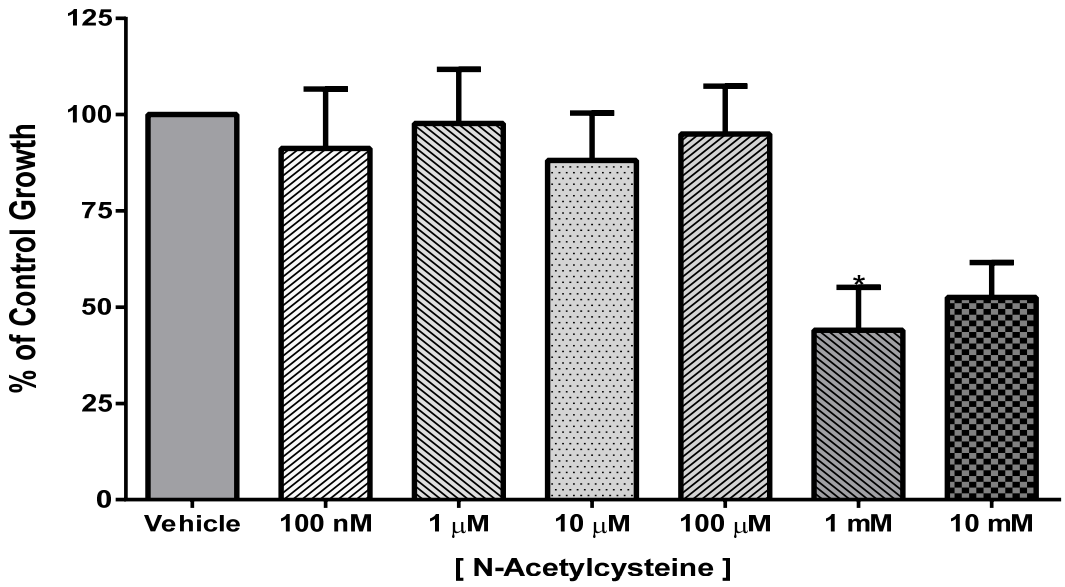

(B)

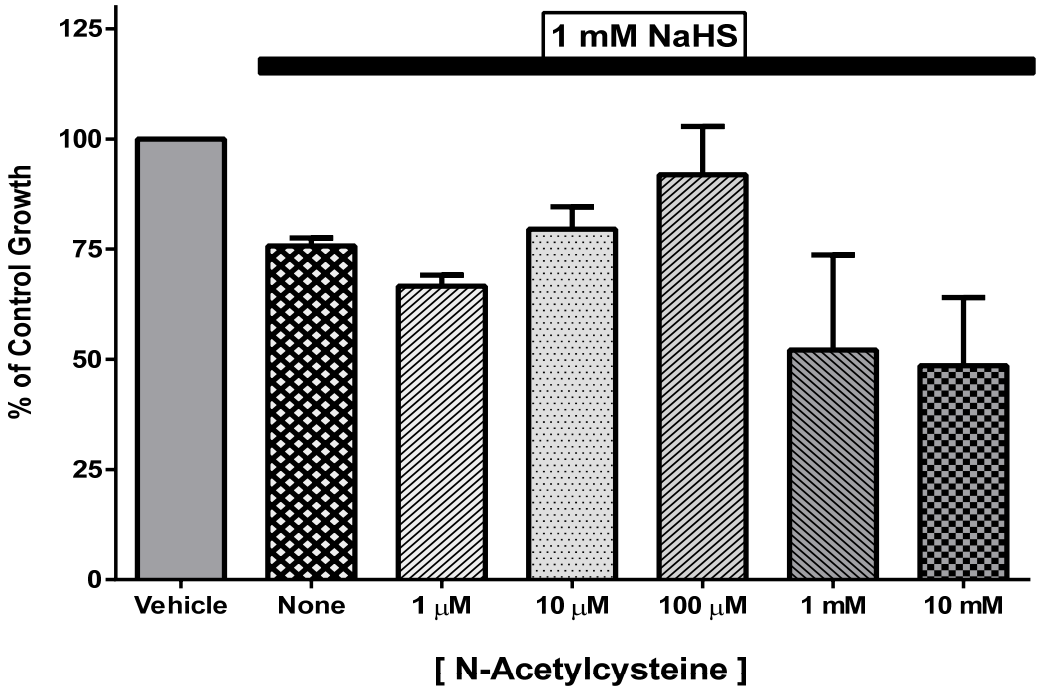

Figure 32: (A) The mean % cell growth ± SEM observed on day 5 following acute treatment (1.5 hours) of HPBF cells with 100 nM – 10 mM NAC. One-way ANOVA revealed a significant effect of NAC on growth P=0.017, only 1 mM NAC had a significantly different growth to vehicle after Dunnett's correction (n=3 independent experiments each with up to 3 repeats). **(B)** The mean % cell growth ± SEM observed on day 5 following acute treatment (1.5 hours) of HPBF cells with 1 M – 10 mM NAC and 30 min of 1 mM NaHS. One-way ANOVA with Dunnett's multiple comparison revealed NAC did not significantly affect cellular growth following 1 mM NaHS treatment P=0.160 (n=3 independent experiments each with up to 3 repeats).

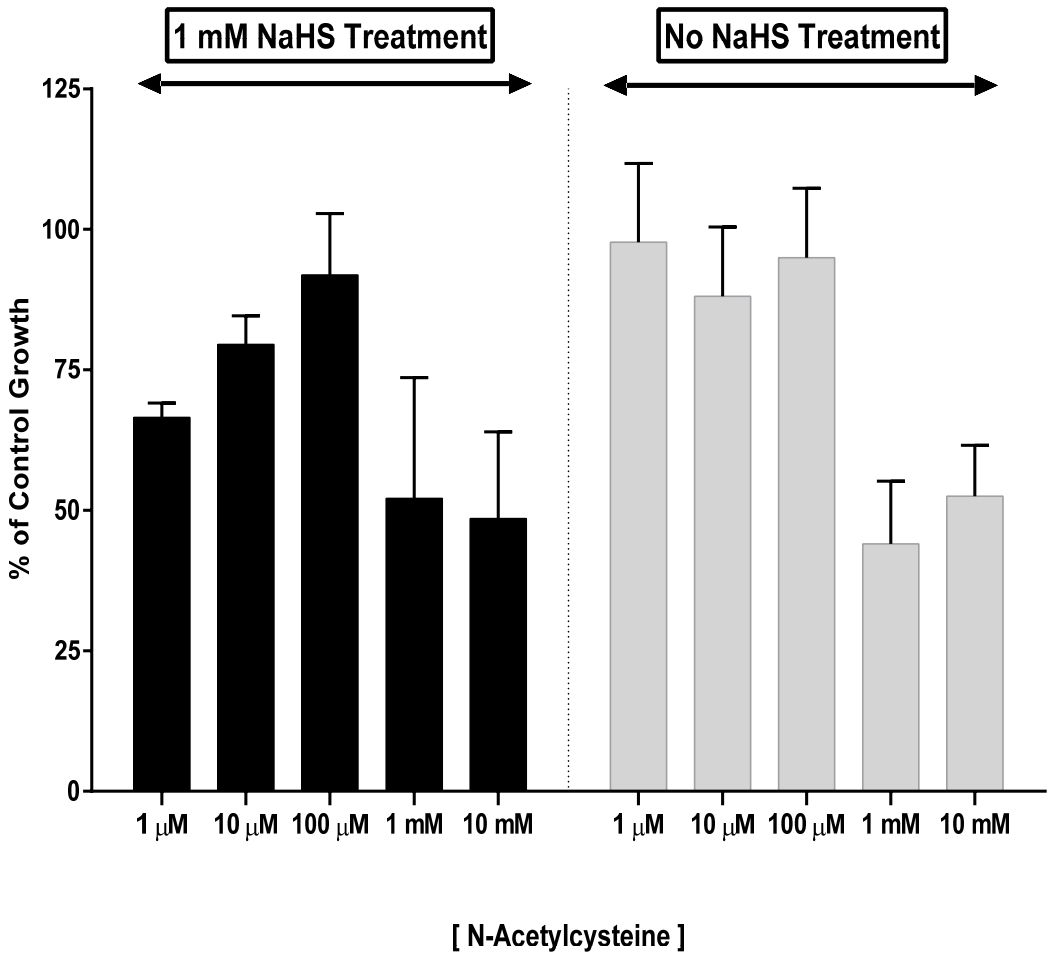

Figure 33: The mean % cell growth ± SEM observed on day 5 following a 1.5 hr treatment of HPBF cells with 1 M – 10 mM NAC with or without a 0.5 hr of 1 mM NaHS. Two-way ANOVA revealed the concentration of NAC had a significant effect on growth (P=0.004), however the effects of 1 mM NaHS were not significant on cell growth P=0.339 (n=3 independent experiments each with up to 3 repeats).

4.5.6. The effect of NaHS on cell cycle in HEK-TRPA1 and HPBF cells

These experiments sought to examine whether the NaHS mediated a reduction in cell growth observed with HEK293-TRPA1 and HPBF was due to cellular quiescence during the cell growth cycle.

4.5.6.1. The effects of NaHS on the cell cycle in HEK-TRPA1 cells

The mean number of cells detected on the flow cytometer per treatment was 11 472, thus the histograms shown in figure 34 represent a large enough sample of cells to provide a respectable estimation of the population characteristics (Riccardi and Nicoletti, 2006).

The results demonstrated that the vehicle treated cells that had not been stained by PI produced a large number of counts at the lower range of the FL2H channel; this is most likely due to autofluorescence from the cells (Figure 34). Vehicle cells stained with PI produced two major peaks one around 180 and another around 360 in the FL2-H channel. These peaks are representative of the G1 and G2/M stages of the cell cycle, and the data are consistent with the peaks reported in the literature when utilising PI staining (Nunez, 2001). The interposing area is regarded as containing cells within the S-phase of the cell cycle. The ModFit algorithm was used to determine the contribution of the different phases of the cell cycle (G1, S, G2/M) to the histogram (Figure 34).

Using this model, treatment with 10 mM NaHS caused a reduction in the proportion of cells in G1 (40.9 ± 2.6 %), an increase in S (59.1 ± 2.6 %) but there were none in the G2/M phase (0 ± 0 %) (Figures 34 and 35A). In comparison, vehicle treated cells displayed a different distribution of cells in the phases of the cell cycle: 42.7 ± 1.2 % (G1), 49.2 ± 1.1 % (S), and 8 ± 0 % (G2/M). Thus over 3 independent experiments, 10 mM NaHS induced a decrease in the proportion of cells in the G1 and G2/M phases with a complementary increase in the S phase of the cell cycle (Figure 35A). This data

suggests that 10 mM NaHS treatment is preventing the normal cellular progression into the G2/M phase of the cell cycle, with cells spending a disproportionate length of time in the S-phase. Nevertheless the HEK293-TRPA1 cells do clearly progress through the cell cycle as section 4.5.3 and Figure 25 have shown that there is an increase in growth on day 5 relative to day 1. The various treatments did not have a statically significant effect on the proportion of cells in each phase of the cell cycle ($P > 0.98$, two-way ANOVA with Bonferroni multiple comparisons, $n = 3$).

A toxic dose of hydrogen peroxide was utilised as a positive control to examine its effects on the populations of cells in various stages of the cell cycle. There was a proportional reduction in the number of cells present at day 5 after treatment with 100 μM H_2O_2 this was evident subjectively under microscopic examination as well as objectively. The later was noted by the persistently lower total cell counts (mean of 7 557) on the flow cytometer, whereas the other treatment groups had a mean of ≥ 10 000 cells per sample. In concordance with this there was a significant decrease in the number of diploid cells observed following treatment with 100 μM H_2O_2 ($P < 0.05$, two-way ANOVA with Bonferroni multiple comparisons, $n = 3$). Furthermore H_2O_2 also caused an increase in amount of cellular debris (50.9 ± 17.5 %) compared with vehicle controls (13.1 ± 3.4 % debris). However acute H_2O_2 treatment did not significantly affect the distribution of cells in the various stages of the cell cycle ($P > 0.05$, two-way ANOVA with Bonferroni multiple comparisons, $n = 3$).

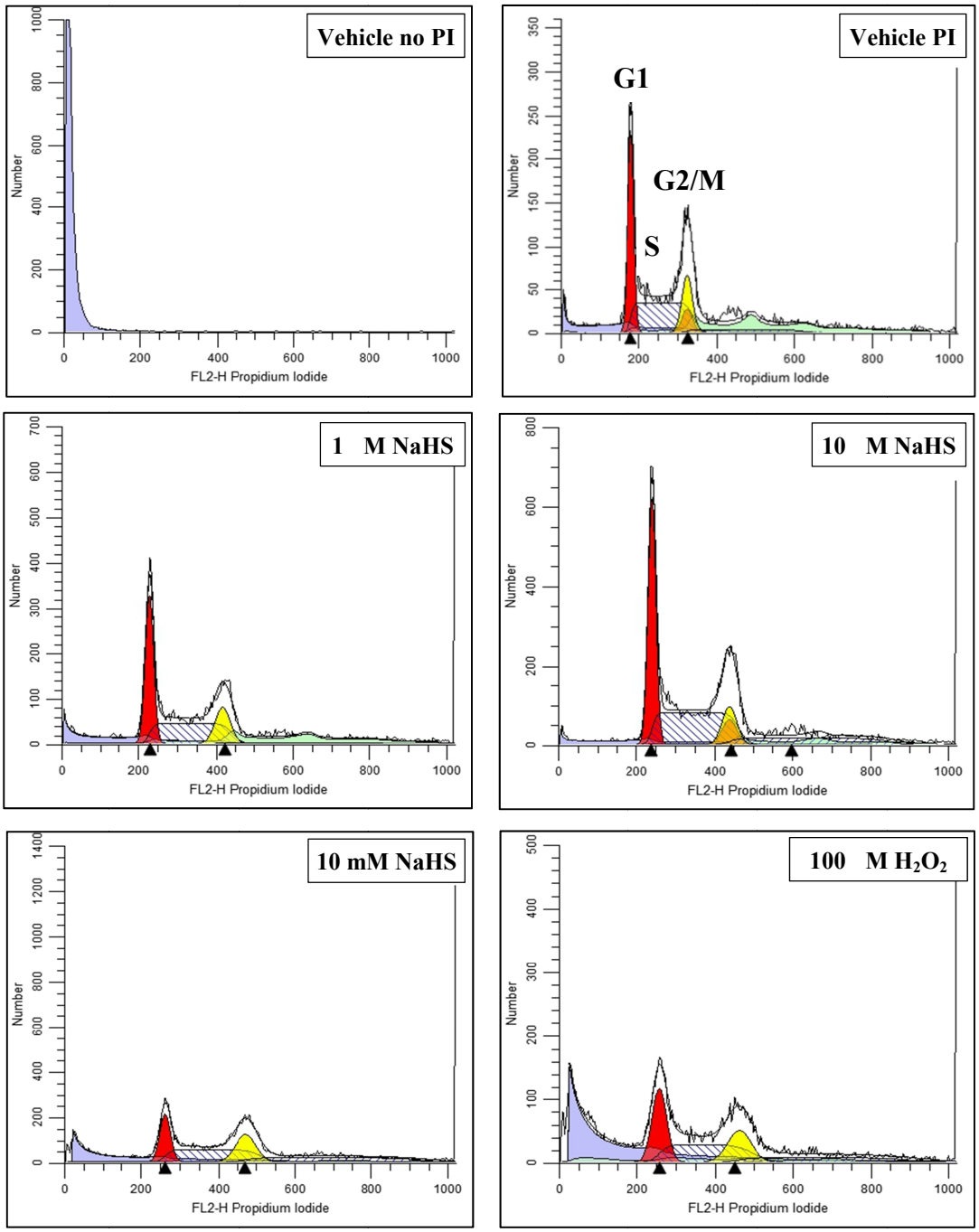

Figure 34: Histograms representing the data obtained using flow cytometry from Propidium Iodide (PI) labelled HEK293-hTRPA1 cells. These cells had been treated with an acute 30 minute treatment of either vehicle, NaHS (1 M- 10 mM) or 100 M H_2O_2 and then allowed to continue growing for 5 days. Cell cycle curves were fitted using ModFIt LT to model the proportion of cells in the different stages of the cell cycle. Red indicates G1, Blue stripes S, and yellow G2/M.

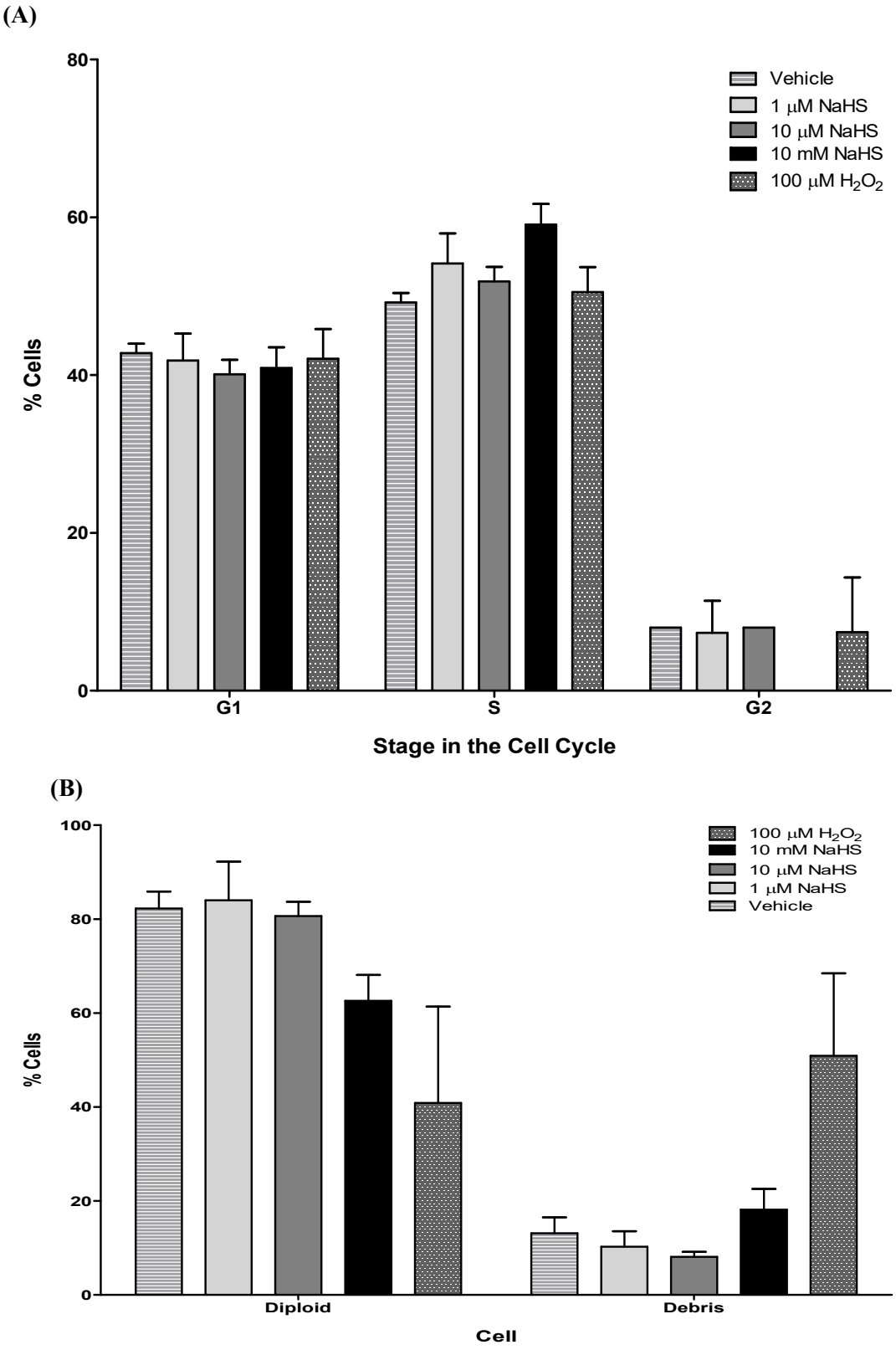

Figure 35: Bar charts representing the pooled data from 3 separate experiments examining the effects of an acute treatment with vehicle, NaHS (1 M- 10 mM) or 100 M H_2O_2 HEK293-TRPA1 cells. Data are the mean ± SEM % of cells in the different stages of the cell cycle on day five **(A)**. In **(B) t**he data represent the proportion of cells found as diploid cells or cell debris on day 5 following the acute treatment. The various treatments did not have an no overall significant effect on the proportions of cellss in different stages of the cell cycle (P = 0.98; Two-way ANOVA with Bonferroni multiple comparisons, n=3) or on the proportion of diploid cells and cell debris (P = 0.94; Two-way ANOVA with Bonferroni multiple comparisons, n=3). The Bonferonni multiple comparisons did reveal there was a significant reduction in the number of diploid cells after 100 M H_2O_2 when compared with vehicle controls ($P<0.05$, n=3).

4.5.6.2. The effects of NaHS on the cell cycle in HPBF cells.

The mean number of cells detected on the flow cytometer per treatment was 10 804, with most of the histograms representing a sufficiently large enough sample of cells to provide a good estimation of the population characteristics (Riccardi and Nicoletti, 2006). The only treatment group that fell short of this was 100 µM H_2O_2 which had a mean count of 1856 cells; a value considered too low to derive accurate conclusions of the population using flow cytometry. Non-PI labelled control cells produced a similar autofluorescence signal to that observed in the HEK-TRPA1 cells (Figures 34 and 36). Furthermore like the HEK-TRPA1 cells, vehicle cells stained with PI also produced two major peaks at around 180 and 360 in the FL2-H channel.

However in contrast to HEK-TRPA1 cells, treatment with 10 mM NaHS produced an increase in the proportion of cells in the G2/M phase (7.8 ± 0.3 %), as well as the S phase (38.5 ± 3.7 %), with a reduced proportion of cells in G1 (53.8 ± 3.4 %) (Figures 36 and 37A). Cells treated with vehicle exhibited a distribution whereby 67 ± 4.3 % were in G1, 27.3 ± 2.4 % in S, and 5.7 ± 2.3 % in the G2/M phase. Not all concentrations of NaHS induced an increase in the proportion of cells in G2/M, as 1 µM - 1 mM NaHS actually prompted a reduction from 5.7 % in vehicle treated cells to between 1.2 – 2.7 % (Figure 37A). The various acute treatment did not have a significant effect of on the proportion of cells in the different stages of the cell cycle ($P > 0.05$, two-way ANOVA with Bonferroni multiple comparisons, n= 3 experiments).

Comparisons between vehicle and NaHS revealed that an increase in the NaHS concentration reduced the amount of cellular debris; vehicle treated samples contained 19.5 ± 8.2 % of cellular debris in contrast to 16.0 ± 5.4 % observed in samples treated with 10 mM NaHS (Figure 37B). Treatment with NaHS or H_2O_2 had no significant effect on the amount of diploid cells or cellular debris ($P > 0.05$, two-way ANOVA with Bonferroni multiple comparisons, n= 3 experiments). However the data examining the effects of H_2O_2 cannot be reliably discussed due to the low cell counts.

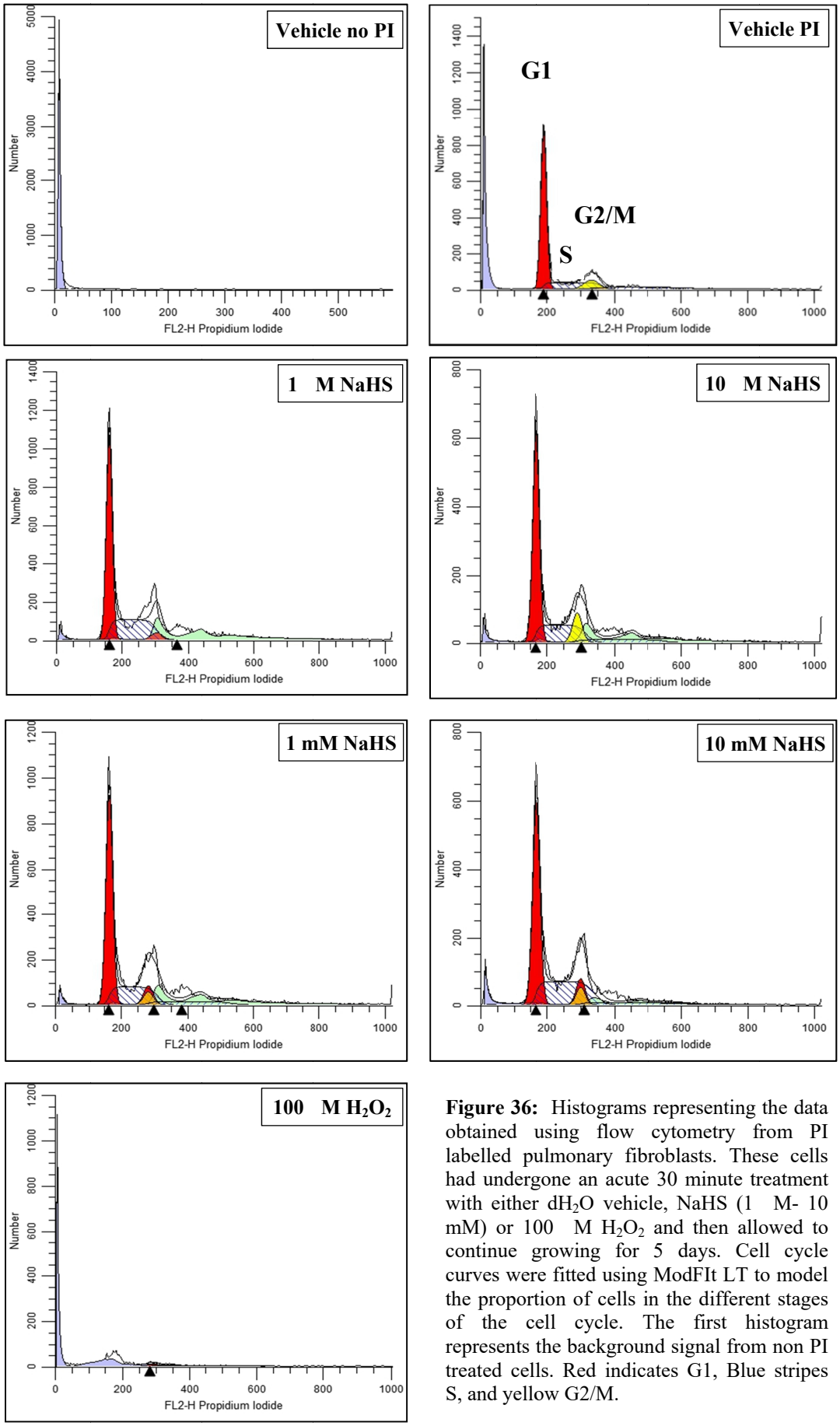

Figure 36: Histograms representing the data obtained using flow cytometry from PI labelled pulmonary fibroblasts. These cells had undergone an acute 30 minute treatment with either dH_2O vehicle, NaHS (1 M- 10 mM) or 100 M H_2O_2 and then allowed to continue growing for 5 days. Cell cycle curves were fitted using ModFIt LT to model the proportion of cells in the different stages of the cell cycle. The first histogram represents the background signal from non PI treated cells. Red indicates G1, Blue stripes S, and yellow G2/M.

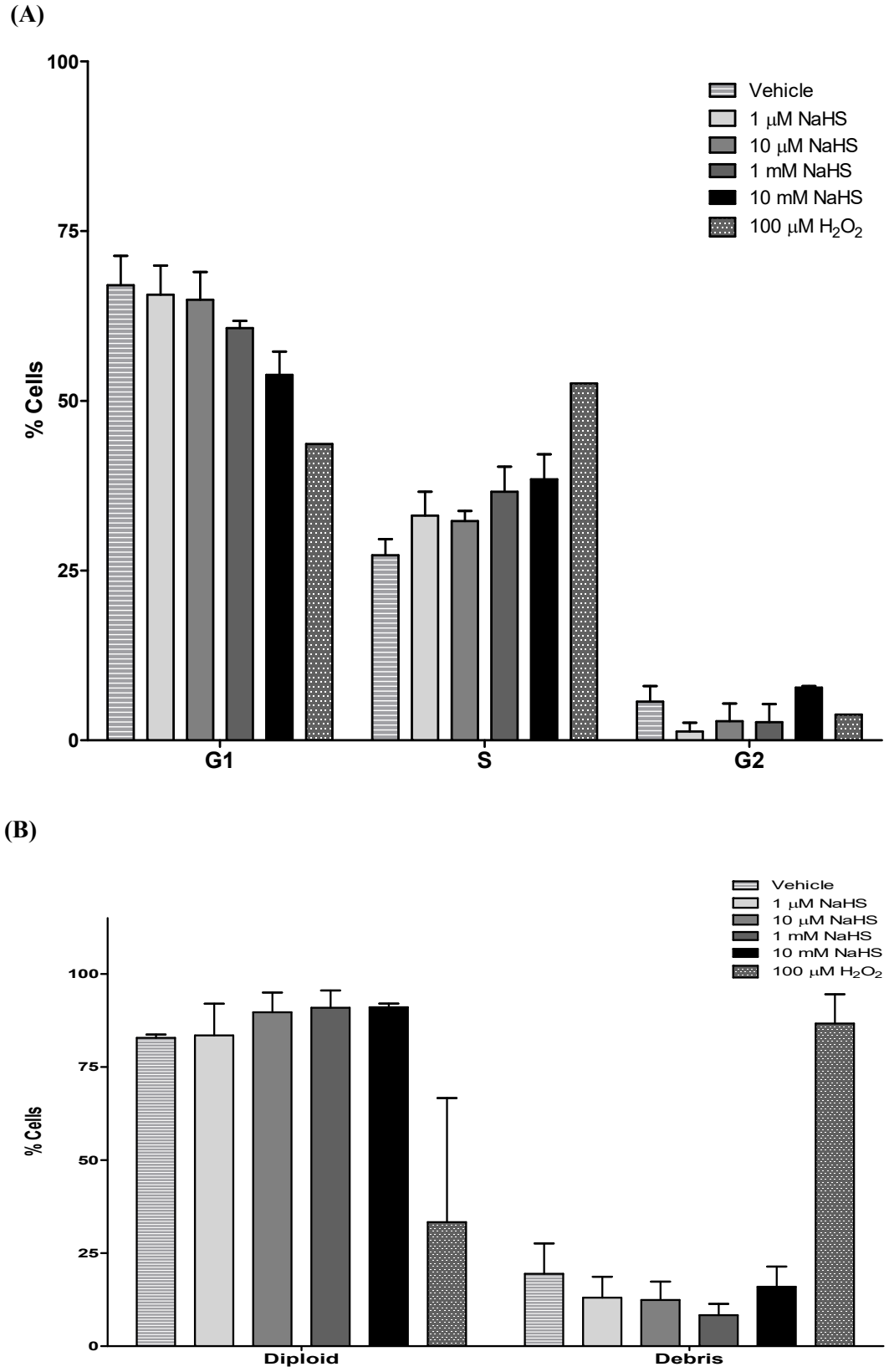

Figure 37: Bar charts representing the pooled data from 3 independent experiments examining the effects of an acute treatment with vehicle, NaHS (1 M- 10 mM) or 100 M H_2O_2 on HPBF. The data are presented as the mean ± SEM % of cell in the different stages of the cell cycle on day five **(A)**. In **(B)** the data represent the proportion of cells found as diploid cells or cell debris on day 5. The treatments did not have a significant effect on the proportion of cells in different stages of the cell cycle ($P > 0.05$; Two-way ANOVA with Bonferroni multiple comparisons, n=3) or on the proportion of diploid cells and cell debris ($P > 0.05$; Two-way ANOVA with Bonferroni multiple comparisons, n=3).

4.6. Discussion

4.6.1. The optimisation of NaHS in cell growth assays

The main investigations described in this chapter have examined the effects of NaHS on cell growth. This has been accomplished through preliminary assays that sought to explore the effects of using the filtered ddH_2O as a vehicle. It was hypothesised that the 1% v/v vehicle would not have an effect on cell growth particularly as the volume utilised was extremely small and water was used instead of solvents such as dimethyl sulfoxide (DMSO) or ethanol which are known to damage cellular membranes and affect membrane protein activity (Sirotkin *et al*., 2001). Indeed the vehicle did not have a significant effect on growth. The next set of experiments examined whether NaHS was altering the pH of the medium as this would clearly confound results given that cells are sensitive to perturbation in pH (Alberts *et al*., 2002). Within the concentrations of NaHS used, it was not found to significantly affect the pH of the medium. Both H^+ and pH data were analysed because from a purely statistical point of view, pH is susceptible to skew due to the logarithm function; this can be overcome by using the direct H^+ concentrations. However Boutelier and Shelton (1980) have provided evidence to suggest that either can be used in biological experiments, although pH is easier to use as it avoids performing the antilogarithm and logarithm steps needed for analysis and then interpretation.

The preliminary assays also provided evidence that the control cells could be incubated in the same incubator as the NaHS treated cells. The benefit of this result was that it negated the need for separate incubators in the ensuing assays and thus avoided the introduction of an additional variable into the experiment. Furthermore it was also found that gaseous H_2S did not appear to interfere with cell growth in neighbouring wells or plates within the shared incubator. This may be due to the kinetics of the plate or that the H_2S was escaping into the atmosphere before it had time to affect neighbouring cells.

4.6.2. The effects of NaHS on HEK293-EV, TRPA1 and HPBF growth

The main experiments then highlighted that chronic treatment with high concentrations of NaHS attenuated cell growth in HEK293 cells transfected with or without TRPA1; this possibly abates the role of TRPA1 in this process. However the experiments performed were not sufficiently extensisve to provide a decisive conclusion, and further repeats would be necessary. The data appeared to indicate that HEK293-EV (IC_{50} of 2.3 mM) cells were slightly more sensitive to chronic NaHS/H_2S treatment compared with HEK-hTRPA1 (IC_{50} of 2.6 mM) which could be explained by several factors, it could be that hTRPA1 is not mediating any anti-proliferative effects of H_2S in this model, on the other hand it could be that it is in fact providing a cytoprotective role from the H_2S gas and hence increasing the concentration of NaHS/ H_2S required to affect cell growth. The other explanation may be that this increased sensitivity is just a result of chance due to the number of repeats and the variability seen in this assay which includes a poorer fit in HEK293-EV (as exemplified by the lower R^2 of 0.76), and/or the cell growth assay is not a sufficiently sensitive assay to use to determine an IC_{50}. The latter could be addressed by performing further experimental repeats to increase the power of the study, whereas the former would need more complex assays involving cell stressors such as reactive oxygen species to tease out the true role of the TRPA1 receptor in these cell growth assays. Nevertheless what these results do show conclusively is that at mM concentrations, NaHS did inhibit cell proliferation regardless of the presence of TRPA1 receptors.

During the course of the experiments it was found that using the OD as the only measure of cell growth was not providing an accurate picture of what was occurring in the experiments (Skehan *et al*., 1990). One reason for the discrepancy between the analyses using absorbance versus the percentage cell growth is skew; the ODs represent the raw data that are not standardised to the initial cell density. Thus to obtain reproducible data, the assay is reliant on an incredibly homogenous method of plating cells onto the growth plates. However what I found was that a number of cells plated initially did vary irrespective of the several techniques utilised to ensure homogeneity. In an ideal world further repeats would help improve the confidence intervals and/or allow outliers to be identified. However the variability in the OD data was partly

overcome by converting to the % of control cell growth as this standardises the treatment groups against the control cell growth on both day zero and the day of cell fixation (Vichai and Kirtikara, 2006). However the confidence intervals were still relatively wide in the data looking at the % of control cell growth over the OD, and thus it could be that the cell growth assays are not sensitive enough to help accurately identify a concentration-response curve without performing many further repeats to overcome the sources of error in the assay such as during cell plating, applying treatments, and changing the medium.

The observed inhibitory effects of NaHS on HEK-293 cells with both control EV as well as those transfected to overexpress a calcium channel (hTRPA1), are consistent with reports from others (Elies *et al*., 2015; Yang *et al*., 2004a). However, Elies *et al*. (2015) presented data showing this inhibition in their HEK control cells was evident by day 4 at a lower concentration of NaHS (100 μM). Several reasons could explain this discrepancy; one could be due to their use of serum-free media (SFM) which is known to increase cell stress due to the absence of growth factors (Freshney and Freshney, 2005). Moreover the use of SFM does not accurately model the *in vivo* environment where a milieu of growth factors and cytokines are present. An additional cause to the discrepancies in the results could be that the authors have used non-transfected HEK293 cells as controls instead of a mock-transfected HEK293 cells used in this thesis. Moreover, the methodological difference used for the quantitative assessment of cells counts may also explain the difference in results, as the tryptan-blue method used by Elies and colleagues has been reported to have an inferior sensitivity relative to the SRB-assay (Vichai and Kirtikara, 2006). Nevertheless there are certain similarities between the models used, as it appears that Elies and colleagues also used a similar chronic treatment paradigm whereby the NaHS was only applied once at the start of the experiment and left for the duration (Elies *et al*., 2015).

In the chronic experiments, NaHS was left for the duration of the experiment in order to investigate how this would compare with a brief exposure of cells to NaHS. The former could be seen as a model of chronic inflammation with the latter as that of an acute inflammatory episode. An important limitation of the model utilised in these chronic treatment models is the variability in exposure to H_2S that is likely to occur. In the

chronic treatment the H_2S may have escaped into the atmosphere within a few hours given that others have shown the sulfide content in stock solutions reduce to under 40% after eight hours (Nagy *et al*., 2014). Furthermore this may even be faster in the presence of cells, as H_2S becomes more unstable in solution by undergoing spontaneous oxidation in the presence of oxygen and metal catalysts (Kashfi and Olson, 2013). To truly appreciate the extent of the loss of NaHS/H_2S, it would be useful to measure temporal changes in the sulfide content as the growth assays progress. Some have reported that half of a dose of H_2S can be lost from open tissue culture wells in 5 minutes (Kashfi and Olson, 2013).

Nevertheless conceptually the acute and chronic treatments did differ and do provide a model of a brief versus a more protracted exposure to H_2S. If one did want to accurately examine the chronic effects of H_2S, a better model would utilise an incubator capable of maintaining a constant H_2S gas concentration. However as alluded to in chapter 3 this would be a much more costly system to set-up and maintain. Interestingly, the comparison between a brief and more protracted NaHS/H_2S exposure did reveal that in both models of application of NaHS there was a concentration dependent chronic inhibition of growth; the long-term effects on growth were reproducible both in primary human lung fibroblasts, as well as in over-expressing systems such as HEK-293. This possibly suggests a conserved molecular mode of action in both cell types. Consistent with this, it has been suggested that part of the toxic effects of H_2S are mediated through the inhibition of cytochrome oxidase (Lindenmann *et al*., 2010; Chen and Wang, 2012), which thus perturbs the normal cellular bioenergetics and reduces the availability of ATP for cellular processes such as growth. Others have provided evidence for the extracellular signal-regulated kinase (ERK)1/2 pathway mediating the H_2S induced inhibition of the cell growth (Yang *et al*., 2004a). The ERK1/2 pathway can activate $p21^{Cip/WAF-1}$ a cdk inhibitory protein which is important for cell cycle arrest (Yang *et al*., 2004a).

It was not known whether the NaHS treatment was causing a reduction in the overall rate of reproduction through induction of the hypometabolic state that has been observed in mice (Blackstone *et al*., 2005), or through cells entering a quiescent stage in the cell cycle (Campisi, 2005), this was addressed using flow cytometry with PI

labelling. This experiment allows quantitative DNA content analysis in tissue culture cells using PI; a fluorescent molecule that binds nucleic acid with little or no sequence preference (Riccardi and Nicoletti, 2006). The PI based flow cytometry experiments found that NaHS did not significantly affect the proportion of cells in each phase of the cell cycle in HEK293-TRPA1 cells. This would suggest that although growth was still occurring in the NaHS over the five day course of the experiment, the reduction in the rate was a global phenomenon rather than cells getting trapped in a specific stage of the cell cycle. Hence, an interesting extension to this experiment would be to repeat it with non-hTRPA1 transfected HEK293, in order to determine whether there are any differences in the proportion of cells found in the various stages of the cell cycle which may then be attributable to the presence hTRPA1.

The acute treatment of HPBF with NaHS produced a similar result to the HEK293-hTRPA1 cells with the proportion of cells in each stage of the cell cycle not altering significantly. Thus, once more it is likely the effect was a global reduction in growth through the cells entering a hypometabolic state. These results seem inconsistent with those of Baskar *et al*. (2007), who found that treatment with 10-75 μM NaHS over 12-48 hours caused a concentration dependent increase in DNA damage (assessed through micronuclei formation) and cell cycle arrest in the G1 phase. The difference in the two sets of data may pertain to Baskar *et al.* (2007), utilising human foetal fibroblasts instead of the adult fibroblasts used in this study, particularly as there is evidence for age related differences in Ca^{2+} handling between the two populations (Papazafiri and Kletsas, 2003). Baskar *et al.* (2007) also provided evidence that NaHS promoted apoptosis in their fibroblast population. This could explain why the cell cycle experiments performed in my study did not show a difference in the cell cycle populations; cells were undergoing apoptosis with a resultant global reduction in cell numbers.

An augmentation of the flow cytometry assay involving the use of dual staining for both PI in conjunction with Annexin 5 would allow the detection of apoptosis (Riccardi and Nicoletti, 2006; Wlodkowic *et al*., 2009). Consistent with the hypothesis that NaHS could be inducing cellular apoptosis in the growth assays, NaHS was shown to induce apoptosis at concentrations < 200 μM but necrosis at > 200 μM in mature cortical

neuronal cells expressing the glutamate receptor (Cheung *et al*., 2007). Although these concentrations are several-fold lower than the concentrations that I used, different cells are known to have varying sensitivities to H_2S/NaHS (Guang-dong and Rui, 2007). Another experimental method that could be utilised to examine such effects in the HEK293 cells and HPBF would be western blots to examine for apoptotic bodies, caspases, ERK and cathepsins (Liu *et al*., 2004; Yang *et al*., 2004b; Medzhitov, 2008). It is also important to be mindful that the lack of effect with NaHS on the proportion of cells in each stage of the cell cycle maybe a false negative secondary to an insufficient number of experimental repeats, or it may be that the ModFit model is not accurate enough to detect the subtle changes that NaHS had induced.

In the flow cytometry assays, Hydrogen peroxide was used as positive control for cell death. It was shown to cause a significant reduction in cell numbers. However others have also reported that H_2O_2 itself activates TRPA1 with an EC_{50} of 230 μM (Streng *et al*., 2008; Módis *et al*., 2013). This EC_{50} is high and does question the validity of their experiments as the 100 μM H_2O_2 that has been used in this experiment is commonly used as a positive control for cell death (Yang, 2004). On the other hand the EC_{50} of 230 μM on TRPA1 may explain why the results for this treatment group were similar to those cells treated with a lower concentration of NaHS e.g. 1 and 10 μM NaHS in HEK-TRPA1 cells (Figure 35A).

4.6.3. The effects of NAC on HEK293- TRPA1 and HPBF growth

As mentioned previously, the drug NAC has been used in the treatment of certain chronic fibrotic conditions such as IPF with a postulated mechanism thought to involve its anti-oxidant properties (Datta *et al*., 2011). To the best of my knowledge, this is the only study to date that has examined the *in vitro* effects of NAC on primary human pulmonary fibroblast growth. A previous study has explored the effects of NAC in human fibroblast cells; however this study did not investigate the effects on growth and used cells of foetal origin rather than adults (Sugiura *et al*., 2009). Sugiura and colleagues did provide evidence for NAC inhibiting the transforming growth factor-β1

(TGF-β1) induced fibrotic process, interestingly TGF-β1 is also known to reduce the cellular glutathione levels and is known to promote tissue remodelling and fibrosis (Finesmith *et al*., 1990; Sugiura *et al*., 2009). On the other hand NAC has been shown to inactivate TGF-β1 from a dimer to monomer through the reduction of its disulphide bonds (Meurer *et al*., 2005). One possible cause for the reduction in growth could be a change in pH induced by NAC unfortunately this was not assessed during the course of the experiments.

The results presented here provide evidence that NAC significantly inhibits cell growth in primary human lung fibroblasts. This observation is consistent with studies on hepatic fibroblasts (Meurer *et al*., 2005), and provides *in vitro* evidence for the potential anti-fibrotic actions of NAC in the lung. These anti- proliferative effects of NAC may be mediated through inhibiting the effects of TGF-β1, likewise NaHS has also been shown to inhibit TGF-β1 induced cellular proliferation (Sheng *et al*., 2013). These findings thus provide a common mechanism underlying how the two agents may inhibit fibroblast proliferation and would be an avenue for further exploration in the future.

4.7. Conclusion

Hydrogen sulfide has been shown to have variable effects on different cells. The *in vitro* data in this chapter have shown that NaHS retards the growth of HEK293 cells transfected with either human TRPA1 or an EV. This inhibitory effect on HEK-293 TRPA1 growth is also present following a brief treatment with NaHS with the mechanism thought to involve a global reduction in cell replication. The global reduction in cell growth following acute treatment with NaHS is also observed in primary human bronchial fibroblasts. These novel findings need to be explored further in order to provide a better understanding of the role that H_2S plays in modulating the progression from inflammation to fibrosis and thus could potentially help in the development of new therapies for respiratory disorders such as COPD, asthma and pulmonary fibrosis.

5. General Discussion & Future Work

Hydrogen sulfide has an odour that everyone is familiar with but most try to avoid it, yet others have embraced its therapeutic potential for centuries by seeking sulphur springs with their medicinal properties or garlic with its putative health benefits. What has changed in the last twenty years is that it is now recognised as the third gasotransmitter and is thus undergoing an immense period of research with over 41 300 publications on PubMed. Nevertheless there is still much to learn about its role in normal health as well as in disease. The fact that enzymes which synthesise H_2S are found to be expressed so diversely in mammalian organs indicate this gasotransmitter has a role in most if not all systems in the body. Furthermore, perturbations in the levels of H_2S have been implicated in various disorders including those affecting the respiratory tract such as COPD, asthma, pulmonary fibrosis and acute lung injury (Olson *et al.*, 2010; Olson, 2011; Chen and Wang, 2012). Furthermore recent data suggests that it mediates part of its effects via the TRPA1 channel. The latter is entirely plausible given that TRPA1 has been known to undergo activation by other sulphur containing ligands such allyl isothiocyanate which is found in mustard, horseradish and wasabi. Furthermore TRPA1 itself is also becoming increasingly appreciated as a sensor and mediator of airway inflammation and in the management of chronic airway diseases such as asthma, COPD and pulmonary fibrosis (Bautista *et al.*, 2006; Caceres *et al.,* 2009; Banner *et al.,* 2011; Raemdonck *et al.,* 2012).

There has been evidence published for the activation of TRPA1 by H_2S, nevertheless this has not been with human TRPA1 receptors. As a consequence the major hypothesis of this study was that H_2S mediates part of its effects on the respiratory system through the activation of human TRPA1 channels and this includes regulating the growth of pulmonary fibroblasts during an episode of inflammation.

1. The major finding in this study supports this hypothesis; an acute 30 minute treatment with 1 mM NaHS inhibited the growth of human pulmonary fibroblast (IC_{50} = 1.2 mM).

   a. This inhibitory effect on growth was evident even 5 days after an acute exposure to NaHS. The finding appeared to be through a global reduction in cell proliferation rather than the cells entering a senescent phase of the cell cycle.

2. A similar effect was also observed with HEK293 cells transfected with hTRPA1, however these cells were not as susceptible to the effects of an acute treatment with NaHS. This inhibition in growth was greater when HEK293-hTRPA1 cells were exposed to a prolonged NaHS treatment (IC_{50} = 2.6 mM).

3. A novel finding was that NAC not only appeared to prevent the NaHS mediated inhibition of cell growth in HPBF, but it had a dual role and in fact it reduced growth in HPBF when it was added independent of NaHS.

4. The final unexpected finding was that fluo-3 the non-esterified analogue of fluo-3AM has been found to directly react with NaHS. This could provide a new type of intracellular H_2S probe and subsequently allow the opportunity for even further research into this gasotransmitter.

The discovery of the effects of an acute NaHS exposure on primary adult human bronchial fibroblasts is unique in that most models examining the effects of NaHS on cell growth apply the drug for the duration of the experiment rather than remove it after a brief 30 minute application (Miyamoto *et al.,* 2011; Elies *et al*., 2015;). This is an incredibly interesting finding as it implies that a brief exposure to H_2S is able to alter the growth trajectory of the cells. This discovery requires further research in order to elucidate the molecular mechanism underlying the attenuated growth. Previously Baskar *et al*. (2007) had reported such reductions in growth occur through the activation of pro-apoptotic pathways, however their conclusions were based on foetal lung fibroblasts which are known to have a more distinct calcium homeostasis when compared with adult fibroblasts (Papazafiri and Kletsas, 2003). Nevertheless examining such apoptotic pathways in adult human bronchial fibroblasts would still provide a

useful foundation to assess the mechanisms underpinning the attenuated growth. The proportion of fibroblasts undergoing apoptosis following NaHS treatment could be assessed using dual labelled (PI and Annexin V) flow cytometry experiments. An alternative method would be to use Western blotting to examine the proportion of apoptotic bodies (Wlodkowic *et al.,* 2009). I would also plan to use immunohistochemistry to assess the extent of TRPA1 receptor expression on the membranes of pulmonary fibroblasts. The activity of the receptors could then be pharmacologically evaluated using the cell suspension based calcium fluorometric assays. Once the presence of active TRPA1 channels are confirmed, one could then try to antagonise the effects of H_2S using a ligand such as HC 030031 prior to the application of NaHS. This compound has been shown to antagonise the AITC evoked calcium currents in TRPA1 channels (Caceres *et al*., 2009).

The *in vitro* fluorometric calcium assays were used to pharmacologically examine the effects of NaHS/H_2S on the hTRPA1 receptor using an overexpressing mammalian vector (HEK293 cells). Unfortunately due to NaHS specifically reacting with the fluorescent probe, the molecular effects of H_2S on TRP channels could not be assessed any further. However what it has opened up is a new avenue of research into a well-known calcium imaging dye that has the potential to be used as a compound to investigate H_2S signalling. It has a favourable toxicity profile, is highly sensitive, allows rapid measurements of calcium flux, has a large fluorescence increase upon activation, is excited in visible light-range thus reducing cellular photo damage, and has been used for cell imaging since the late 1980s (Kao *et al.*, 1989; Thomas *et al*., 2000). This is particularly pertinent as there are several research groups trying to develop H_2S probes that are safe, sensitive and specific (Lippert, 2014). It would be interesting to see whether other H_2S donating drugs such as Na_2S or GYY 4137 are also able to produce the same effect with fluo-3. If so it would indicate that the dye was reacting with H_2S rather than NaHS. If the reaction was specific to H_2S, then analysis of the chemical reaction occurring could help in the development of improved probes capable of detecting H_2S. It would be particularly useful if a ratiometric H_2S dye could be developed as it would allow an estimation of the concentration of H_2S present in cells thus solving a major hurdle in H_2S research.

The *in vitro* anti-proliferative effects of NAC on fibroblasts however does not appear to clearly translate to the clinical context as the most recent randomised-control clinical trial in IPF found that NAC did not offer a significant benefit in patients with mild-to-moderate impairment in lung function (Martinez *et al.*, 2014). The difference between the clinical and laboratory findings may relate to the differences in the concentration of NAC at the cellular level given the trial used a 600 mg dose which would likely result in the presence of a much lower concentration at the cellular level than those used by me.

The concentrations of NAC used in my experiments were derived from the observation that most studies using various experimental paradigms to investigate the antioxidant properties of NAC used between 1 – 10 mM (Kim *et al.*, 2014; Nishio *et al.*, 2013). On the other hand, it could be that although NAC does show *in vitro* effects on fibroblasts, these are not directly translatable to the more elaborate whole organ level due to several factors including the effects of becoming marginalised by the contribution of other cellular systems *in vivo*, as well as the process of fibrosis and the clinical manifestations of therapy representing a much more complex system that is oversimplified in the *in vitro* models. It may also be that the therapeutic benefits of NAC though present, did not manifest as a change in lung function which was the primary outcome of the trial. The mixed results observed with NAC pre-treatment also require further investigations to assess whether this compound has a biphasic effect in bronchial fibroblasts.

The discussions above highlight that there are many questions that still need to be addressed to help understand the interaction between H_2S, TRPA1 and bronchial fibroblasts. This current work has provided some data to show that H_2S (in the form of NaHS) modulates the growth of pulmonary fibroblasts as well as HEK293-hTRPA1 cells. As pulmonary fibroblasts are thought to express TRPA1 particularly during the onset of an inflammatory process (Mukhopadhyay *et al.,* 2011; Nassini *et al.*, 2012), it could be hypothesised that the endogenous H_2S acts to modulate the proliferation of fibroblasts and thus prevents the inflammatory reaction cascading out of control and/or entering into a pathological chronic stage. The chronic phase would then presents clinically as respiratory conditions such as asthma and COPD (Alkhouri *et al.*, 2014). Thus one may be able to develop novel H_2S compound that are able to modulate the inflammatory process through activating the TRPA1 channel. However the situation is

much more complex than this as the activation of the TRPA1 channel itself has been found to mediate lung hypersensitivity and promote neurogenic and non-neurogenic inflammation (Bautista *et al*., 2006; Nassini *et al*., 2012; Kichko *et al*., 2015). These findings highlight the need for further research into this system in order to better understand such chronic inflammatory processes, and help develop effective treatments against them in the future.

6. References

Abdullah, H., Heaney, L.G., Cosby, S.L., McGarvey, L.P. a, 2014. Rhinovirus upregulates transient receptor potential channels in a human neuronal cell line: implications for respiratory virus-induced cough reflex sensitivity. Thorax 69, 46–54.

Abe, K., Kimura, H., 1996. The possible role of hydrogen sulfide as an endogenous neuromodulator. J. Neurosci. 16, 1066–71.

Alberts, B., Johnson, A., Lewis, J., Raff, M., Roberts, K., Walter, P., 2002. Molecular biology of the cancer, 4th ed. Garland Science.

Alkhouri, H., Poppinga, W.J., Tania, N.P., Ammit, A., Schuliga, M., 2014. Regulation of pulmonary inflammation by mesenchymal cells. Pulm. Pharmacol. Ther. 29, 156–65.

Almeida, A.S., Figueiredo-Pereira, C., Vieira, H.L.A., 2015. Carbon monoxide and mitochondria-modulation of cell metabolism, redox response and cell death. Front. Physiol. 6, 33.

Andersson, D. a., Gentry, C., Bevan, S., 2012. TRPA1 Has a key role in the somatic pro-nociceptive actions of hydrogen sulfide. PLoS One 7, e46917.

Ang, S.-F., Sio, S.W.S., Moochhala, S.M., MacAry, P.A., Bhatia, M., 2011. Hydrogen sulfide upregulates cyclooxygenase-2 and prostaglandin E metabolite in sepsis-evoked acute lung injury via transient receptor potential vanilloid type 1 channel activation. J. Immunol. 187, 4778–87.

Bandell, M., Story, G.M., Hwang, S.W., Viswanath, V., Eid, S.R., Petrus, M.J., Earley, T.J., Patapoutian, A., 2004. Noxious cold ion channel TRPA1 is activated by pungent compounds and bradykinin. Neuron 41, 849–57.

Banner, K.H., Igney, F., Poll, C., 2011. TRP channels: Emerging targets for respiratory disease. Pharmacol. Ther. 130, 371–84.

Baskar, R., Li, L., Moore, P.K., 2007. Hydrogen sulfide-induces DNA damage and changes in apoptotic gene expression in human lung fibroblast cells. Fed. Am. Soc. Exp. Biol. J. 21, 247–55.

Baskar, R., Sparatore, A., Del Soldato, P., Moore, P.K., 2008. Effect of S-diclofenac, a novel hydrogen sulfide releasing derivative inhibit rat vascular smooth muscle cell proliferation. Eur. J. Pharmacol. 594, 1–8.

Baskar, R., Bian, J., 2011. Hydrogen sulfide gas has cell growth regulatory role. Eur. J. Pharmacol. 656, 5–9.

Bates, M.N., Garrett, N., Shoemack, P., 2002. Investigation of health effects of hydrogen sulfide from a geothermal source. Arch. Environ. Health 57, 405–11.

Bautista, D.M., Jordt, S.E., Nikai, T., Tsuruda, P.R., Read, A.J., Poblete, J., Yamoah, E.N., Basbaum, A.I., Julius, D., 2006. TRPA1 mediates the inflammatory actions of environmental irritants and proalgesic agents. Cell 124, 1269–82.

Bautista, D.M., Movahed, P., Hinman, A., Axelsson, H.E., Sterner, O., Högestätt, E.D., Julius, D., Jordt, S.-E., Zygmunt, P.M., 2005. Pungent products from garlic activate the sensory ion channel TRPA1. Proc. Natl. Acad. Sci. U. S. A. 102, 12248–52.

Baxter, M., Eltom, S., Dekkak, B., Yew-Booth, L., Dubuis, E.D., Maher, S.A., Belvisi, M.G., Birrell, M.A., 2014. Role of transient receptor potential and pannexin channels in cigarette smoke-triggered ATP release in the lung. Thorax 69, 1080–9.

Beasley, R., Semprini, A., Mitchell, E.A., 2015. Risk factors for asthma: is prevention possible? Lancet 386, 1075–85.

Bhambhani, Y., Singh, M., 1991. Physiological effects of hydrogen sulfide inhalation during exercise in healthy men. J. Appl. Physiol. 71, 1872–7.

Bhambhani, Y., Burnham, R., Snydmiller, G., MacLean, I., Martin, T., 1996. Effects of 5 ppm hydrogen sulfide inhalation on biochemical properties of skeletal muscle in exercising men and women. Am. Ind. Hyg. Assoc. J. 57, 464–8.

Bhatia, M., Sidhapuriwala, J.N., Sparatore, A., Moore, P.K., 2008. Treatment with H2S-releasing diclofenac protects mice against acute pancreatitis-associated lung injury. Shock 29, 84–8.

Bhatia, M., Wong, F.L., Fu, D., Lau, H.Y., Moochhala, S.M., Moore, P.K., 2005. Role of hydrogen sulfide in acute pancreatitis and associated lung injury. FASEB J. 19, 623–5.

Bianchi, B.R., Zhang, X.-F., Reilly, R.M., Kym, P.R., Yao, B.B., Chen, J., 2012. Species comparison and pharmacological characterization of human, monkey, rat, and mouse TRPA1 channels. J. Pharmacol. Exp. Ther. 341, 360–8.

Blackstone, E., Morrison, M., Roth, M.B., 2005. H2S induces a suspended animation-like state in mice. Science 308, 518.

Bos, E.M., van Goor, H., Joles, J. a, Whiteman, M., Leuvenink, H.G.D., 2014. Hydrogen sulfide - physiological properties and therapeutic potential in ischaemia. Br. J. Pharmacol. 1479–93.

Boutilier, R., Shelton, G., 1980. The statistical treatment of hydrogen ion concentration and pH. J. Exp. Biol. 335–9.

Brancaleone, V., Roviezzo, F., Vellecco, V., De Gruttola, L., Bucci, M., Cirino, G., 2008. Biosynthesis of H2S is impaired in non-obese diabetic (NOD) mice. Br. J. Pharmacol. 155, 673–80.

Brunelli, A., Ferguson, M.K., Rocco, G., Pieretti, P., Vigneswaran, W.T., Morgan-Hughes, N.J., Zanello, M., Salati, M., 2008. A scoring system predicting the risk for intensive care unit admission for complications after major lung resection: a multicenter analysis. Ann. Thorac. Surg. 86, 213–8.

Caceres, A.I., Brackmann, M., Elia, M.D., Bessac, B.F., del Camino, D., D'Amours, M., Witek, J.S., Fanger, C.M., Chong, J. a, Hayward, N.J., Homer, R.J., Cohn, L., Huang, X., Moran, M.M., Jordt, S.-E., 2009. A sensory neuronal ion channel essential for airway inflammation and hyperreactivity in asthma. Proc. Natl. Acad. Sci. U. S. A. 106, 9099–104.

Camelliti, P., Borg, T.K., Kohl, P., 2005. Structural and functional characterisation of cardiac fibroblasts. Cardiovasc. Res. 65, 40–51.

Campisi, J., 2005. Senescent cells, tumor suppression, and organismal aging: good citizens, bad neighbors. Cell 120, 513–22.

Carbone, E., Sher, E., Clementi, F., 1990. Ca currents in human neuroblastoma IMR32 cells: kinetics, permeability and pharmacology. Pflügers Arch. Eur. J. Physiol. 416, 170-9.

Chang, H.Y., Chi, J.-T., Dudoit, S., Bondre, C., van de Rijn, M., Botstein, D., Brown, P.O., 2002. Diversity, topographic differentiation, and positional memory in human fibroblasts. Proc. Natl. Acad. Sci. U. S. A. 99, 12877–82.

Channick, R., Preston, I., Klinger, J.R., 2013. Oral therapies for pulmonary arterial hypertension: endothelin receptor antagonists and phosphodiesterase-5 inhibitors. Clin. Chest Med. 34, 811–24.

Chattopadhyay, M., Kodela, R., Nath, N., Dastagirzada, Y.M., Velázquez-Martínez, C. a., Boring, D., Kashfi, K., 2012. Hydrogen sulfide-releasing NSAIDs inhibit the growth of human cancer cells: A general property and evidence of a tissue type-independent effect. Biochem. Pharmacol. 83, 715–22.

Chen, J., Zhang, X.-F., Kort, M.E., Huth, J.R., Sun, C., Miesbauer, L.J., Cassar, S.C., Neelands, T., Scott, V.E., Moreland, R.B., Reilly, R.M., Hajduk, P.J., Kym, P.R., Hutchins, C.W., Faltynek, C.R., 2008. Molecular determinants of species-specific activation or blockade of TRPA1 channels. J. Neurosci. 28, 5063–71.

Chen, Y.-H., Yao, W.-Z., Geng, B., Ding, Y.-L., Lu, M., Zhao, M.-W., Tang, C.-S., 2005. Endogenous hydrogen sulfide in patients with COPD. Chest 128, 3205–11.

Chen, Y.-H., Wang, P.-P., Wang, X.-M., He, Y.-J., Yao, W.-Z., Qi, Y.-F., Tang, C.-S., 2011. Involvement of endogenous hydrogen sulfide in cigarette smoke-induced changes in airway responsiveness and inflammation of rat lung. Cytokine 53, 334–41.

Chen, Y.H., Wu, R., Geng, B., Qi, Y.F., Wang, P.P., Yao, W.Z., Tang, C.S., 2009. Endogenous hydrogen sulfide reduces airway inflammation and remodeling in a rat model of asthma. Cytokine 45, 117–23.

Chen, Y., Zhao, J., Du, J., Xu, G., Tang, C., Geng, B., 2012. Hydrogen sulfide regulates cardiac sarcoplasmic reticulum Ca2+ uptake via KATP channel and PI3K/Akt pathway. Life Sci. 91, 271–8.

Chen, Y., Wang, R., 2012. The message in the air: hydrogen sulfide metabolism in chronic respiratory diseases. Respir Physiol Neurobiol 184, 130–8.

Cheung, N.S., Peng, Z.F., Chen, M.J., Moore, P.K., Whiteman, M., 2007. Hydrogen sulfide induced neuronal death occurs via glutamate receptor and is associated with calpain activation and lysosomal rupture in mouse primary cortical neurons. Neuropharmacology 53, 505–14.

Chrysanthopoulou, A., Mitroulis, I., Apostolidou, E., Arelaki, S., Mikroulis, D., Konstantinidis, T., Sivridis, E., Koffa, M., Giatromanolaki, A., Boumpas, D.T., Ritis, K., Kambas, K., 2014. Neutrophil extracellular traps promote differentiation and function of fibroblasts. J. Pathol. 233, 294–307.

Chung, K.F., 2015. Targeting the interleukin pathway in the treatment of asthma. Lancet 386, 1086–96.

Chunyu, Z., Junbao, D., Dingfang, B., Hui, Y., Xiuying, T., Chaoshu, T., 2003. The regulatory effect of hydrogen sulfide on hypoxic pulmonary hypertension in rats. Biochem. Biophys. Res. Commun. 302, 810–6.

Datta, A., Scotton, C.J., Chambers, R.C., 2011. Novel therapeutic approaches for pulmonary fibrosis. Br. J. Pharmacol. 163, 141–72.

Decramer, M., Janssens, W., Miravitlles, M., 2012. Chronic obstructive pulmonary disease. Lancet 379, 1341–51.

Deering-Rice, C.E., Shapiro, D., Romero, E.G., Stockmann, C., Bevans, T.S., Phan, Q.M., Stone, B.L., Fassl, B., Nkoy, F., Uchida, D.A., Ward, R.M., Veranth, J.M., Reilly, C.A., 2015. Activation of TRPA1 by insoluble particulate material and association with asthma. Am. J. Respir. Cell Mol. Biol. 53, 893-901.

Dekhuijzen, P.N., van Beurden, W.J., 2006. The role for N-acetylcysteine in the management of COPD. Int. J. Chron. Obstruct. Pulmon. Dis. 1, 99-106.

Deplancke, B., Gaskins, H.R., 2003. Hydrogen sulfide induces serum-independent cell cycle entry in nontransformed rat intestinal epithelial cells. FASEB J. 17, 1310–2.

Di Meo, I., Lamperti, C., Tiranti, V., 2015. Mitochondrial diseases caused by toxic compound accumulation: from etiopathology to therapeutic approaches. EMBO Mol. Med. 20, 1257-66

Di, a, Malik, a B., 2010. TRP channels and the control of vascular function. Curr Opin Pharmacol 10, 127–32.

Diehl, J.A., Ponugoti, B., 2010. Ubiquitin-dependent proteolysis in G1/S phase control and its relationship with tumor susceptibility. Genes Cancer 1, 717–24.

Dombkowski, R.A., Russell, M.J., Schulman, A.A., Doellman, M.M., Olson, K.R., 2005. Vertebrate phylogeny of hydrogen sulfide vasoactivity. Am. J. Physiol. Regul. Integr. Comp. Physiol. 288, R243–52.

Dorman, D.C., Moulin, F.J.-M., McManus, B.E., Mahle, K.C., James, R.A., Struve, M.F., 2002. Cytochrome oxidase inhibition induced by acute hydrogen sulfide inhalation: correlation with tissue sulfide concentrations in the rat brain, liver, lung, and nasal epithelium. Toxicol. Sci. 65, 18–25.

Dubaj, V., Mazzolini, A., Wood, A., 2007. Monitoring of neuronal and glial calcium activity using a novel direct-contact probe. J. Microsc. 226, 83–9.

Duffield, J.S., Lupher, M., Thannickal, V.J., Wynn, T.A., 2013. Host responses in tissue repair and fibrosis. Annu. Rev. Pathol. 8, 241–76.

Durham, A.L., Adcock, I.M., 2015. The relationship between COPD and lung cancer. Lung Cancer. 90, 121-7.

Elies, J., Johnson, E., Boyle, J.P., Scragg, J.L., Peers, C., 2015. H2S does not regulate proliferation via T-type Ca2+ channels. Biochem. Biophys. Res. Commun. 461, 659–64.

Elrod, J.W., Calvert, J.W., Morrison, J., Doeller, J.E., Kraus, D.W., Tao, L., Jiao, X., Scalia, R., Kiss, L., Szabo, C., Kimura, H., Chow, C.-W., Lefer, D.J., 2007. Hydrogen sulfide attenuates myocardial ischemia-reperfusion injury by preservation of mitochondrial function. Proc. Natl. Acad. Sci. U. S. A. 104, 15560–5.

Fago, A., Jensen, F.B., Tota, B., Feelisch, M., Olson, K.R., Helbo, S., Lefevre, S., Mancardi, D., Palumbo, A., Sandvik, G.K., Skovgaard, N., 2012. Integrating nitric oxide, nitrite and hydrogen sulfide signaling in the physiological adaptations to hypoxia: A comparative approach. Comp. Biochem. Physiol. A. Mol. Integr. Physiol. 162, 1–6.

Fang, L.P., Lin, Q., Tang, C.S., Liu, X.M., 2009. Hydrogen sulfide suppresses migration, proliferation and myofibroblast transdifferentiation of human lung fibroblasts. Pulm. Pharmacol. Ther. 22, 554–61.

Fang, L.-P., Lin, Q., Tang, C.-S., Liu, X.-M., 2010. Hydrogen sulfide attenuates epithelial-mesenchymal transition of human alveolar epithelial cells. Pharmacol. Res. 61, 298–305.

Fernandes, V.S., Ribeiro, A.S.F., Barahona, M.V., Orensanz, L.M., Martínez-Sáenz, A., Recio, P., Martínez, A.C., Bustamante, S., Carballido, J., García-Sacristán, A., Prieto, D., Hernández, M., 2013. Hydrogen sulfide mediated inhibitory neurotransmission to the pig bladder neck: Role of KATP channels, sensory nerves and calcium signaling. J. Urol. 190, 746–56.

Fiedler, N., Kipen, H., Ohman-Strickland, P., Zhang, J., Weisel, C., Laumbach, R., Kelly-McNeil, K., Olejeme, K., Lioy, P., 2008. Sensory and cognitive effects of acute exposure to hydrogen sulfide. Environ. Health Perspect. 116, 78–85.

Finesmith, T.H., Broadley, K.N., Davidson, J.M., 1990. Fibroblasts from wounds of different stages of repair vary in their ability to contract a collagen gel in response to growth factors. J. Cell. Physiol. 144, 99–107.

Fitzgerald, R., DeSantiago, B., Lee, D.Y., Yang, G., Kim, J.Y., Foster, D.B., Chan-Li, Y., Horton, M.R., Panettieri, R.A., Wang, R., An, S.S., 2014. H2S relaxes isolated human airway smooth muscle cells via the sarcolemmal K(ATP) channel. Biochem. Biophys. Res. Commun. 446, 393–8.

Flavell, S.J., Hou, T.Z., Lax, S., Filer, A.D., Salmon, M., Buckley, C.D., 2008. Fibroblasts as novel therapeutic targets in chronic inflammation. Br. J. Pharmacol. 153 Suppl , S241–6.

Frantzias, J., Logan, J., Mollat, P., Sparatore, A., Del Soldato, P., Ralston, S., Idris, A., 2012. Hydrogen sulphide-releasing diclofenac derivatives inhibit breast cancer-induced osteoclastogenesis in vitro and prevent osteolysis ex vivo. Br. J. Pharmacol. 165, 1914–25.

Freshney, R.I., Freshney, R.I., 2005. Serum-free media. in: culture of animal cells. John Wiley & Sons, Inc.

Furchgott, R.F., Vanhoutte, P.M., 1989. Endothelium-derived relaxing and contracting factors. FASEB J. 3, 2007–18.

Furne, J., Saeed, A., Levitt, M.D., 2008. Whole tissue hydrogen sulfide concentrations are orders of magnitude lower than presently accepted values. Am. J. Physiol. Regul. Integr. Comp. Physiol. 295, R1479–85.

Garantziotis, S., Steele, M.P., Schwartz, D.A., 2004. Pulmonary fibrosis: thinking outside of the lung. J. Clin. Invest. 114, 319–21.

Geppetti, P., Materazzi, S., Nicoletti, P., 2006. The transient receptor potential vanilloid 1: role in airway inflammation and disease. Eur J Pharmacol 533, 207–14.

Geppetti, P., Patacchini, R., Nassini, R., Materazzi, S., 2010. Cough: the emerging role of the trpa1 channel. Lung 188, S63-8.

Givvimani, S., Munjal, C., Gargoum, R., Sen, U., Tyagi, N., Vacek, J.C., Tyagi, S.C., 2011. Hydrogen sulfide mitigates transition from compensatory hypertrophy to heart failure. J. Appl. Physiol. 110, 1093–100.

Goodwin, L.R., Francom, D., Dieken, F.P., Taylor, J.D., Warenycia, M.W., Reiffenstein, R.J., Dowling, G., 1989. Determination of sulfide in brain tissue by gas dialysis/ion chromatography: postmortem studies and two case reports. J. Anal. Toxicol. 13, 105–9.

Gracheva, E.O., Ingolia, N.T., Kelly, Y.M., Cordero-Morales, J.F., Hollopeter, G., Chesler, A.T., Sánchez, E.E., Perez, J.C., Weissman, J.S., Julius, D., 2010. Molecular basis of infrared detection by snakes. Nature 464, 1006–11.

Graham, F.L., Smiley, J., Russell, W.C., Nairn, R., 1977. Characteristics of a human cell line transformed by DNA from human adenovirus type 5. J. Gen. Virol. 36, 59–72.

Gratzke, C., Streng, T., Waldkirch, E., Sigl, K., Stief, C., Andersson, K.E., Hedlund, P., 2009. Transient receptor potential A1 (TRPA1) activity in the human urethra-evidence for a functional role for TRPA1 in the outflow region. Eur. Urol. 55, 696–704.

Guang-dong, Y., Wang, R., 2007. H_2S and cellular proliferation and apoptosis. Sheng Li Xue Bao.59, 133–40.

Guo, Z., Chen, G., Zeng, G., Li, Z., Chen, A., Wang, J., Jiang, L., 2015. Fluorescence chemosensors for hydrogen sulfide detection in biological systems. Analyst 140, 1772–86.

Hall, J., 2010. Guyton and Hall textbook of medical physiology, 12th ed. Saunders.

Han, W., Dong, Z., Dimitropoulou, C., Su, Y., 2011. Hydrogen sulfide ameliorates tobacco smoke-induced oxidative stress and emphysema in mice. Antioxid. Redox Signal. 15, 2121–34.

Hinman, A., Chuang, H.-H., Bautista, D.M., Julius, D., 2006. TRP channel activation by reversible covalent modification. Proc. Natl. Acad. Sci. U. S. A. 103, 19564–8.

Hoo, Z.H., Whyte, M.K.B., 2012. Idiopathic pulmonary fibrosis. Thorax 67, 742–6.

Hosoki, R., Matsuki, N., Kimura, H., 1997. The possible role of hydrogen sulfide as an endogenous smooth muscle relaxant in synergy with nitric oxide. Biochem. Biophys. Res. Commun. 237, 527–31.

Hsu, C.-C., Lin, R.-L., Lee, L.-Y., Lin, Y.S., 2013. Hydrogen sulfide induces hypersensitivity of rat capsaicin-sensitive lung vagal neurons: role of TRPA1 receptors. Am. J. Physiol. Regul. Integr. Comp. Physiol. 305, R769–79.

Huang, J., Luo, Y., Hao, Y., Zhang, Y., Chen, P., Xu, J., Chen, M., Luo, Y., Zhong, N.-S., Xu, J., Zhou, W., 2014. Cellular mechanism underlying hydrogen sulfide induced mouse tracheal smooth muscle relaxation: role of BKCa. Eur. J. Pharmacol. 741, 55–63.

Jaquemar, D., Schenker, T., Trueb, B., 1999. An ankyrin-like protein with transmembrane domains is specifically lost after oncogenic transformation of human fibroblasts. J. Biol. Chem. 274, 7325–33.

Jha, A., Sharma, P., Anaparti, V., Ryu, M.H., Halayko, A.J., 2015. A role for transient receptor potential ankyrin 1 cation channel (TRPA1) in airway hyper-responsiveness? Can. J. Physiol. Pharmacol. 93, 171–6.

Jiang, Y., Lee, A., Chen, J., Ruta, V., Cadene, M., Chait, B.T., MacKinnon, R., 2003. X-ray structure of a voltage-dependent K+ channel. Nature 423, 33–41.

Jordt, S.-E., Bautista, D.M., Chuang, H.-H., McKemy, D.D., Zygmunt, P.M., Högestätt, E.D., Meng, I.D., Julius, D., 2004. Mustard oils and cannabinoids excite sensory nerve fibres through the TRP channel ANKTM1. Nature 427, 260–5.

Kabil, O., Banerjee, R., 2010. Redox biochemistry of hydrogen sulfide. J. Biol. Chem. 285, 21903–7.

Kamijo, Y., Takai, M., Fujita, Y., Hirose, Y., Iwasaki, Y., Ishihara, S., 2013. A multicenter retrospective survey on a suicide trend using hydrogen sulfide in Japan. Clin. Toxicol. (Phila). 51, 425–8.

Kaneko, Y., Szallasi, A., 2014. Transient receptor potential (TRP) channels: A clinical perspective. Br. J. Pharmacol. 171, 2474–507.

Kao, J.P., Harootunian, A.T., Tsien, R.Y., 1989. Photochemically generated cytosolic calcium pulses and their detection by fluo-3. J. Biol. Chem. 264, 8179–84.

Kashfi, K., Olson, K.R., 2013. Biology and therapeutic potential of hydrogen sulfide and hydrogen sulfide-releasing chimeras. Biochem. Pharmacol. 85, 689–703.

Kastan, M.B., Bartek, J., 2004. Cell-cycle checkpoints and cancer. Nature 432, 316–23.

Kendall, R.T., Feghali-Bostwick, C.A., 2014. Fibroblasts in fibrosis: novel roles and mediators. Front. Pharmacol. 5, 1-13.

Kichko, T.I., Niedermirtl, F., Leffler, A., Reeh, P.W., 2015. Irritant volatile anesthetics induce neurogenic inflammation through TRPA1 and TRPV1 channels in the isolated mouse trachea. Anesth. Analg. 120, 467–71.

Kim, S., Lee, H.G., Park, S.A., Kundu, J.K., Keum, Y.S., Cha, Y.N., Na, H.K., Surh, Y.J., 2014. Keap1 cysteine 288 as a potential target for diallyl trisulfide-induced Nrf2 activation. PLoS One. 9, e85984.

Kimura, H., 2014. Production and physiological effects of hydrogen sulfide. Antioxid. Redox Signal. 20, 783–93.

Kubo, S., Doe, I., Kurokawa, Y., Kawabata, A., 2007. Hydrogen sulfide causes relaxation in mouse bronchial smooth muscle. J. Pharmacol. Sci. 104, 392–6.

Laursen, W.J., Anderson, E.O., Hoffstaetter, L.J., Bagriantsev, S.N., Gracheva, E.O., 2015. Species-specific temperature sensitivity of TRPA1. Temperature, 1–14.

Li, L., Salto-Tellez, M., Tan, C.-H., Whiteman, M., Moore, P.K., 2009. GYY4137, a novel hydrogen sulfide-releasing molecule, protects against endotoxic shock in the rat. Free Radic. Biol. Med. 47, 103–13.

Li, L., Whiteman, M., Guan, Y.Y., Neo, K.L., Cheng, Y., Lee, S.W., Zhao, Y., Baskar, R., Tan, C.-H., Moore, P.K., 2008. Characterization of a novel, water-soluble hydrogen sulfide-releasing molecule (GYY4137): new insights into the biology of hydrogen sulfide. Circulation 117, 2351–60.

Li, S.-B., Tong, X.-S., Wang, X.-X., Jin, X.-H., Ye, H., 2010. [Regulative mechanism of budesonide on endogenous hydrogen sulfide, cystathionine-gamma-lyase and cystathionine-beta-synthase system in asthmatic rats]. Zhongguo Dang Dai Er Ke Za Zhi 12, 654–7.

Li, T., Zhao, B., Wang, C., Wang, H., Liu, Z., Li, W., Jin, H., Tang, C., Du, J., 2008. Regulatory effects of hydrogen sulfide on IL-6, IL-8 and IL-10 levels in the plasma and pulmonary tissue of rats with acute lung injury. Exp. Biol. Med. (Maywood). 233, 1081–7.

Libby, P., 2002. Inflammation in atherosclerosis. Nature 420, 868–74.

Linden, P.A., Bueno, R., Colson, Y.L., Jaklitsch, M.T., Lukanich, J., Mentzer, S., Sugarbaker, D.J., 2005. Lung resection in patients with preoperative FEV1 < 35% predicted. Chest 127, 1984–90.

Lindenmann, J., Matzi, V., Anegg, U., Neuboeck, N., Porubsky, C., Fell, B., Raber, T., Ratzenhofer-Komenda, B., Renner, H., Klemen, H., Greilberger, J., Haas, J., Maier, A., Smolle-Juettner, F., 2010. Hyperbaric oxygen in the treatment of hydrogen sulphide intoxication. Acta Anaesthesiol. Scand. 54, 784–5.

Lippert, A.R., 2014. Designing reaction-based fluorescent probes for selective hydrogen sulfide detection. J. Inorg. Biochem. 133, 136–42.

Liu, X., Yue, P., Zhou, Z., Khuri, F.R., Sun, S.Y., 2004. Death receptor regulation and celecoxib-induced apoptosis in human lung cancer cells. J. Natl. Cancer Inst. 96, 1769–80.

Louhivuori, L.M., Bart, G., Larsson, K.P., Louhivuori, V., Näsman, J., Nordström, T., Koivisto, A.P., Åkerman, K.E.O., 2009. Differentiation dependent expression of TRPA1 and TRPM8 channels in IMR-32 human neuroblastoma cells. J. Cell. Physiol. 221, 67–74.

Lu, M., Liu, Y.-H., Goh, H.S., Wang, J.J.X., Yong, Q.-C., Wang, R., Bian, J.-S., 2010. Hydrogen sulfide inhibits plasma renin activity. J. Am. Soc. Nephrol. 21, 993–1002.

Macpherson, L.J., Dubin, A.E., Evans, M.J., Marr, F., Schultz, P.G., Cravatt, B.F., Patapoutian, A., 2007. Noxious compounds activate TRPA1 ion channels through covalent modification of cysteines. Nature 445, 541–5.

Mancardi, D., Penna, C., Merlino, A., Del Soldato, P., Wink, D. a., Pagliaro, P., 2009. Physiological and pharmacological features of the novel gasotransmitter: Hydrogen sulfide. Biochim. Biophys. Acta - Bioenerg. 1787, 864–72.

Martinez, F.J., de Andrade, J.A., Anstrom, K.J., King, T.E., Raghu, G., 2014. Randomized trial of acetylcysteine in idiopathic pulmonary fibrosis. N. Engl. J. Med. 370, 2093–101.

Martinez, F.D., Vercelli, D., 2013. Asthma. Lancet 382, 1360–72.

McCully, K.S., 1996. Homocysteine and vascular disease. Nat. Med. 2, 386–9.

McGarvey, L.P., Butler, C.A., Stokesberry, S., Polley, L., McQuaid, S., Abdullah, H., Ashraf, S., McGahon, M.K., Curtis, T.M., Arron, J., Choy, D., Warke, T.J., Bradding, P., Ennis, M., Zholos, A., Costello, R.W., Heaney, L.G., 2014. Increased expression of bronchial epithelial transient receptor potential vanilloid 1 channels in patients with severe asthma. J. Allergy Clin. Immunol. 133, 704–12.e4.

Medzhitov, R., 2008. Origin and physiological roles of inflammation. Nature 454, 428–35.

Meng, G., Wang, J., Xiao, Y., Bai, W., Xie, L., Shan, L., Moore, P.K., Ji, Y., 2015. GYY4137 protects against myocardial ischemia and reperfusion injury by attenuating oxidative stress and apoptosis in rats. J. Biomed. Res. 29, 203–13.

Merritt, J.E., McCarthy, S.A., Davies, M.P., Moores, K.E., 1990. Use of fluo-3 to measure cytosolic Ca2+ in platelets and neutrophils. Loading cells with the dye, calibration of traces, measurements in the presence of plasma, and buffering of cytosolic Ca2+. Biochem. J. 269, 513–9.

Meurer, S.K., Lahme, B., Tihaa, L., Weiskirchen, R., Gressner, A.M., 2005. N-Acetyl-L-cysteine suppresses TGF-B signaling at distinct molecular steps: The biochemical and biological efficacy of a multifunctional, antifibrotic drug. Biochem. Pharmacol. 70, 1026–34.

Mitchell, J.E., Campbell, A.P., New, N.E., Sadofsky, L.R., Kastelik, J.A., Mulrennan, S.A., Compton, S.J., Morice, A.H., 2005. Expression and characterization of the intracellular vanilloid receptor (TRPV1) in bronchi from patients with chronic cough. Exp. Lung Res. 31, 295–306.

Miyamoto, R., Otsuguro, K.I., Ito, S., 2011. Time- and concentration-dependent activation of TRPA1 by hydrogen sulfide in rat DRG neurons. Neurosci. Lett. 499, 137–42.

Módis, K., Asimakopoulou, A., Coletta, C., Papapetropoulos, A., Szabo, C., 2013. Oxidative stress suppresses the cellular bioenergetic effect of the 3-mercaptopyruvate sulfurtransferase/hydrogen sulfide pathway. Biochem. Biophys. Res. Commun. 433, 401-7.

Mok, Y.-Y.P., Atan, M.S.B.M., Yoke Ping, C., Zhong Jing, W., Bhatia, M., Moochhala, S., Moore, P.K., 2004. Role of hydrogen sulphide in haemorrhagic shock in the rat: protective effect of inhibitors of hydrogen sulphide biosynthesis. Br. J. Pharmacol. 143, 881–9.

Moncada, S., Higgs, E. a, 2006. The discovery of nitric oxide and its role in vascular biology. Br. J. Pharmacol. 147 Suppl , S193–201.

Morgan, D.O., 1997. Cyclin-dependent kinases: engines, clocks, and microprocessors. Annu. Rev. Cell Dev. Biol. 13, 261–91.

Morgan, K., Sadofsky, L.R., Crow, C., Morice, A.H., 2014. Human TRPM8 and TRPA1 pain channels, including a gene variant with increased sensitivity to agonists (TRPA1 R797T), exhibit differential regulation by SRC-tyrosine kinase inhibitor. Biosci. Rep. 34, e00131.

Mukhopadhyay, I., Gomes, P., Aranake, S., Shetty, M., Karnik, P., Damle, M., Kuruganti, S., Thorat, S., Khairatkar-Joshi, N., 2011. Expression of functional TRPA1 receptor on human lung fibroblast and epithelial cells. J. Recept. Signal Transduct. 31, 350–8.

Munaron, L., Avanzato, D., Moccia, F., Mancardi, D., 2013. Hydrogen sulfide as a regulator of calcium channels. Cell Calcium 53, 77–84.

Myers, P.R., Minor, R.L., Guerra, R., Bates, J.N., Harrison, D.G., 1990. Vasorelaxant properties of the endothelium-derived relaxing factor more closely resemble S-nitrosocysteine than nitric oxide. Nature 345, 161–3.

Nagy, P., Pálinkás, Z., Nagy, A., Budai, B., Tóth, I., Vasas, A., 2014. Chemical aspects of hydrogen sulfide measurements in physiological samples. Biochim. Biophys. Acta - Gen. Subj. 1840, 876–91.

Nagy, P., Pálinkás, Z., Nagy, A., Budai, B., Tóth, I., Vasas, A., 2014. Chemical aspects of hydrogen sulfide measurements in physiological samples. Biochim. Biophys. Acta - Gen. Subj. 1840, 876–91.

Nair, G.B., Niederman, M.S., 2015. Ventilator-associated pneumonia: present understanding and ongoing debates. Intensive Care Med. 41, 34–48.

Nassini, R., Pedretti, P., Moretto, N., Fusi, C., Carnini, C., Facchinetti, F., Viscomi, A.R., Pisano, A.R., Stokesberry, S., Brunmark, C., Svitacheva, N., McGarvey, L., Patacchini, R., Damholt, A.B., Geppetti, P., Materazzi, S., 2012. Transient receptor potential ankyrin 1 channel localized to non-neuronal airway cells promotes non-neurogenic inflammation. PLoS One 7.

Nishio, N., Taniguchi, W., Sugimura, Y.K., Takiguchi, N., Yamanaka, M., Kiyoyuki, Y., Yamada, H., Miyazaki, N., Yoshida, M., Nakatsuka, T., 2013. Reactive oxygen species enhance excitatory synaptic transmission in rat spinal dorsal horn neurons by activating TRPA1 and TRPV1 channels. Neuroscience 247, 201–12.

Nunez, R., 2001. DNA measurement and cell cycle analysis by flow cytometry. Curr. Issues Mol. Biol. 3, 67–70.

O'Brien, J., Vetter, R.D., 1990. Production of thiosulphate during sulphide oxidation by mitochondria of the symbiont-containing bivalve Solemya reidi. J. Exp. Biol. 149, 133–48.

Ogawa, H., Takahashi, K., Miura, S., Imagawa, T., Saito, S., Tominaga, M., Ohta, T., 2012. H2S functions as a nociceptive messenger through transient receptor potential ankyrin 1 (TRPA1) activation. Neuroscience 218, 335–43.

Ojo, O., Lagan, A.L., Rajendran, V., Spanjer, A., Chen, L., Sohal, S.S., Heijink, I., Jones, R., Maarsingh, H., Hackett, T.L., 2014. Pathological changes in the COPD lung mesenchyme--novel lessons learned from in vitro and in vivo studies. Pulm. Pharmacol. Ther. 29, 121–8.

Okada, Y., Reinach, P.S., Shirai, K., Kitano, A., Kao, W.W.-Y., Flanders, K.C., Miyajima, M., Liu, H., Zhang, J., Saika, S., 2011. TRPV1 involvement in inflammatory tissue fibrosis in mice. Am. J. Pathol. 178, 2654–64.

Okubo, K., Matsumura, M., Kawaishi, Y., Aoki, Y., Matsunami, M., Okawa, Y., Sekiguchi, F., Kawabata, A., 2012. Hydrogen sulfide-induced mechanical hyperalgesia and allodynia require activation of both Cav3.2 and TRPA1 channels in mice. Br. J. Pharmacol. 166, 1738–43.

Olson, K.R., 2011. Hydrogen sulfide is an oxygen sensor in the carotid body. Respir. Physiol. Neurobiol. 179, 103–10.

Olson, K.R., 2011. The therapeutic potential of hydrogen sulfide: separating hype from hope. Am. J. Physiol. Regul. Integr. Comp. Physiol. 301, R297–312.

Olson, K.R., 2012. A practical look at the chemistry and biology of hydrogen sulfide. Antioxid. Redox Signal. 17, 32–44.

Olson, K.R., 2013. Hydrogen sulfide: both feet on the gas and none on the brake? Front. Physiol. 4, 1-3.

Olson, K.R., DeLeon, E.R., Liu, F., 2014. Controversies and conundrums in hydrogen sulfide biology. Nitric Oxide 1, 11–26.

Olson, K.R., Dombkowski, R.A., Russell, M.J., Doellman, M.M., Head, S.K., Whitfield, N.L., Madden, J.A., 2006. Hydrogen sulfide as an oxygen sensor/transducer in vertebrate hypoxic vasoconstriction and hypoxic vasodilation. J. Exp. Biol. 209, 4011–23.

Olson, K.R., Whitfield, N.L., Bearden, S.E., St Leger, J., Nilson, E., Gao, Y., Madden, J. a, 2010. Hypoxic pulmonary vasodilation: a paradigm shift with a hydrogen sulfide mechanism. Am. J. Physiol. Regul. Integr. Comp. Physiol. 298, R51–60.

Papapetropoulos, A., Pyriochou, A., Altaany, Z., Yang, G., Marazioti, A., Zhou, Z., Jeschke, M.G., Branski, L.K., Herndon, D.N., Wang, R., Szabó, C., 2009. Hydrogen sulfide is an endogenous stimulator of angiogenesis. Proc. Natl. Acad. Sci. U. S. A. 106, 21972–7.

Papazafiri, P., Kletsas, D., 2003. Developmental and age-related alterations of calcium homeostasis in human fibroblasts. Exp. Gerontol. 38, 307–11.

Pasparakis, M., Vandenabeele, P., 2015. Necroptosis and its role in inflammation. Nature 517, 311–20.

Patacchini, R., Santicioli, P., Giuliani, S., Maggi, C.A., 2005. Pharmacological investigation of hydrogen sulfide (H2S) contractile activity in rat detrusor muscle. Eur. J. Pharmacol. 509, 171–7.

Pedersen, S.F., Owsianik, G., Nilius, B., 2005. TRP channels: an overview. Cell Calcium 38, 233–52.

Peng, Y.-J., Nanduri, J., Raghuraman, G., Souvannakitti, D., Gadalla, M.M., Kumar, G.K., Snyder, S.H., Prabhakar, N.R., 2010. H2S mediates O2 sensing in the carotid body. Proc. Natl. Acad. Sci. U. S. A. 107, 10719–24.

Perry, M.M., Hui, C.K., Whiteman, M., Wood, M.E., Adcock, I., 2013. Europe PMC funders group hydrogen sulfide inhibits proliferation and release of IL-8 from human airway smooth muscle cells 45, 746–52.

Pozsgai, G., Hajna, Z., Bagoly, T., Boros, M., Kemény, Á., Materazzi, S., Nassini, R., Helyes, Z., Szolcsányi, J., Pintér, E., 2012. The role of transient receptor potential ankyrin 1

(TRPA1) receptor activation in hydrogen-sulphide-induced CGRP-release and vasodilation. Eur. J. Pharmacol. 689, 56–64.

Prandelli, C., Parola, C., Buizza, L., Delbarba, A., Marziano, M., Salvi, V., Zacchi, V., Memo, M., Sozzani, S., Calza, S., Uberti, D., Bosisio, D., 2013. Sulphurous thermal water increases the release of the anti-inflammatory cytokine IL-10 and modulates antioxidant enzyme activity. Int. J. Immunopathol. Pharmacol. 26, 633–46.

Predmore, B.L., Lefer, D.J., Gojon, G., 2012. Hydrogen sulfide in biochemistry and medicine. Antioxid. Redox Signal. 17, 119–40.

Puranik, M., Weeks, C.L., Lahaye, D., Kabil, O., Taoka, S., Nielsen, S.B., Groves, J.T., Banerjee, R., Spiro, T.G., 2006. Dynamics of carbon monoxide binding to cystathionine beta-Synthase. J. Biol. Chem. 281, 13433-8.

Qingyou, Z., Junbao, D., Weijin, Z., Hui, Y., Chaoshu, T., Chunyu, Z., 2004. Impact of hydrogen sulfide on carbon monoxide/heme oxygenase pathway in the pathogenesis of hypoxic pulmonary hypertension. Biochem. Biophys. Res. Commun. 317, 30–7.

Raemdonck, K., de Alba, J., Birrell, M. a., Grace, M., Maher, S. a., Irvin, C.G., Fozard, J.R., O'Byrne, P.M., Belvisi, M.G., 2012. A role for sensory nerves in the late asthmatic response. Thorax 67, 19–25.

Ramachandran, R., Morice, A.H., Compton, S.J., 2006. Proteinase-activated receptor2 agonists upregulate granulocyte colony-stimulating factor, IL-8, and VCAM-1 expression in human bronchial fibroblasts. Am. J. Respir. Cell Mol. Biol. 35, 133–41.

Rashid, S., Heer, J.K., Garle, M.J., Alexander, S.P.H., Roberts, R.E., 2013. Hydrogen sulphide-induced relaxation of porcine peripheral bronchioles. Br. J. Pharmacol. 168, 1902–10.

Reiffenstein, R.J., Hulbert, W.C., Roth, S.H., 1992. Toxicology of hydrogen sulfide. Annu. Rev. Pharmacol. Toxicol. 32, 109–34.

Riccardi, C., Nicoletti, I., 2006. Analysis of apoptosis by propidium iodide staining and flow cytometry. Nat. Protoc. 1, 1458–61.

Rouzé, A., Cottereau, A., Nseir, S., 2014. Chronic obstructive pulmonary disease and the risk for ventilator-associated pneumonia. Curr. Opin. Crit. Care 20, 525–31.

Ruan, T., Lin, Y.-J., Hsu, T.-H., Lu, S.-H., Jow, G.-M., Kou, Y.R., 2014. Sensitization by pulmonary reactive oxygen species of rat vagal lung C-fibers: the roles of the TRPV1, TRPA1, and P2X receptors. PLoS One 9, e91763.

Rubin, H., 1997. Cell aging in vivo and in vitro. Mech. Ageing Dev. 98, 1–35.

Sadofsky, L.R., Boa, A.N., Maher, S.A., Birrell, M.A., Belvisi, M.G., Morice, A.H., 2011. TRPA1 is activated by direct addition of cysteine residues to the N-hydroxysuccinyl esters of acrylic and cinnamic acids. Pharmacol. Res. 63, 30–6.

Sadofsky, L.R., Campi, B., Trevisani, M., Compton, S.J., Morice, A.H., 2008. Transient receptor potential vanilloid-1-mediated calcium responses are inhibited by the alkylamine antihistamines dexbrompheniramine and chlorpheniramine. Exp. Lung Res. 34, 681–93.

Sadofsky, L.R., Ramachandran, R., Crow, C., Cowen, M., Compton, S.J., Morice, A.H., 2012. Inflammatory stimuli up-regulate transient receptor potential vanilloid-1 expression in human bronchial fibroblasts. Exp. Lung Res. 38, 75–81.

Salloum, F.N., 2015. Hydrogen sulfide and cardioprotection — Mechanistic insights and clinical translatability. Pharmacol. Ther. 152, 11–17.

Schaefer, E.A.M., Stohr, S., Meister, M., Aigner, A., Gudermann, T., Buech, T.R.H., 2013. Stimulation of the chemosensory TRPA1 cation channel by volatile toxic substances promotes cell survival of small cell lung cancer cells. Biochem. Pharmacol. 85, 426–38.

Scholey, J.M., Brust-Mascher, I., Mogilner, A., 2003. Cell division. Nature 422, 746–52.

Shaw, G., Morse, S., Ararat, M., Graham, F.L., 2002. Preferential transformation of human neuronal cells by human adenoviruses and the origin of HEK 293 cells. FASEB J. 16, 869–71.

Sheng, J., Shim, W., Wei, H., Lim, S.Y., Liew, R., Lim, T.S., Ong, B.H., Chua, Y.L., Wong, P., 2013. Hydrogen sulphide suppresses human atrial fibroblast proliferation and transformation to myofibroblasts. J. Cell. Mol. Med. 17, 1345–54.

Shohrati, M., Karimzadeh, I., Saburi, A., Khalili, H., Ghanei, M., 2014. The role of N-acetylcysteine in the management of acute and chronic pulmonary complications of sulfur mustard: a literature review. Inhal. Toxicol. 26, 507–23.

Sirotkin, V.A., Zinatullin, A.N., Solomonov, B.N., Faizullin, D.A., Fedotov, V.D., 2001. Calorimetric and Fourier transform infrared spectroscopic study of solid proteins immersed in low water organic solvents. Biochim. Biophys. Acta 1547, 359–69.

Skehan, P., Storeng, R., Scudiero, D., Monks, a, McMahon, J., Vistica, D., Warren, J.T., Bokesch, H., Kenney, S., Boyd, M.R., 1990. New colorimetric cytotoxicity assay for anticancer-drug screening. J. Natl. Cancer Inst. 82, 1107–12.

Squadrone, E., Frigerio, P., Fogliati, C., Gregoretti, C., Conti, G., Antonelli, M., Costa, R., Baiardi, P., Navalesi, P., 2004. Noninvasive vs invasive ventilation in COPD patients with severe acute respiratory failure deemed to require ventilatory assistance. Intensive Care Med. 30, 1303–10.

Steffensen, B., Häkkinen, L., Larjava, H., 2001. Proteolytic events of wound-healing--coordinated interactions among matrix metalloproteinases (MMPs), integrins, and extracellular matrix molecules. Crit. Rev. Oral Biol. Med. 12, 373–98.

Stein, A., Bailey, S.M., 2013. Redox biology of hydrogen sulfide: Implications for physiology, pathophysiology, and pharmacology. Redox Biol. 1, 32–9.

Stipanuk, M.H., Beck, P.W., 1982. Characterization of the enzymic capacity for cysteine desulphhydration in liver and kidney of the rat. Biochem. J. 206, 267–77.

Streng, T., Axelsson, H.E., Hedlund, P., Andersson, D. a., Jordt, S.E., Bevan, S., Andersson, K.E., Högestätt, E.D., Zygmunt, P.M., 2008. Distribution and function of the hydrogen sulfide-sensitive TRPA1 ion channel in rat urinary bladder. Eur. Urol. 53, 391–400.

Sugiura, H., Ichikawa, T., Liu, X., Kobayashi, T., Wang, X.Q., Kawasaki, S., Togo, S., Kamio, K., Mao, L., Ann, Y., Ichinose, M., Rennard, S.I., 2009. N-acetyl-l-cysteine inhibits TGF-β1-induced profibrotic responses in fibroblasts. Pulm. Pharmacol. Ther. 22, 487–91.

Szabó, C., 2007. Hydrogen sulphide and its therapeutic potential. Nat. Rev. Drug Discov. 6, 917–35.

Szabo, C., Coletta, C., Chao, C., Módis, K., Szczesny, B., Papapetropoulos, A., Hellmich, M.R., 2013. Tumor-derived hydrogen sulfide, produced by cystathionine-β-synthase, stimulates bioenergetics, cell proliferation, and angiogenesis in colon cancer. Proc. Natl. Acad. Sci. U. S. A. 110, 12474–9.

Szabó, C., Papapetropoulos, A., 2011. Hydrogen sulphide and angiogenesis: Mechanisms and applications. Br. J. Pharmacol. 164, 853–65.

Szczesny, B., Módis, K., Yanagi, K., Coletta, C., Le Trionnaire, S., Perry, A., Wood, M.E., Whiteman, M., Szabo, C., 2014. AP39, a novel mitochondria-targeted hydrogen sulfide donor, stimulates cellular bioenergetics, exerts cytoprotective effects and protects against the loss of mitochondrial DNA integrity in oxidatively stressed endothelial cells in vitro. Nitric Oxide 41, 120–30.

Takahashi, N., Kozai, D., Mori, Y., 2012. TRP channels: Sensors and transducers of gasotransmitter signals. Front. Physiol. 3, 1–14.

Thomas, D., Tovey, S.C., Collins, T.J., Bootman, M.D., Berridge, M.J., Lipp, P., 2000. A comparison of fluorescent Ca2+ indicator properties and their use in measuring elementary and global Ca2+ signals. Cell Calcium 28, 213–23.

Thomas, P., Smart, T.G., 2005. HEK293 cell line: A vehicle for the expression of recombinant proteins. J. Pharmacol. Toxicol. Methods 51, 187–200.

Toombs, C.F., Insko, M.A., Wintner, E.A., Deckwerth, T.L., Usansky, H., Jamil, K., Goldstein, B., Cooreman, M., Szabo, C., 2010. Detection of exhaled hydrogen sulphide gas in healthy human volunteers during intravenous administration of sodium sulphide. Br. J. Clin. Pharmacol. 69, 626–36.

Trevisani, M., Patacchini, R., Nicoletti, P., Gatti, R., Gazzieri, D., Lissi, N., Zagli, G., Creminon, C., Geppetti, P., Harrison, S., 2005. Hydrogen sulfide causes vanilloid receptor 1-mediated neurogenic inflammation in the airways. Br. J. Pharmacol. 145, 1123–31.

Tumilowicz, J.J., Nichols, W.W., Cholon, J.J., Greene, A.E., 1970. Definition of a continuous human cell line derived from neuroblastoma definition of a continuous human cell Line Derived from 30, 2110–8.

Tyagi, N., Moshal, K.S., Sen, U., Vacek, T.P., Kumar, M., Hughes, W.M., Kundu, S., Tyagi, S.C., 2009. H2S protects against methionine-induced oxidative stress in brain endothelial cells. Antioxid. Redox Signal. 11, 25–33.

Vichai, V., Kirtikara, K., 2006. Sulforhodamine B colorimetric assay for cytotoxicity screening. Nat. Protoc. 1, 1112-6.

Viscomi, C., Burlina, A.B., Dweikat, I., Savoiardo, M., Lamperti, C., Hildebrandt, T., Tiranti, V., Zeviani, M., 2010. Combined treatment with oral metronidazole and N-acetylcysteine is effective in ethylmalonic encephalopathy. Nat. Med. 16, 869–71.

Wagner, F., Asfar, P., Calzia, E., Radermacher, P., Szabó, C., 2009. Bench-to-bedside review: Hydrogen sulfide--the third gaseous transmitter: applications for critical care. Crit. Care 13, 213.

Wallace, J.L., Ianaro, A., Flannigan, K.L., Cirino, G., 2015. Gaseous mediators in resolution of inflammation. Semin. Immunol. 27, 227–33.

Wallace, J.L., Wang, R., 2015. Hydrogen sulfide-based therapeutics: exploiting a unique but ubiquitous gasotransmitter. Nat. Rev. Drug Discov. 14(5):329-45

Wang, L., Cvetkov, T.L., Chance, M.R., Moiseenkova-Bell, V.Y., 2012. Identification of in vivo disulfide conformation of TRPA1 ion channel. J. Biol. Chem. 287, 6169–76.

Wang, R., 2012. Physiological implications of hydrogen sulfide: a whiff exploration that blossomed. Physiol. Rev. 92, 791–896.

Weller, K., Reeh, P.W., Sauer, S.K., 2011. TRPV1, TRPA1, and CB1 in the isolated vagus nerve - Axonal chemosensitivity and control of neuropeptide release. Neuropeptides 45, 391–400.

White, B.J.O., Smith, P. a., Dunn, W.R., 2013. Hydrogen sulphide mediated vasodilatation involves the release of neurotransmitters from sensory nerves in pressurized mesenteric small arteries isolated from rats. Br. J. Pharmacol. 168, 785–93.

Wild, V., Messlinger, K., Fischer, M.J.M., 2015. Hydrogen sulfide determines HNO-induced stimulation of trigeminal afferents. Neurosci. Lett. 602, 104–9.

Wlodkowic, D., Skommer, J., Darzynkiewicz, Z., 2009. Flow cytometry-based apoptosis detection. Methods Mol. Biol. 559, 19–32.

Wu, L.-J., Sweet, T.-B., Clapham, D.E., 2010. International union of basic and clinical pharmacology. LXXVI. Current progress in the mammalian TRP ion channel family. Pharmacol. Rev. 62, 381–404.

Wu, R., Yao, W., Chen, Y., Geng, B., Tang, C., 2008. [Plasma level of endogenous hydrogen sulfide in patients with acute asthma]. Beijing Da Xue Xue Bao. 40, 505–8.

Yanfei, W., Lin, S., Junbao, D., Chaoshu, T., 2006. Impact of l-arginine on hydrogen sulfide/cystathionine-gamma-lyase pathway in rats with high blood flow-induced pulmonary hypertension. Biochem. Biophys. Res. Commun. 345, 851–7.

Yang, G., 2011. Hydrogen sulfide in cell survival: a double-edged sword. Expert Rev. Clin. Pharmacol. 4, 33–47.

Yang, G., Cao, K., Wu, L., Wang, R., 2004a. Cystathionine γ-lyase overexpression inhibits cell proliferation via a H2S-dependent modulation of ERK1/2 phosphorylation and p21 Cip/WAK-1. J. Biol. Chem. 279, 49199–205.

Yang, G., Sun, X., Wang, R., 2004b. Hydrogen sulfide-induced apoptosis of human aorta smooth muscle cells via the activation of mitogen-activated protein kinases and caspase-3. FASEB J. 18, 1782–4.

Yang, K.-T., 2004. Mitochondrial Na+ overload is caused by oxidative stress and leads to activation of the caspase 3-dependent apoptotic machinery. FASEB J. 18, 1442–4.

Yuan, S., Patel, R.P., Kevil, C.G., 2015. Working with nitric oxide and hydrogen sulfide in biological systems. Am. J. Physiol. - Lung Cell. Mol. Physiol. 308, L403-15.

Zhao, Y., Biggs, T.D., Xian, M., 2014. Hydrogen sulfide (H2S) releasing agents: chemistry and biological applications. Chem. Commun. (Camb). 50, 11788–805.

Zhong, G., Chen, F., Cheng, Y., Tang, C., Du, J., 2003. The role of hydrogen sulfide generation in the pathogenesis of hypertension in rats induced by inhibition of nitric oxide synthase. J. Hypertens. 21, 1879–85.